University of Stavanger

FACULTY OF SCIENCE AND TECHNOLOGY

# Bachelor's Thesis

| | |
|---|---|
| Study program/specialization:<br><br>**Petroleum Engineering/ Drilling Technology** | Spring/Autumn semester, 2021<br><br>Open |
| Author: **Jiwar Nori** | ……<br>(Signature of author) |
| Program coordinator:<br><br>Supervisor(s): **Mesfin Belayneh** | |
| Title of bachelor's thesis:<br>***Effect of $SiO_2$ and $TiO_2$ Nanoparticles on Cementitious Materials: Experimental and Modelling Studies***<br><br>Tittel på bacheloroppgave på norsk:<br>***Effekt av $SiO_2$ og $TiO_2$ nanopartikler på sementholdige materialer: Eksperimentelle og modelleringsstudier*** | |
| Credits: 20 | |
| **Keywords:**<br><br>Portland cement<br>Industry cement<br>Environmental cement<br>Nanoparticles<br>$SiO_2$<br>$TiO_2$<br>UCS<br>Tensile Strength<br>Rheology<br>E-modulus<br>Resilience | Number of pages: ……68……<br><br>+ Supplemental material/other: 24<br><br>Date/year 15/05/2021<br><br>Stavanger |

# ACKNOWLEDGEMENTS

I am highly fortunate to have professor **Mesfin Belayneh** as my academic supervisor. I would like to thank him immensely for his guidance, mentoring, great support, and kind advice throughout my thesis work. His office doors are always open, and he has always been available and happy to be in assistance from the earliest of mornings to the latest of evenings. His enthusiasm and dedication for his students is beyond measure and is greatly appreciated.

Additionally, I want to warmly show appreciation for the contribution of the generous senior engineer **Samdar Kakay** for the technical assistance rendered and instructing me in the use of the compressive strength testing apparatus located in his laboratory, which allowed me to perform more destructive test on my cement samples.

Lastly, I strongly thank my parents for their aspiration for me to successfully write this thesis. I also thank them for my moral upbringing and their unflagging encouragement.

# ABSTRACT

Cement is one of the crucial well barrier elements in the oil well. The well barrier performances of cement depend on the cement composition and good cement job during placement. NORSOK D-010 defined the criterial for cement properties. However, well integrity survey study in the North Sea wells showed that cement related integrity failure recorded about 11% [7]. This shows that the conventional cement slurry does not satisfy the standards requirement.

In the recent years, the application of nanotechnology has shown excellent effect on cement properties. This thesis work experimentally investigates the impact of $SiO_2$ nanoparticle solution on the properties of neat industry cement (C-class) and environmental cement. Moreover, the effect of hybrid $SiO_2$-$TiO_2$ nanoparticles solution on the properties of neat Portland G-class cement.

Results showed that the optimum concentration of the nanoparticles improved the elastic, energy absorption, rheology, heat development, and load carrying capacity of the cement plugs. Among the best results:

- The addition of an optimal 0.56 % $SiO_2$ by weight of C-class cement increased the uniaxial compressive strength of the neat cement by 16.7%
- The mixture of an optimal 0.13% SiO2 by weight of environmental cement increased the uniaxial compressive strength of the neat cement by 49.6%
- The blending of an optimal 0.264 %$SiO_2$ / 0.044% $TiO_2$ by weight of G-class cement increased the uniaxial compressive strength of the neat cement by 8.5%

However, changing the curing temperature and pressure, one may achieve different results.

# TABLE OF CONTENTS

# LIST OF FIGURES

# LIST OF TABLES

# LIST OF ABBREVIATIONS

API = American Petroleum Institute

BOP = Blow Out Preventor

HSR = High Sulphate Resistant

I.R = Insoluble Residue

ISO = International Organization for Standardization

MSR = Moderate Sulphate Resistant

NCS = Norwegian Continental Shelf

OPC = Ordinary Portland Cement

P&A = Plug and Abandonment

PSA = Petroleum Safety Authority

RPM = Revolution Per Minute

SEM = Scan Electron Microscope

UCS = Uniaxial Compressive Strength

WCR = Water to Cement Ratio

Wt% = Weight percent

%bwoc = Percent by weight of cement

# LIST OF SYMBOLS

A = cross-sectional area of specimen ($mm^2$)

E = Young´s modulus = (MPa)

Fmax = force at time of failure (N)

G = Shear modulus (GPa)

K = Bulk modulus (GPa)

M = Modulus of Elasticity (GPa)

P = applied force at moment the sample breaks (N)

R = Resilience ($J/m^3$)

Vp = Compressional wave velocity (km/s)

$\rho$ = density ($kg/m^3$)

$\sigma_t$ = tensile strength ($\frac{N}{m^2}$)

$\tau$ = Shear stress (Pa)

$\tau_c$ = Yield stress (Pa)

$\mu_c$ = Viscosity (Pa.s)

$\gamma$ = Shear rate ($sec^{-1}$)

$\Delta M$ = change of mass

$\Delta\sigma$ = Change in stress

$\Delta\varepsilon$ = Change in strain

# 1 INTRODUCTION

This BSc thesis presents experimental and modelling works. The experimental study part investigates the effect of Silica oxide ($SiO_2$) and Titanium oxide ($TiO_2$) nanoparticles on C-class, G-class, and environmental cements with the aim of improving their mechanical and elastic properties. The cement plugs have been characterized through destructive (Uniaxial compressive strength and Tensile strength) methods and non-destructive (sonic, mass absorption, rheology, and heat development) methods. The modelling part deals with the development of a new uniaxial compressive strength (UCS) and compressional wave velocity ($V_p$) based empirical model.

## 1.1 Background

During well construction, production and abandonment phases, cement is an important well barrier element. Cementing job in well construction is categorized into two operations namely, primary cementing and remedial cementing. Primary cementing is the process of placing cement around a casing. The main functions are to provide zonal isolation to prevent migration of fluids in the annulus, support for the casing or liner string, and protection of the casing string from corrosive formation fluids [1].

In case of primary cementing failure, the remedial cementing operations are performed to repair primary cementing problems by squeeze cementing and plug cementing. Plug cementing is performed by the operators typically when they are abandoning a well because of its reach to the end of its productive life [1].

Figure 1.1 illustrates the process of cement placement and the final constructed well structure. Figure 1.2 shows the application of cement on the plug and abandonment (P&A) well. Here, the cement plugs are placed as primary, secondary, and surface plugs.

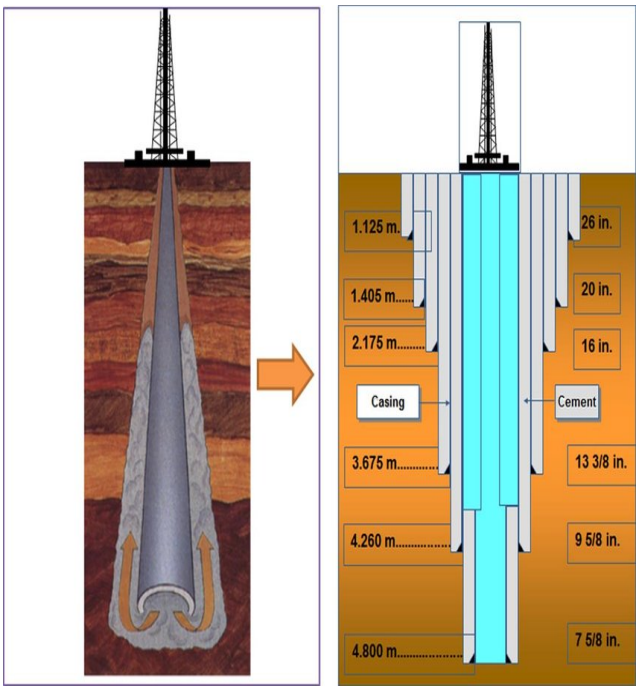


Figure 1.1 Process of oil well cementing [2]

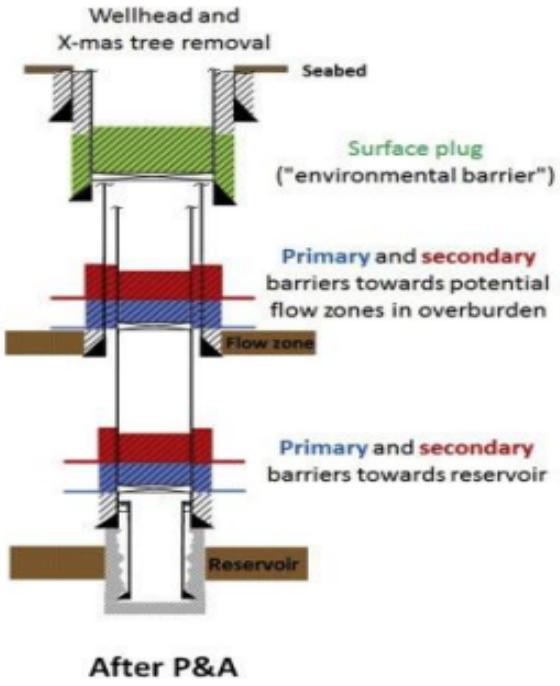


Figure 1.2 Application of cement plug (P&A) [3]

Cement quality and good cementing job are the main factors to ensure a long-term integrity of the well. However, due to pressure and temperature loading the permeability of cement will be increased by cracking, debonding, and shear failure mechanisms as well [4]. This as a result allows reservoir fluid leakage.

Figure 1.3 illustrates the possible reservoir fluids leakage pathways to the surface. (1) between cement and outside of casing, (2) between cement and inside of casing, (3) through cement, (4) through casing, (5) in cement fractures, (6) between cement and rock [5].
The mechanisms (1), (2), and (6) describe transport through micro annuli, where tiny gaps between the components become the preferred flow path.

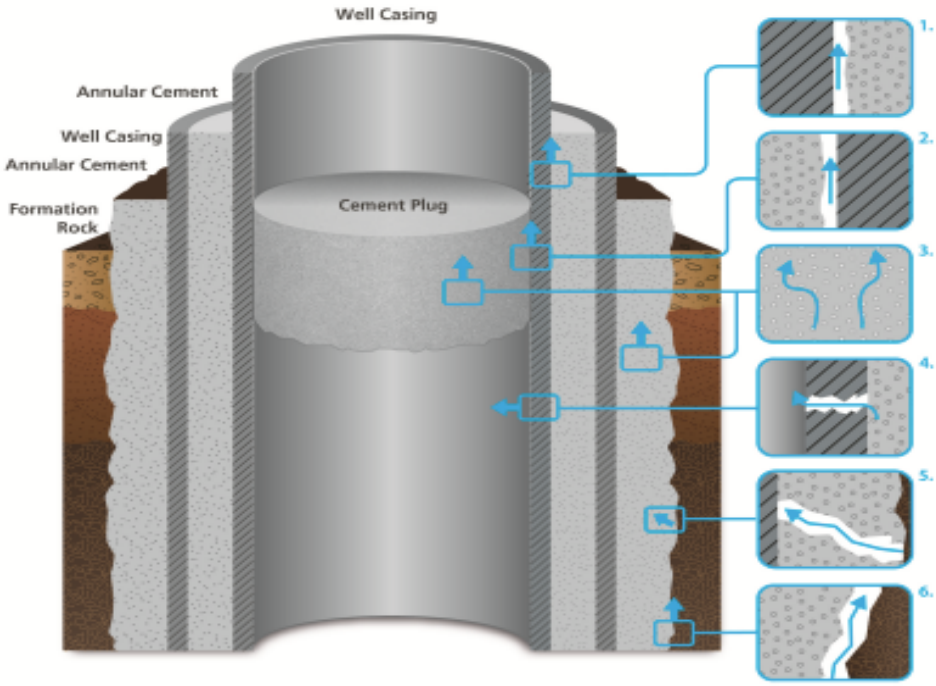


Figure 1.3 Potential leakage pathways, Celia et al. (2005) [5]

For long terms structural integrity, NORSOK D-010 defined the well integrity as the "*Application of technical, operational, and organizational solutions to reduce risk level of undesired formation fluids leaks throughout the life cycle of a well.*" [6]

Moreover, the NORSOK D-010 demands a criterial for cement properties to be:

a) Impermeable
b) Long term integrity
c) Non shrinking
d) Ductile – (non-brittle) – able to withstand mechanical loads/impact
e) Resistance to different chemicals / substances ($H_2S$, $CO_2$ and hydrocarbons)
f) Wetting, to ensure bonding to steel

However, well integrity surveys indicated that several wells have shown integrity issues. For instance, the petroleum safety authority (PSA) of Norway has well integrity survey conducted on 71 wells (31 production and 40 injection). Results as illustrated in Figure 1.4 indicated that cement recorded 11% failure [7].

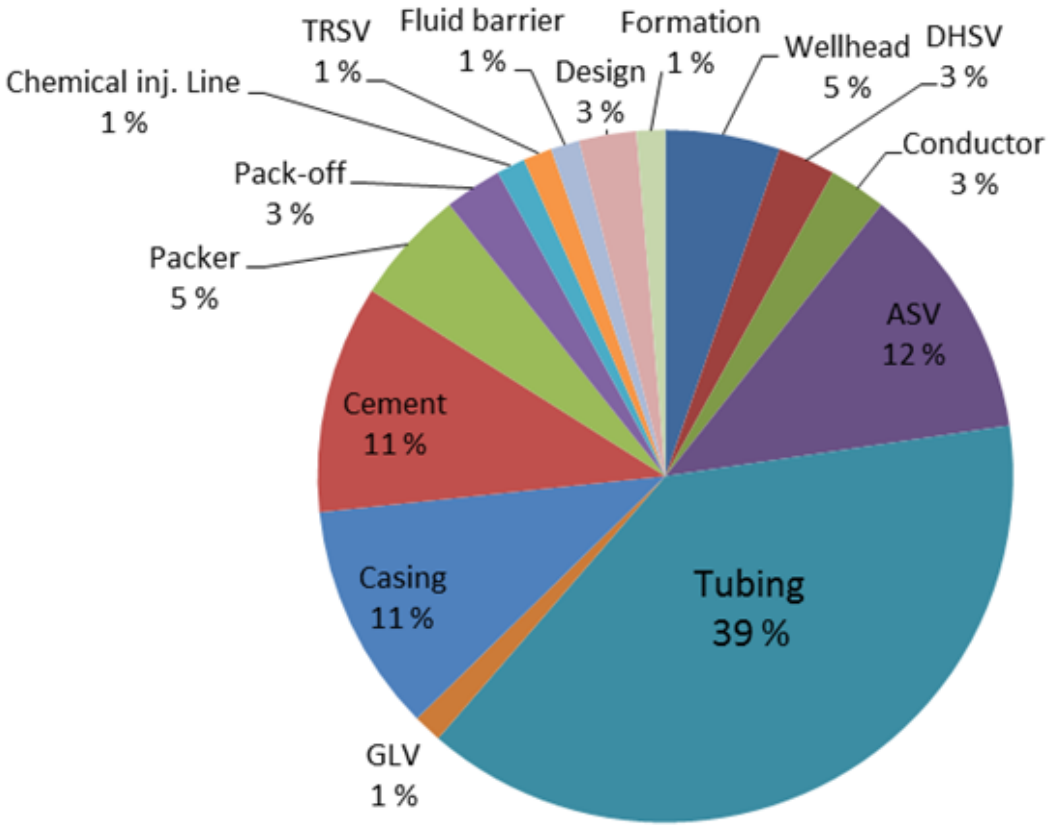


Figure 1.4 Barrier element failure [7]

From the integrity survey, it is evident that the cement does not satisfy the NORSOK D-010 criteria, and this suggests the need to improve the conventional cement.

## 1.2 Problem Formulations

During well construction phase, the surface casing is cemented all the way to the surface. During drilling operation, the well head is connected with the surface casing and on the top of it, blow out preventor (BOP) is landed. During production phase, the BOP is replaced by Christmas tree. In order to provide good structural integrity, the top section is cemented with C-class cement, which is commonly known as industry cement. However, studies from Alberta,

Canada, show that most of the leaks are observed at the top section [8]. As shown in Figure 1.4, the conventional cement in the NCS showed integrity issues [7]. In the recent years, the application of nanoparticles has shown impressive effect on cement properties. Therefore, the main focus of this thesis is to improve the conventional cement properties. The issues to be addressed in this thesis are:

- $SiO_2$ nanoparticle concentration effect on the mechanical, elastic, and physical properties of the industry cement
- $SiO_2$ nanoparticle concentration effect on the mechanical, elastic, and physical properties of environmental cement
- $SiO_2$ - $TiO_2$ hybrid nanoparticle effect on the Portland G-class cement

## 1.3 Scope and Objectives

The primary objective of the thesis is to investigate the research questions addressed in the problem formulations part. This is done through some experimental works like destructive and non-destructive techniques. The activities are:

- Review of nanoparticles in the oil and gas industry
- Conduct experimental study on the effect of nanoparticles on industry, environmental and Portland cement. The cement plugs will be characterized with destructive and non-destructive test
- Finally, develop new empirical UCS vs compressional wave velocity model

## 1.4 Research Methods

Figure 1.5 displays an overview of the structure of the thesis work, which comprises of three parts. The first part deals with literature study on the cement and nanoparticles application in the petroleum industry. The second part experimentally investigates the impact of nanoparticles on the conventional neat cements. Based on the experimental destructive and non-destructive test datasets, the modelling part will develop new empirical models.

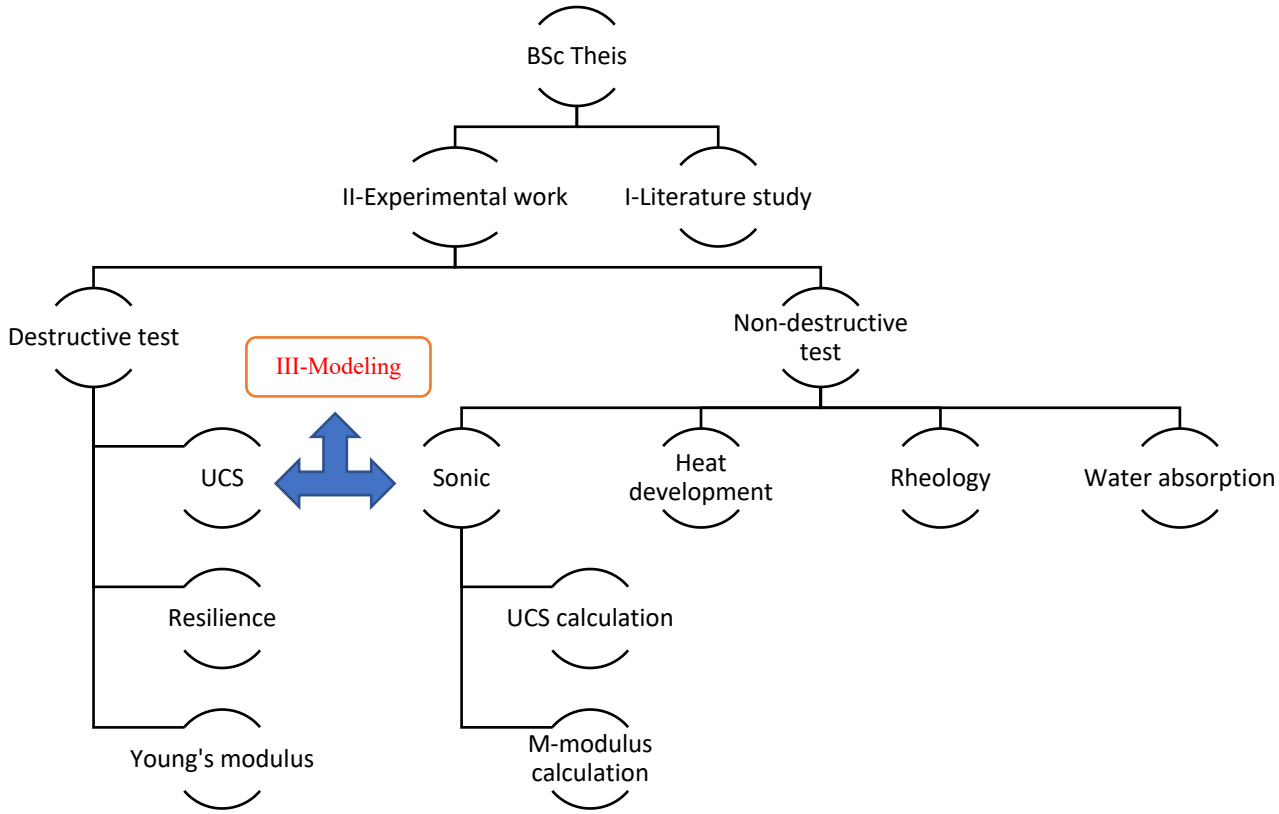


Figure 1.5 Research methodology

# 2 LITERATURE STUDY

Chapter 2 presents a literature review of Portland cement, nanotechnology, and some applications in the petroleum industry and a description of the nanoparticles selected for use in the thesis.

## 2.1 API Classification of Portland Cement

Ordinary Portland Cement (OPC) is the commonly used cement in oil and gas industry. The American Petroleum Institute (API) has set up standard specific physical and chemical properties. Portland cement satisfy the API standard requirements.

Portland cement is classified into eight API classes, indicated with the letters from A to H with three grades ordinary (O), moderate sulphate resistant (MSR), and high sulphate resistant (HSR). Nowadays, the cement of class E and F are infrequently used worldwide, and they are deleted from the latest edition of (API 10 A) which is also similar to International Organization for Standardization (ISO 10426-1) [4].

Table 2.1 presents the description of the API cement classes briefly.

Table 2.1 A brief description of the API classes [4]

| | |
|---|---|
| **Class A** | **Used for situations where no special properties are required.** |
| **Class B** | Used for situations where moderate or high sulphate resistance is required. |
| **Class C** | Used for situations where high early strength development is required. |
| **Classes D, E and F** | Were intended for use in deeper wells, the number of faster-hydrating phases are reduced, and the grain size of the particles are increased. Because the technology has improved greatly since the retarders used in these classes were first made and are today outdated, these classes are rarely used today. |
| **Classes G and H** | These classes were developed after improvement of retarders and accelerators. They are used as a basic well cement. |

## 2.2 Portland Cement´s Hydration Process

Portland cement is a hydraulic cement, which sets and harden when cement reacts with water. The strength is obtained by a process known as hydration.

Portland cement is made up of four main compounds which are referred to as clinker minerals and they are the followings: $C_3S$, $C_2S$, $C_3A$, and $C_4AF$. Hydration of $C_3S$ is mostly used as a model for the Portland cement hydration. The hydration of these individual clinker phases is different to the hydration of multicomponent system Portland cement. The individual clinker phases can affect each other, as the presence of hydrating $C_3S$ cause the hydration of $C_3A$ to be modified [4].

Table 2.2 shows us the composition of minerals of the major compounds.

Table 2.2 Mineralogical composition of Portland cement

| Shorthand form | Formula | Mineral name | Mass% |
|---|---|---|---|
| **$C_3S$** | $3CaO*SiO_2$ | Alite | 60-65 |
| **$C_2S$** | $2CaO*SiO_2$ | Belite | 20-25 |
| **$C_3A$** | $3CaO*Al_2O_3$ | Aluminate | 5-12 |
| **$C_4AF$** | $4CaO*\ Al_2O_3*Fe_2O_3$ | Ferrite | 6-12 |

$C_3S$ and $C_2S$ are the two most responsible compounds for the strength development. These compounds of silica phase form up 80-90 wt% of the cement. Portland cement hydration results in the production of calcium silicate hydrate and calcium hydroxide according to the chemical reaction [4].

$$\mathbf{2C_3S \rightarrow C_3S_2H_3 + 3CH}$$

$$\mathbf{2C_2S + 4H \rightarrow C_3S_2H_3 + CH}$$

The hydration of $C_3S$ and $C_2S$ form similar C-S-H phase. Hydration of $C_3S$ is primarily responsible for setting and early strength development, while the final strength is mostly due to the hydration of $C_2S$ [4].

Figure 2.1 illustrates the exothermic process of hydration of $C_3S$ which undergoes through five different stages:

I. Preinduction period

II. Induction period

III. Acceleration period

IV. Deceleration Period

V. Diffusion period

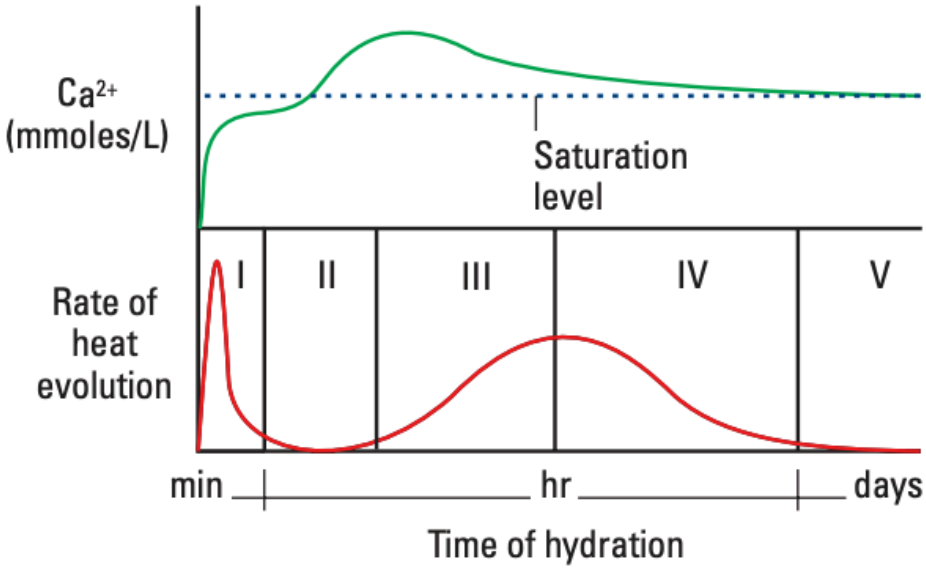


Figure 2.1 Schematic representation of changes occurring during hydration of $C_3S$ [4]

## 2.3 Nanotechnology

The application of nanotechnology (1-100 nanometres) has shown proven solution in several industries such as biomedical and electronics. The surface area of nanoparticle is higher

than the micro sized particles. Through chemical and physical interactions, nanoparticle creates a new material having properties such as light weight and stronger [9].

The application of nanomaterials in the petroleum industry has shown promising results. However, its application is not fully investigated. Therefore, this thesis work is designed to test the impact of $SiO_2$ and $TiO_2$ on the selected cement types. The following presents the review of the effect of nanoparticles in the petroleum industry.

## 2.4 Application of Nanoparticle on Cement

The performance of nanoparticle for a given application depends on several factors. Among these, the surface chemistry, the concentration, the size as well as its interaction with the base system in which the nanomaterial is mixed with. Basically, nanomaterial is synthesized in two methods, namely, "top down" and "bottom-up". Figure 2.2 illustrates these.

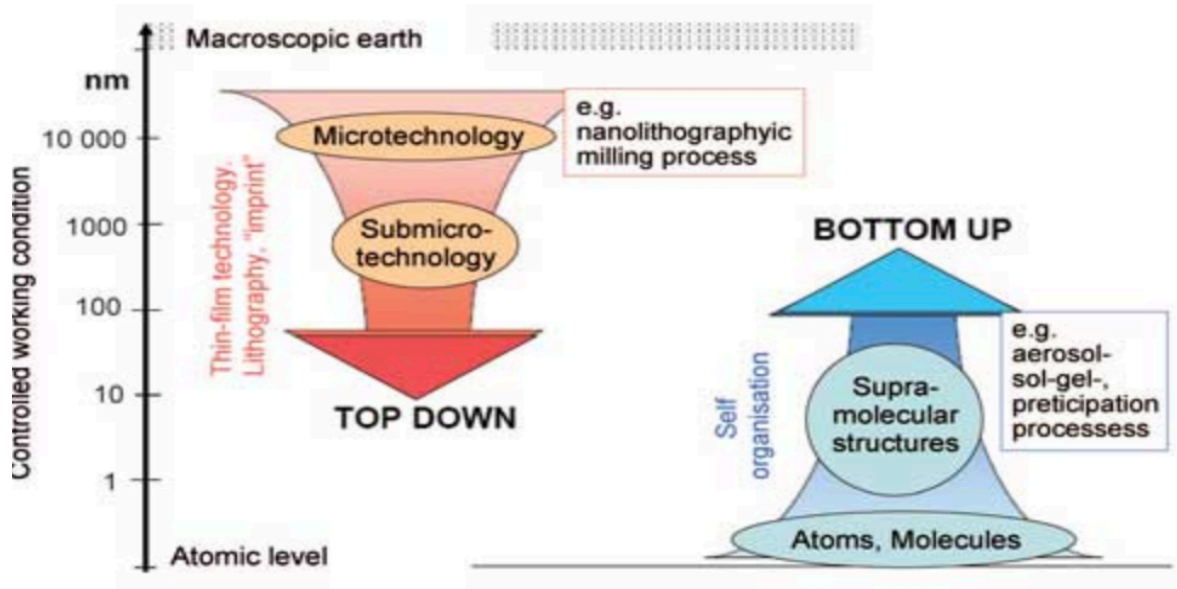


Figure 2.2 An illustration of top-down and bottom-up methods for synthesis of nanoparticles [10]

The "top-down" method is reducing macro materials into nano sized through mechanical milling techniques. The "bottom-up" method synthesis is by using chemical processes. All the nanoparticles used in this thesis are synthesized by the bottom up commercial nanofluids.

### 2.4.1 Application of Nanotechnology in the Oil and Gas Industry

The nanoparticle research results documented in literature have shown impressive impact on drilling fluid, cement, and enhanced oil recovery. The industry believes that the nanotechnology would bring more solution for the problems associated with the conventional technology. For instance:

**In drilling fluid:**

- Nanoparticles in drilling fluids have shown reduced filtrate loss and mud cake thickness [11-12], improved the rheological parameters [11,13,14], increased the lubricity of the drilling fluid [15], improved the thermal and electrical conductivity [16], and increased the wellbore strength [17].

**For enhanced oil recovery:**

- In enhanced oil recovery, nanoparticles increased the recovery [18-21].

Figure 2.3 illustrates the application of nanoparticles in the oil and gas industry. The application is diverse in exploration, refining and processing, production, reservoir management, and drilling.


Figure 2.3 Application of nanotechnology in the oil and gas industry [22]

### 2.4.2 Applications of Nanotechnology in Oil-well Cementing

Several investigators have tested different types of nanoparticles in cement. Results have shown that nanoparticles improve the mechanical, elastic, and rheological properties of cements. In the following, some of the selected research papers reviewed and summarized their main results.

Table 2.3 Review of effect of nanoparticles on cement [23-37]

| Author [23-37] | Nanoparticles and Characterization | Key findings |
|---|---|---|
| Li et al. (2003) [23] | Nanoparticle<br>• $SiO_2$ and $Fe_2O_3$<br>Test:<br>• Compressive strength<br>• Flexural strength | Results:<br>• Compressive strength increased with decreasing amount of $Fe_2O_3$<br>• Compressive strength increased with increasing amount of $SiO_2$<br>• Increased flexural strength |
| Ershadi et al. (2011) [24] | Nano silica<br>Test<br>• Early strength<br>• Permeability<br>• Porosity<br>• Fluid loss<br>• Thickening time | Results:<br>• High early strength<br>• 99% reduction of permeability<br>• 33.3% reduction of porosity<br>• Reduced fluid loss<br>• Reduced thickening time |
| Rahimirad et al. (2012) [25] | Nanoparticle<br>• Nanotube<br>Test<br>• Physical property<br>• Mechanical property<br>• Thermal property<br>• Heat conductivity | Results:<br>• Density of cement reduction by 6%<br>• Enhancement of compressive strength by 70%<br>• Reduction of heat conductivity of cement by 20% |
| Roji et al. (2012) [26] | Particles:<br>• API Class G cement<br>• Nano-engineered API Class G cement<br>Tests:<br>• Mechanical strength<br>• Physical property | Results:<br>Nano-engineered particle effect in 24hrs:<br>• Bending force increased by 45%<br>• Compressional strength increased by 56%<br>• Density reduced by 1.5% |
| Patil & Deshpande (2012) [27] | Nanoparticle<br>- Nano silica<br>Tests: | Results:<br>adding 0.2 gal/sk of nano silica |

| | | |
|---|---|---|
| | - using API standards and procedures | - the rate of strength development increased from 172 to 460 psi/hr, which is an increase in 167.44%<br>- Fluid loss receded from 52 ml/30min to 34 ml/30min (reduced by 34.6 %) |
| Pang et al. (2014) [28] | Nanoparticle<br>- Nano silicas<br>Test<br>- if additive used as accelerators for shortening the WOC time | Results:<br>- Small concentration of nano silica particle sizes increases the cement-set acceleration |
| Moradi & Nikolaev (2015) [29] | Particles<br>- Portland cement<br>- weighting material<br>- silica flour or silica sand<br>Test.<br>- Compressive strength<br>- free fluid test<br>- thickening time and<br>- flow ability | Results:<br>The compressive strength for the<br>100% Portland cement:<br>- was 15.21 MPa<br>70 % cement + 15% hematite and 15 % silica flour<br>- 20.18 MPa<br>In the free fluid test<br>- a reduction free fluid content by adding polyvinyl alcohol<br>Flowability<br>- decreases by adding lignosulfonate<br>Thickening time<br>- Lignosulfonate increases the thickening time |
| Murtaza et al. (2016) [30] | Test<br>compressive strength<br>permeability and porosity<br>Nano clay<br>(1%, 2% and 3%) | Results:<br>after 24 hours, 1% Nano clay to the base mix reduced<br>- permeability decrease by 76%<br>- porosity by 9% |
| Rehman et al. (2016) [31] | Nanoparticle: MWCNT<br>3% of MWCNT as nanomaterials and various concentrations of CNT varying from 0.1%, 0.25% to 0.5%<br>Test<br>compressive strength (UCS)<br>rheological properties | Results:<br>Compared to the base mix<br>• UCS increase respectively with 19%, 10% and 9% for the 0.1%, 0.25% and 0.5% CNT component recipes<br>***Yield point testing***<br>• a decrease for the 0.1% and 0.25% with respectively 38% and 17%, while for the 0.5% mix the yield point increased 14% |

| | | |
|---|---|---|
| | | ***Gel strength***<br>• The gel strength after 10 seconds for the 0.1%, 0.25% and 0.5% recipes, resulted a decrease in gel strength with respectively 56%, 44% and 44%<br>• The gel strength after 10 minutes resulted an increase for 0.1%, 0.25% and 0.5% recipes with respectively 37%, 41% and 48% compared to the base mix |
| Jafariesfad et al. (2016) [32] | Issue<br>- Shrinkage with oil well cement<br><br>Nanoparticle:<br>- MgO | Results:<br>• NPs system reduced shrinkage<br><br>Lowest and highest improvement:<br>***After 1 day***<br>• Lowest 0% after day 1 and highest 200%<br>***After 14 days***<br>• Lowest was 8% and highest was 122% improvement |
| Heathman et al. (2017) [33] | Two issues addressed:<br>- if steel was hydrophobic<br>- if cement and steel do not form a chemical bond<br><br>Test:<br>- contact angle before and after nano treatment<br>- shear bond test strength | Results:<br><br>Decrease in contact angle<br>- Lower the contact angle of steel substrates from 58o to 14o, a decrease in 76%<br><br>Shear bond tests<br>- an increase in shear bond by lowering the contact angle<br><br>- 75% increase in water wettability and 50% increase in shear bond |
| Peyvandi et al. (2017) [34] | Nanoparticle<br>- Graphite nanoplatelet<br>Tests<br>- Rheological<br>- shrinkage<br>- flexural<br>- tensile<br>- compressive strength | Results:<br><br>0.2 vol% NP<br>- improvement 20% in flexibility<br>- 0% in tensile strength<br>- 50% improvement in shrinkage<br><br>Rheological test; with 0.2vol% GnP, 0.4vol% GnP and 0.8 vol%<br>- Result at 300 rpm gave 131, 201 and 282, respectively<br>- Results 3 rpm gave 31, 50 and 55 respectively |
| Baig et al. (2017) "Application of" [35] | Nanoparticles<br><br>Nano zeolite 1%, 2% 3% | Result:<br>- Early compressive strength is highest for Nano zeolite 2<br>Compressive strength<br>- Nano zeolite 1 and Nano zeolite 2 increased 0.75% and 14.6%, respectively<br>- Nano zeolite 3 was reduced with 10.2 % after 6 hours<br>Nano zeolite 1 |

| | | |
|---|---|---|
| | | - highest strength after 24 hours. NZ1 increased with 4.77 %<br>Nano zeolite 2<br>- increased with 2.88 %<br>Nano zeolite 3<br>- Reduced with -13.58%<br>• The porosity for<br>- Nano zeolite 1<br>- Porosity reduced 17%, and the permeability was reduced 98 %<br><br>- Nano zeolite 3<br>- Porosity increased 25.76 %, while the permeability decreased 8.55% |
| Nazari et al. (2010) [36] | Nanoparticle<br>• Nano Titanium Dioxide<br><br>Test<br>• Compressive strength<br>• Workability | Results:<br>• The ultimate strength was gained at 1.0% of cement replacement<br>• $TiO_2$ improves compressive strength but decreases its workability |
| Jay Sorathiya et al. (2017) [37] | Nanoparticle<br>• Anatase Nano Titanium Dioxide<br><br>Test<br>• Compressive strength<br>• Workability | Results:<br>• Higher compressive strength<br>• Cement strength increases when the added nano $TiO_2$ particle up to maximum limit of 1.0% with average particle sizes of 15 nm<br>• By increasing percentage of $TiO_2$ more than 1%, compressive strength of the concrete is decreased |

From the literature study, we can observe that $SiO_2$ performance on G-class cement enhanced the mechanical, setting, and filtrate loss properties. Moreover, the positive effect of $TiO_2$ on G-class cement is reported. However, in this thesis the effect of silica on C-class and environmental cement will be tested. In addition, the impact of the hybrid ($SiO_2$+$TiO_2$) nanoparticles on G-class will be investigated.

# 3 EXPERIMENTAL WORK

Chapter 3 presents the materials, the cement slurry preparation, the characterization methods, and theories used to quantify the mechanical, elastic, and rheological parameters.

## 3.1 Materials and Methods

All the materials used have been provided by the University of Stavanger or its collaborating companies.

### 3.1.1 Description of Cements

Different cements were purchased and used in this thesis, the industry C-class cement and Portland G-class cement were provided by NORCEM, and the environmental cement was provided by CEMEX. The cement compositions will be described briefly below.

#### 3.1.1.1 Industry Cement

The Industry C-class cement used was provided by NORCEM [38]. The Industry C-class cement is the most common cement used on the top section of the wellbore to resist and prevent the wells from collapsing because of its unique strength.

Table 3.1 Properties of the utilized Industry C-class cement [38]

| ***Properties*** | | **Declared values** | **Requirements according to NS-EN 197-1:2011** |
|---|---|---|---|
| *Fineness (Blaine $m^2/kg$)* | | 550 | |
| *Specific weight ($kg/dm^3$)* | | 3.13 | |
| *Soundness (mm)* | | 1 | ≤ 10 |
| *Initial setting time (min)* | | 110 | ≥ 45 |
| *Compressive strength (MPa)* | 24 hrs | 33 | |
| | 48 hrs | 41 | ≥ 30 |
| | 7 days | 50 | |
| | 28 days | 59 | ≥ 52.5 |
| *Sulfate (% $SO_3$)* | | ≤ 4.0 | ≤ 4.0 |
| *Chloride (% $Cl^-$)* | | ≤ 0.085 | ≤ 0.10 |
| *Water soluble chromium (ppm $Cr^{6}+$)* | | ≤ 2 | ≤ 2 [1] |
| *Alkalis (% $Na_2O_{ekv}$)* | | 1.3 | |
| *Clinker (%)* | | 96 | 95-100 |
| *Minor additional components (%)* | | 4 | 0-5 |

### 3.1.1.2 Environmental Cement

The environmental cement used was provided by CEMEX [39]. In Norway, it is paid a lot of attention to the environment which makes it a very big concern to the Norwegian society. The environmental cement is prepared and utilized in an environmentally way which can help the Norwegian society to relief their concerns about environment when it comes to cements. It also has a great strength which can make it be considered to become a candidate cement for use in the top section of a wellbore in the oil industry.

Table 3.2 Chemical and physical composition of the utilized environmental cement [39]

| ***Chemical data*** | | **Wt%** |
|---|---|---|
| *Calcium* | (CaO) | 56 |
| *Silicon* | ($SiO_2$) | 25 |
| *Aluminium* | ($Al_2O_3$) | 6.3 |
| *Iron* | ($Fe_2O_3$) | 2.1 |
| *Magnesium oxide* | (MgO) | 4.0 |
| *Sulfate* | ($SO_3$) | 3.1 |
| *Potassium* | ($K_2O$) | 0.82 |
| *Sodium* | ($Na_2O$) | 0.31 |
| *Sodium oxide Equivalent* | ($Na_2O_{ekv}$) | 0.85 |
| *($C_3A$)* | | 5.3 |
| *Loss of glow* | | 1.7 |
| *Insoluble residue* | | 0.6 |
| *Water soluble Chloride* | ($Cl^-$) | 0.07 |
| *Water soluble Chromium* | Cr(VI) | < 2 mg/kg |
| ***Physical data*** | | |
| *Fineness (Blaine $m^2/kg$)* | | 460 m2/kg |
| *Density* | | 3.06 g/cm3 |
| *Bulk density* | | 1.1 g/cm3 |
| *Proportion slag* | | Ca 33% |
| *Binding time* | | 170 min |
| *Expansion* | | 1.0 mm |
| *Compressive strength* | 1 d | 16 MPa |
| | 2 d | 28 MPa |
| | 28 d | 59 MPa |

#### 3.1.1.3 Portland G-class Cement

The Portland G-class cement was obtained from NORCEM Co., Ltd. (Stavanger, Norway). The Portland G-class cement is the most commonly oil well cement. In accordance with API SPEC 10A/NS-EN ISO 10426-1 [38], the G-class cement is tested having a higher sulfate resistance. The chemical composition and the physical properties of the cement are provided in Table 3.3 and 3.4.

Table 3.3 Physical properties of Portland cement [38]

| Density (lb/gal) | Surface Area ($m^2$/kg) | Max. Consistency Bc | Thickening time Min |
|---|---|---|---|
| 16 | 317 | 13 | 108 |

Table 3.4 Chemical compositions of Portland cement (*I.R = Insoluble residue) [38]

| Cr(VI) | $SO_3$ | $C_3A$ | $C_2S$ | $C_4AF+2C_3A$ | $Na_3O$ | MgO | I.R* | Loss on Ignition |
|---|---|---|---|---|---|---|---|---|
| 0.00 | 1.73% | 1.7% | 55.6% | 15.2% | 0.48% | 1.43 | 0.1% | 0.79% |

### 3.1.2 Description of Nanoparticle

To investigate the effect of nanoparticles on the cements described in the previous section, we used two types of nanoparticles in water solution namely, colloidal silica nanoparticle solution and titanium oxide nanoparticle solution. The description of the nanoparticles will be presented below.

#### 3.1.2.1 Colloidal Silica Nanoparticle Solution

In this thesis a colloidal silica solution with a concentration of 50wt% suspension in $H_2O$ is used [40]. The solution has a density of 1,4 g/mL at 25°C with a pH ranged from 9,0 - 10,5. The nanoparticles utilized was purchased in solution form from Merck Life Science AS/Sigma Aldrich Norway AS and US Research Nanomaterials, Inc.

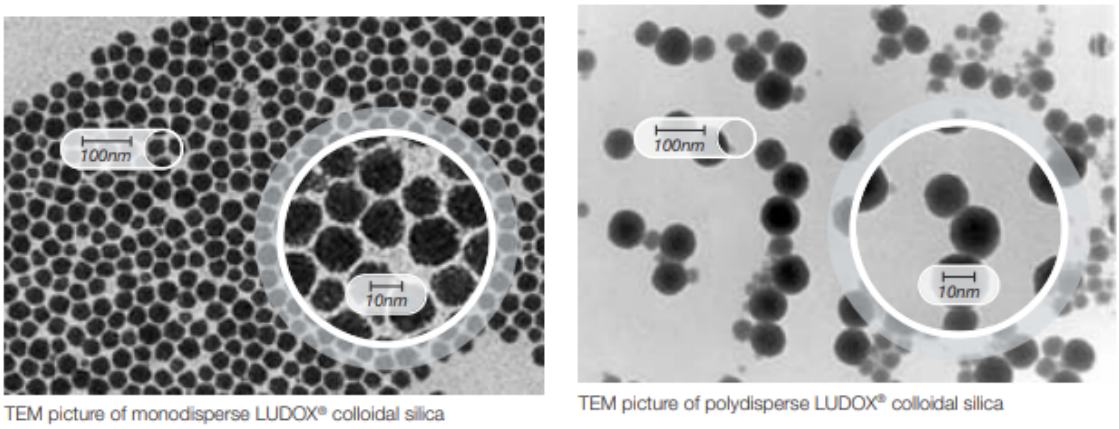


Figure 3.1 TEM picture of monodisperse and polydisperse LUDOX colloidal silica [40]

### 3.1.2.2 Titanium Oxide Nanoparticle Solution

In this thesis rutile-titanium oxide solution with a concentration of 15wt% suspension in $H_2O$ is used [41]. The nanoparticle suspensions are anatase aqueous dispersions with a particle size which ranges from 5-15nm. The nano-solution was purchased from the US Research Nanomaterials, Inc.

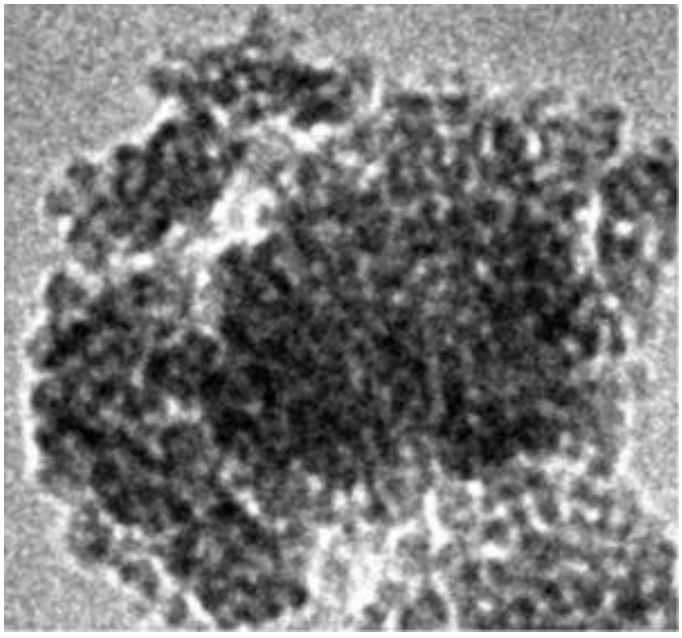

Figure 3.2 TEM picture of titanium oxide [41]

### 3.1.3 Characterization Methods

The characterization methods of the cement plug specimens are summarized in figure 3.3. The first phase of testing is non-destructive tests, where the samples are characterized through mass absorption, ultrasonic, rheology, and heat development. The second phase is mechanical destructive test with uniaxial compressive and Brazilian tests.

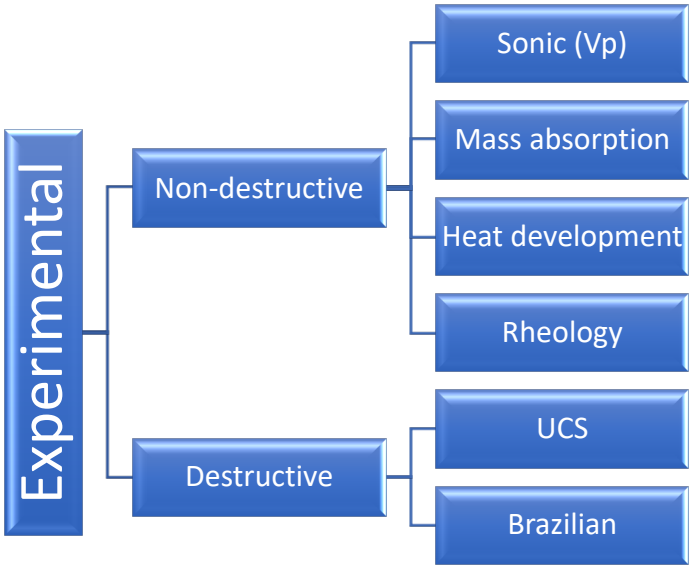


Figure 3.3 Scope of experimental work

#### 3.1.3.1 Compressive Strength

Uniaxial compressive strength is the strength measurement of a material to resist compressive loading until it fractures. It is one of the oldest methods used in destructive testing to compute the compressive strength of a material. Although, compressive strength can also be computed through non-destructive tests as well.

Figure 3.4 illustrates the Zwick apparatus which was used to run series of tests. The software program testXpert II is connected to the apparatus and the compressive data is logged. The start position is fixed according to the height of the specimen and then the specimen is firmly placed and centralized between those two loading plates to be crushed. Before running the test, the force is set to zero and then started. During testing, the axial load is continuously applied on the plug until it crushes the specimen. Figure 3.5 shows the uniaxial compressive stress – strain test result.

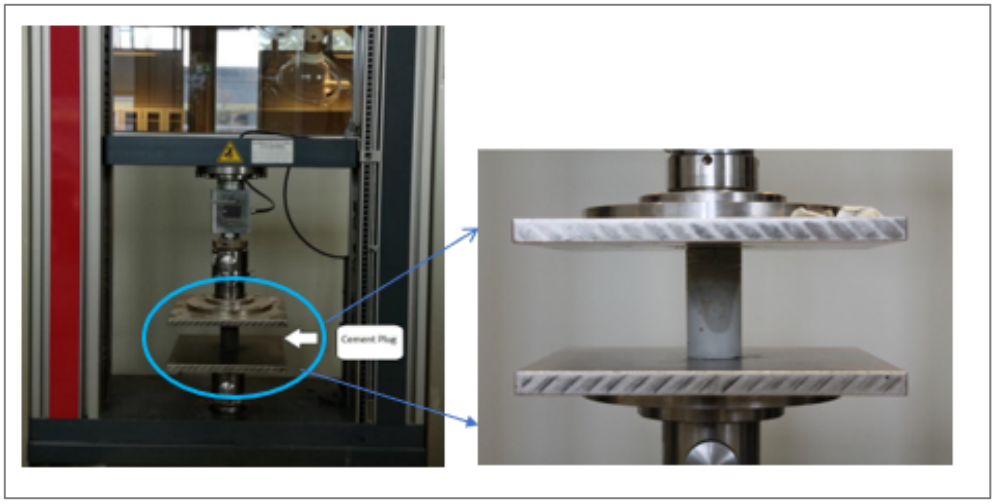

Figure 3.4 Zwick Z020 apparatus for destructive compressive testing

The uniaxial compressive strength (UCS) is calculated by dividing the force required to crush the cement plug specimens by the cross-sectional area of the specimens [42].

$$UCS = \frac{F_{max}}{A} \qquad 3.1$$

Where;

- $UCS$ is the Uniaxial compressive strength ($MPa$)
- $F_{max}$ is the force at the time of failure (N)
- $A$ is the cross-sectional area of the specimen ($mm^2$)

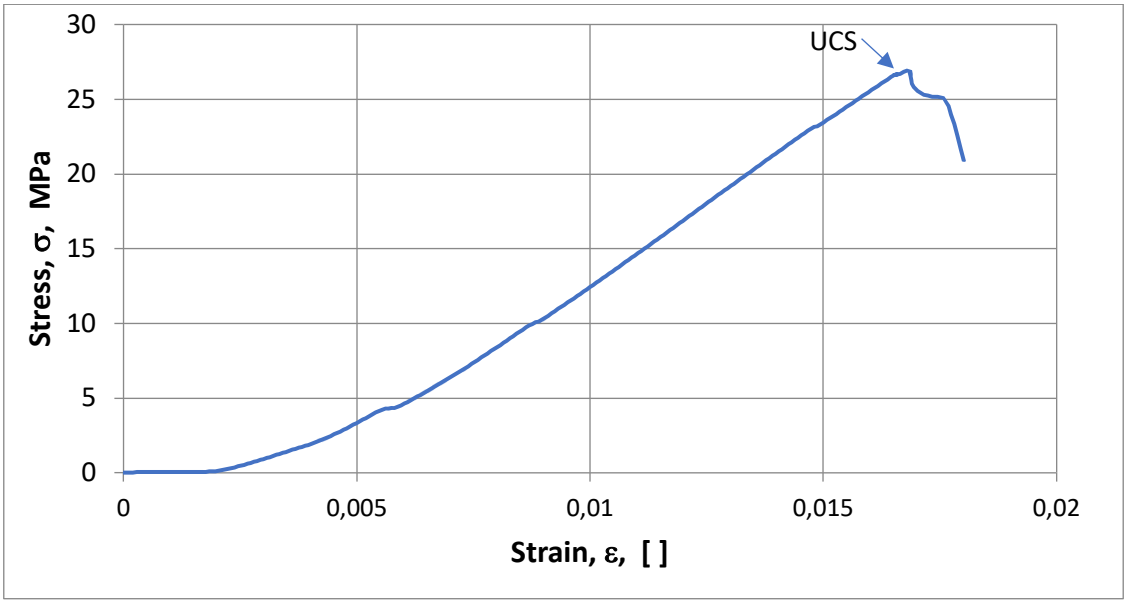


Figure 3.5 Illustration of the Ultimate tensile strength determination from uniaxial stress - strain test result

### 3.1.3.2 Brazilian Tensile Test

Brazilian or splitting tensile strength is the maximum stress a material can resist under axial loading until it induces physical deformation along two axials lines. Compressive load is the most frequently stress subjected to structures, while the value of the tensile strength is of practical significance in slab design, shear strength, and resistance to cracking, because cracking is due to tensile failure regardless of loading or environmental conditions. The value of tensile strength and compressive strength is closely related with a low magnitude than the compressive strength [42].

The tensile strength was calculated with the following equation [42].

$$\sigma_t = \frac{2P}{\pi DL} \qquad 3.2$$

Where;

- $\sigma_t$ is the tensile strength ($\frac{N}{m^2}$)
- P is the applied force at the moment the sample breaks (N)
- D is the sample's diameter (m)
- L is the sample's length (m)

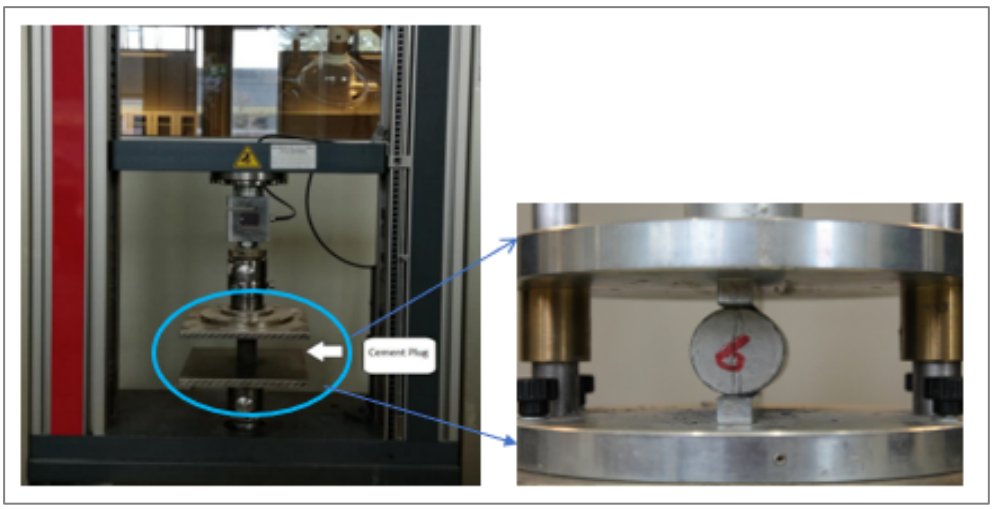

Figure 3.6 Zwick Z050 apparatus for destructive tensile testing

### 3.1.3.3 Sonic Travel Time

Ultrasonic inspection is a non-destructive method of investigating the materials ability to transmit mechanical sonic wave through its body. If structure contains cracks, pores, trapped air, and not very well cemented, the travel time will be higher than the very well compacted and strong materials. During testing as shown in Figure 3.6, the ultrasonic pulses are emitted through the specimens, and then the travel time from the transmitter to receiver on the other side of the bulk material is recorded.

The compressional wave velocity is calculated from the length of the plug specimen and the travel time as

$$V_p = \frac{l}{t} \qquad 3.2$$

Where;

- $V_p$ is the P-wave's velocity (m/s)
- l is the length of a plug (m)
- t is the P-wave's travel time through a plug (sec)

Figure 3.6 shows the photograph picture of the CNS Farnell Pundit 7 device used to measure the travel time through the cement specimens. Before testing, the measuring equipment is calibrated with calibration plug having the travel time of 25 μs. The surface of the plugs at the bottom and at the top should have very good contact with the source and the receiver transducer metallic surfaces.

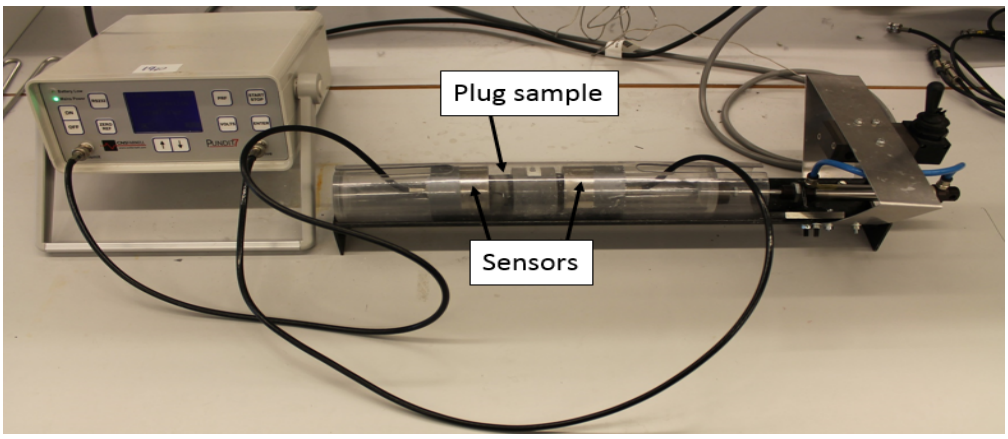


Figure 3.7 CNS Farnell Pundit 7 device for sonic travel time measurement

### 3.1.3.4 Fluid Absorption

The internal structure of the plugs is quantified by the degree of the porosity and the permeability that describe the ability of the plugs to allow fluid flow. However, due to the absence of measuring equipment, in this thesis, the internal structure is analysed indirectly by studying the mass absorption. The percentile changes of mass absorbed after the plugs have been immersed in water with respect to the before immersion mass is calculated as:

$$\Delta M = \frac{M_t - M_0}{M_0} * 100 \qquad 3.4$$

Where;

- $\Delta M$ is the change of mass (%)
- $M_0$ is the mass before immersed in water
- $M_t$ is the mass after the plug were taken out of the water

### 3.1.3.5 Elastic Properties of Plugs

The compressional wave velocity is related with the bulk and shear modulus [42].

$$v_p = \sqrt{\frac{K + \frac{4}{3}G}{\rho}} \qquad 3.5$$

Where;

- K is the bulk modulus, (Gpa)
- G is the shear modulus, (Gpa)
- $V_p$ is the P-wave's velocity $(m/s)$
- $\rho$ is the density $(kg/m^3)$

During non-destructive test, we measure the compressional wave velocity and the density of the plugs. From the above equation the modulus of elasticity is estimated as:

$$M = K + \frac{4}{3} * G = V_p^2 * \rho * 10^{-9} \qquad 3.6$$

Where;

- $M = K + \frac{4}{3} * G$ = Dynamic modulus of elasticity
- K = bulk modulus, which is the measure of the resistance of the material for hydrostatic loading (GPa)
- G is the shear modulus, which is the measure of the resistance of the material for the shear loading (GPa)

### 3.1.3.6 Youngs´s Modulus

For further evaluation of the effect of nanoparticles, the elastic/stiffness and energy absorbing capacity of the plugs were quantified.

The Young´s modulus is the measure of the stiffness of solid materials. As illustrated in Figure 3.8, the Young´s modulus of the material is calculated from the slope of the linear elastic region of the stress-strain test as [43].

$$E = \frac{\Delta\sigma}{\Delta\varepsilon} \qquad 3.7$$

Where; E is the Young´s modulus (MPa), Δσ is the change in stress, and Δε is the change in strain.

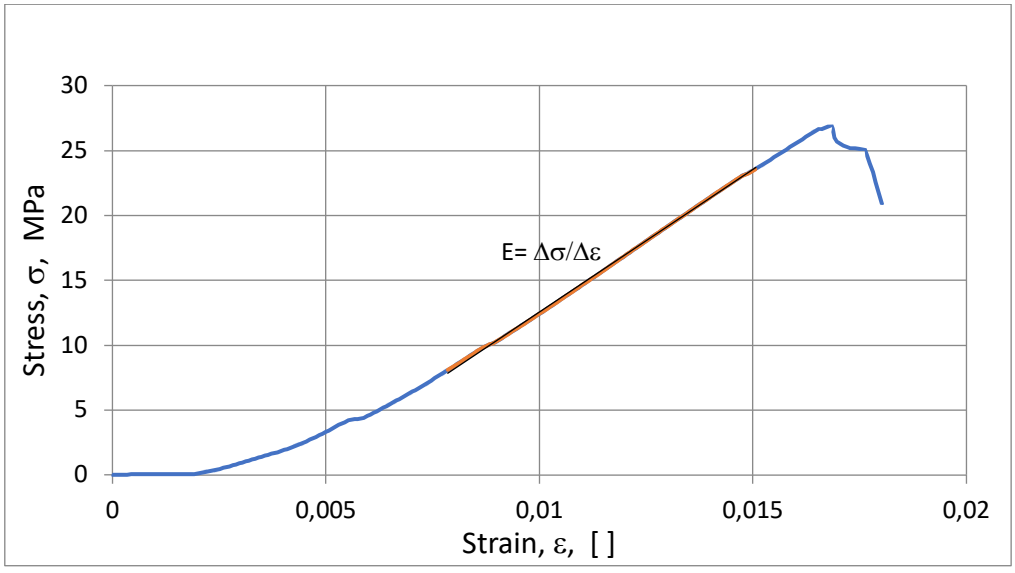


Figure 3.8 Illustration of Young´s modulus determination from the uniaxial stress - strain test result

### 3.1.3.7 Resilience

Resilience of the material is the energy absorbed by the material until reaching the yield stress quantified to compare the plugs [43]. The yields stress of the test is not shown clearly and assumed that the value is at the Uniaxial compressive stress. As shown in Figure 3.9, the resilience of the plugs is estimated by integrating the area under the ultimate strength as:

$$R = \sum \frac{(Strain(i+1) - Strain(i)) * (Stress(i+1) + Stress(i))}{2} \quad 3.8$$

Where;

- R is the resilience ($J/m^3$)
- Stress (i) and Stress (i+i) (Pa) are the stresses of the trapezoid, where corresponding are strain (i) and strain (i+1) (m/m).

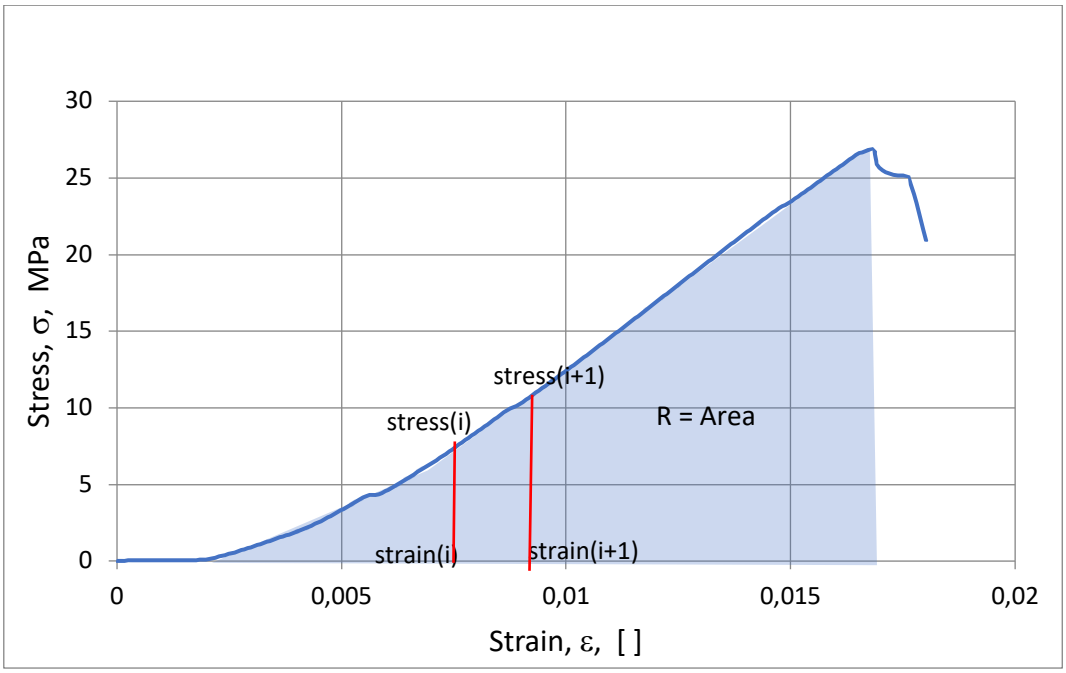


Figure 3.9 Illustration of Resilience determination from the area under the maximum uniaxial stress - strain test result

### 3.1.3.8 Rheology of Cement Slurry

Figure 3.10 shows the viscometer used to measure the viscosity of cement slurries. The measurements are at RPM of 300, 200, 100, 6, and 3 Revolution per minute (RPM). There are several rheological models that are used for describing the rheology of cements. Among others, the Casson rheological model can be mentioned. The Casson model is two parameter models, which describe visco-elastic fluids at high and low shear rate. The model is a function of Yield stress and plastic viscosity. Mathematically, the model is expressed as [4].

$$\tau^{0.5} = \tau_c^{0.5} + \mu_c^{0.5}\gamma^{0.5} \quad \text{For} \quad \tau < \tau_c \tag{3.9}$$

$$\gamma = 0 \quad \text{For} \quad \tau \geq \tau_c \tag{3.10}$$

Where;

- $\tau$ is measured shear stress (Pa)
- $\tau_c$ is yield stress (Pa)
- $\mu_c$ is viscosity (Pa.s)
- $\gamma$ is shear rate ($sec^{-1}$)

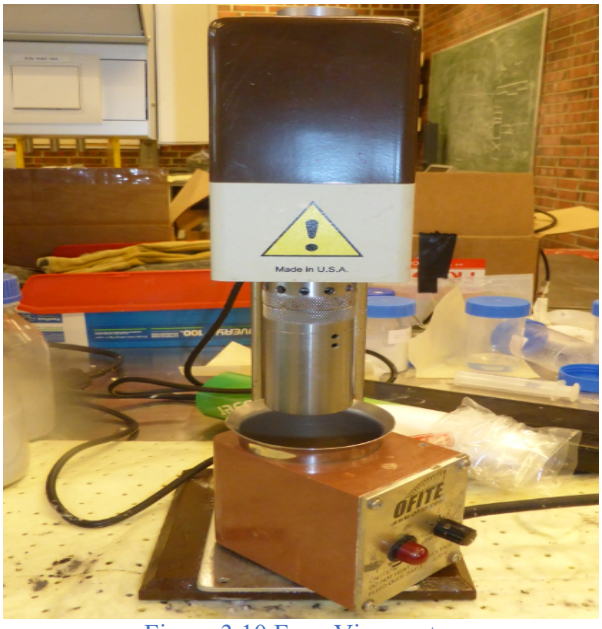


Figure 3.10 Fann Viscometer

#### 3.1.3.9 Heat development

An exothermic reaction occurs when cement is in contact with water. The release of heat will increase the temperature of cement during hydration process. Based on the Uniaxial compressive strength test results, the optimum nanoparticle concentration and its effect will be compared with the neat cement slurries. Figure 3.11 and Figure 3.12 show the cement slurries placed in insulated compartments and connected with temperature sensors.

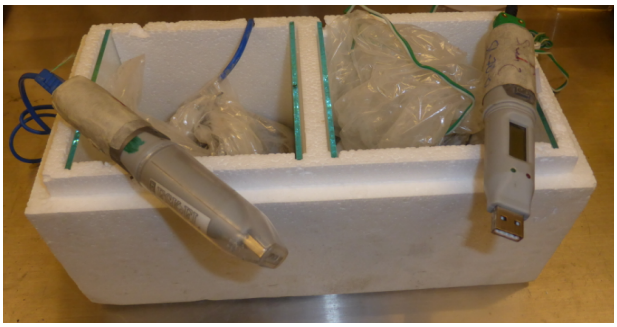

Figure 3.11 Temperature sensors immersed in cement slurries

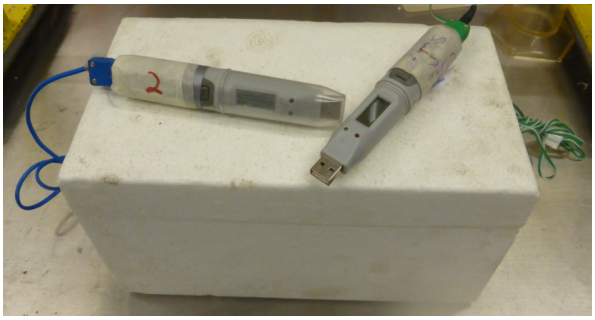

Figure 3.12 Cement slurries being locked on the top during three days temperature logging

### 3.1.4 Experimental Test Matrix Design

#### 3.1.4.1 Slurry and Cement Moulds

As shown in Figure 3.13, the cement slurry for the synthesis of cement plugs is molded in plastic cylinders having a dimension of 34.50mm inner diameter and 69.25mm length. This gives the length to diameter ratio of 2.0, which are the recommended sizes [42].

Figure 3.13 Cement mold cup, cement filled and top unpolished, cement top polished for testing

As shown in the figure, the top of the cement plug has uneven surface. While the plugs were within the plastic cup, the top surface was polished with sandpaper in order to make it flat. Before destructive test, the samples were characterized with non-destructive tests. During mass absorption, the samples were first immersed in water for consecutive days until the plugs are being saturated. Mass and sonic travel times are measured.

For the modelling purpose, the non-destructive tests are measured the day when the plugs are being tested with destructive test. The plugs are aged and tested at 3 days, 7 days, and 28 days. The experimental tests were designed based on the three cements. In the following the design background along with the compositions will be presented.

### 3.1.4.2 Test Matrix 1- Investigation of Silica on C-class Cement

As reviewed, the top section of a well requires a higher strength cement. Being informed to know from Oil company that the top section cement used in the NCS is industry cement, which is C-class. The first test matrix is therefore designed to investigate the effect of nano-silica solution on the C-class cement. The composition of the slurry is water/cement ratio of $100/178.57 \approx 0.56$.

A total of 5 nano-based cement plugs and one nanoparticle free plug were synthesized. For statistical purpose, four samples were made for plug #1-5. To evaluate the impact of the higher concentration of nanoparticles, plug #6 with 0.84wt% concentration was synthesized having only one sample.

Table 3.5 shows the amount of water, cement, and silica nanoparticles for test matrix 1. The nano-free plugs are referred as a reference of control, with which the nano treated cements plugs will be compared with. To maintain the concentration of fluids (i.e., 100g), as the concentration of nano-solution increases, the same amount of water was reduced.

During cement slurry preparation, 178.57g cement is blended with 100g fluid. The mixture is mixed with hand until the solution becomes homogenous. The slurry was then poured into the plastic cup. While filling up the slurry, the cup was repeatedly pounded against a flat surface in order to compact and prevent the possible air from being trapped.

Table 3.5 Test Matrix 1

| **Plug (#)** | **Freshwater (g)** | **Cement (g)** | **$SiO_2$ (g) (aq) (50% sol)** | **% $SiO_2$ by weight of cement (% bwoc)** | #of samples |
|---|---|---|---|---|---|
| **1** | 100 | 178.57 | 0.00 | 0wt% | 4 |
| **2** | 99.75 | 178.57 | 0.25 | 0.14wt% | 4 |
| **3** | 99.50 | 178.57 | 0.50 | 0.28wt% | 4 |
| **4** | 99.25 | 178.57 | 0.75 | 0.42wt% | 4 |
| **5** | 99.00 | 178.57 | 1.00 | 0.56wt% | 4 |
| **6** | 98.50 | 178.57 | 1.50 | 0.84wt% | 1 |

### 3.1.4.3 Test Matrix 2- Investigation of Silica on Environmental Cement

The design idea here is the possibility of using environmental cement for the oil and gas well provided that it qualifies the industry requirement. At this level of research due to time, detail investigation was not conducted except for the evaluation of Silica nanoparticle on the environmental cement. Up to the knowledge of the author, this type of study is not found within the intended research period.

The slurry was synthesized with a water/cement ratio of $100/192.3 \approx 0.52$. For statistical analysis purpose, a total of eight samples were synthesized. Four of the samples were used for the Uniaxial compressive strength test and the rest of the samples were used for Brazilian test. In table 3.6, only the concentration of the compositions is presented.

Table 3.6 Test Matrix 2

| Plug (#) | Freshwater (g) | Cement (g) | Silica(g) (aq) | % Silica (aq) by weight of cement (bwoc) | Number of samples |
|---|---|---|---|---|---|
| **1** | 100 | 192.3 | 0.00 | 0wt% | 8 |
| **2** | 99.75 | 192.3 | 0.25 | 0.13wt% | 8 |
| **3** | 99.50 | 192.3 | 0.50 | 0.26wt% | 8 |
| **4** | 99.25 | 192.3 | 0.75 | 0.39wt% | 8 |

### 3.1.4.4 Test Matrix 3- Silica and Titanium Oxide Hybrid on G-class Cement

In test matrix 1 and 2, it is shown that silica improved the performance of the neat C-class and the environmental cement. To investigate if there is synergy between nanoparticles, the background best silica concentration was blended with different concentrations of Titanium oxide. For this, the effect of hybrid is tested on G-class cement.

The water cement ratio according to API G-class cement is 100g water/227.27g cement ≈ 0.44. For each sample two plugs were synthesized for the average value. Table 3.7 presents the composition of the $SiO_2$ & $TiO_2$ solutions.

Table 3.7 Test Matrix 3

| **Plug (#)** | **Freshwater (g)** | **Cement (g)** | **$SiO_2$ (g) (50% sol)** | **TiO2 (g) (3%sol)** | **Number of samples** |
|---|---|---|---|---|---|
| **1** | 100 | 227.27 | 0.0 | 0.0 | 2 |
| **2** | 99.3 | 227.27 | 0.6 | 0.1 | 2 |
| **3** | 99.2 | 227.27 | 0.6 | 0.2 | 2 |
| **4** | 99.1 | 227.27 | 0.6 | 0.3 | 2 |

# 4 RESULTS AND DISCUSSION

This chapter presents the experimental test results obtained from the three test matrices. Both the destructive and non-destructive results of the nano-treated slurries are compared with the nano-free neat cement. The results presented in this chapter are the average values of the samples.

## 4.1 Effect of $SiO_2$ on C-class - Industry Cement

As reviewed early, $SiO_2$ nanoparticle improved the mechanical, filtrate and enhance the hydration rate that reduced undesired wait on cement of the G-class [26]. In this thesis, the impact of $SiO_2$ on C-class is experimentally investigated. The samples are aged 3 days, 7 days, and 28 days. However, for the analysis, the results presented are the 28 days curing. The 3 days and 7 days test results are attached in Appendix.

### 4.1.1 Effect of $SiO_2$ on Fluid Absorption of C-class Cement

After the 28 days, the samples were first weighed before immersion in water. The samples were then again weighed after three days in water. The mass of fluid (or volume) absorbed in the plugs are calculated based on the difference between the mass of the plugs before and after water absorption. Figure 4.1 displays the percentile water absorption of the plugs. Results show that the fluid absorption decreases as the concentration of $SiO_2$ increases. This indirectly shows that the nanoparticles improved the internal structure of the plugs.

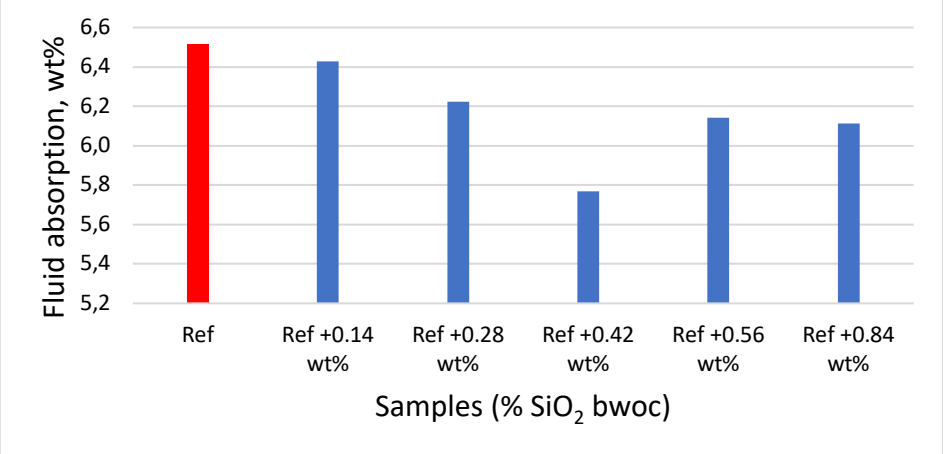


Figure 4.1 Effect of $SiO_2$ on water absorption of C-class cement

### 4.1.2 Effect of $SiO_2$ on the Modulus of Elasticity of C-class Cement

One of the NORSOK D-010 requirements that a cement should have is Ductile – (non-brittle). The modulus of elasticity (M = K + 4/3G) is the measurement which describes a substance´s ability to withstand mechanical loads/impact, which is the combined effect of the bulk modulus and the shear modulus. The bulk modulus is the resistance of the material for hydrostatic loading and the shear modulus is the resistance of the material for the shear or torsional loading. Figure 4.2 shows the Modulus of elasticity (M) of the plugs. As the concentration of $SiO_2$ increases, the Modulus of elasticity (M) increases compared to the nanoparticle free reference samples.

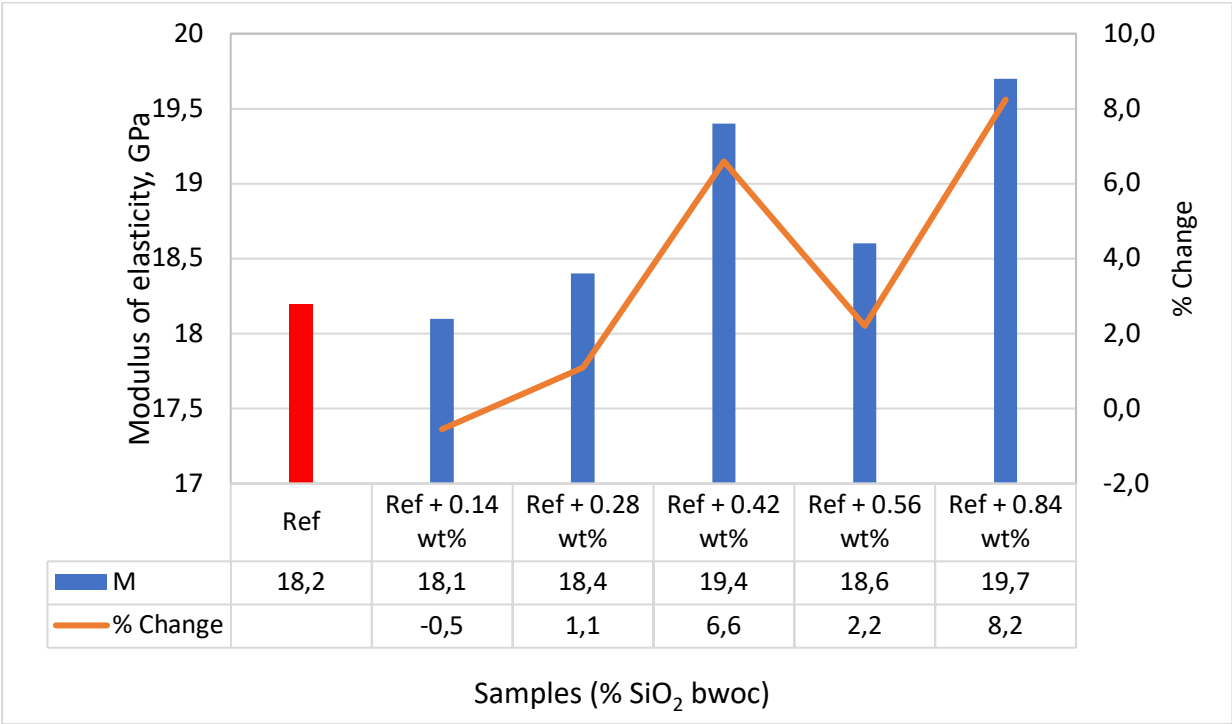


Figure 4.2 Effect of $SiO_2$ on the modulus of elasticity of C-class cement

### 4.1.3 Effect of $SiO_2$ on Uniaxial Compressive Strength of C-class Cement

The UCS of the plugs is obtained from the destructive test results. The UCS average values of the plugs after 28 days of curing are displayed in Figure 4.3. Results in general shows that all the addition of $SiO_2$ increases the UCS of the neat cement. However, the 0.28 %bwoc nanoparticle reduced the UCS. Up to this level of research the reason for the reduction was not investigated. There are several possible explanations for this among others, the sample might not have a perfect flat surface so that during testing a point load at local contact will generate a

huge stress and resulting an early failure. Moreover, the sample might have a trapped air in the plugs, which results in internal defect and it weakens the plugs load carrying capacity. The internal structure could have been inspected through scan electron microscope. Unfortunately, the equipment was down during this thesis work. Repeat test could also had provided answer if the result is repetitive. However, due to short research period, the nanoparticle concentration was not re-evaluated. Among the considered $SiO_2$, the 0.56 %bwoc increased the UCS of the neat cement by 17%.

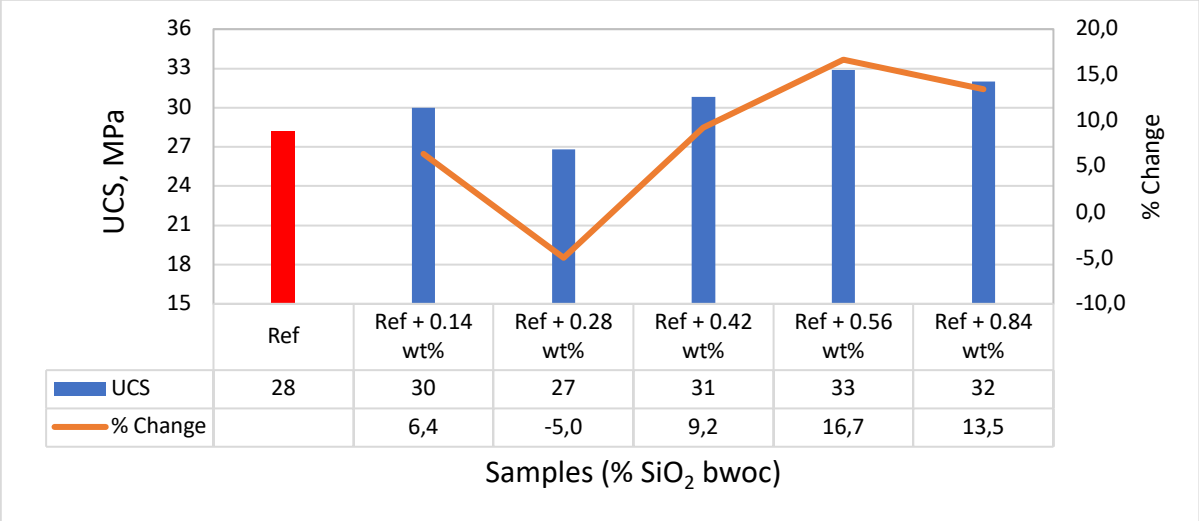


Figure 4.3 Effect of $SiO_2$ on the Uniaxial compressive strength of C-class cement

### 4.1.4 Effect of $SiO_2$ on Tensile Strength of C-class Cement

The tensile strength of the cement plugs was indirectly determined from the Brazilian test. Unlike the compression tests, only three nanoparticle blended plugs along with the reference were selected for the testing. Figure 4.4 shows the tensile test results. As shown, the test results trend is like the compressional strengths. It is interesting to observe that 0.28wt% $SiO_2$ produced a weaker tensile strength as observed for the compressional test result. This may be interpreted that the performance of $SiO_2$ is a non-linear effect and the reason for the weak effect can be investigated by the molecular level. However, due to the scan electron microscope and element analysis equipment failure, the samples were not analyzed further. Results from the test show that the 0.14wt% $SiO_2$ increased the tensile strength of the neat cement plug by 5.2%.

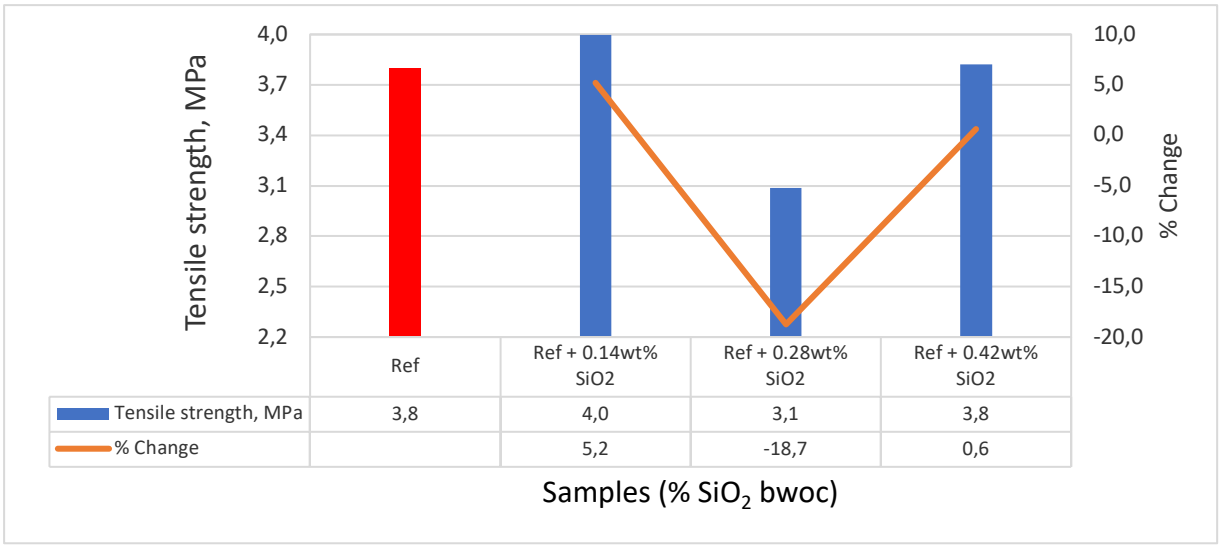


Figure 4.4 Effect of $SiO_2$ on Tensile strength of C-class cement

## 4.1.5 Effect of $SiO_2$ on Young´s Modulus (E) of C-class Cement

The Young´s modulus of the plugs was calculated from the linear elastic strain curve of the compression tests. Results in Figure 4.5 show that all the nano treated plugs Young´s moduli are higher than the neat cement plugs. This shows that the nanoparticles increase the cement grain-grain cementation and hence becomes stiffer. Among the nanoparticle systems, here again the 0.28wt% $SiO_2$ system relatively showed lower Young´s modulus.

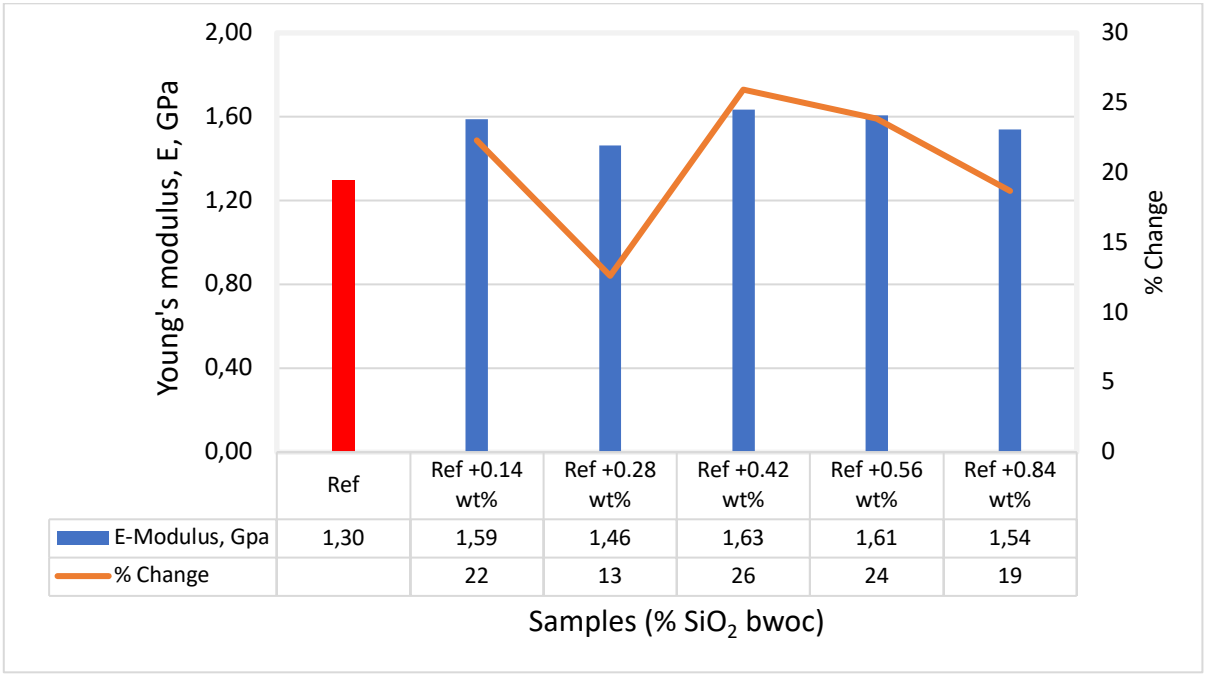


Figure 4.5 Effect of $SiO_2$ on Youngs modulus (E) of C-class cement

### 4.1.6 Effect of $SiO_2$ on Resilience of C-class Cement

The amount of energy absorbed by the cement plug until reaching to the higher stress is calculated by integrating the area under the stress strain. Figure 4.6 shows that except for the 0.28wt% $SiO_2$, all the nanoparticle concentrations exhibited a higher resilience as compared with the neat cement plug. As shown in the figure, the highest resilience is acquired from the concentration 0.14wt% $SiO_2$ by an increase of 63%, while the lowest resilience is acquired from the concentration 0.28wt% $SiO_2$ which decreases by a change of 22%.

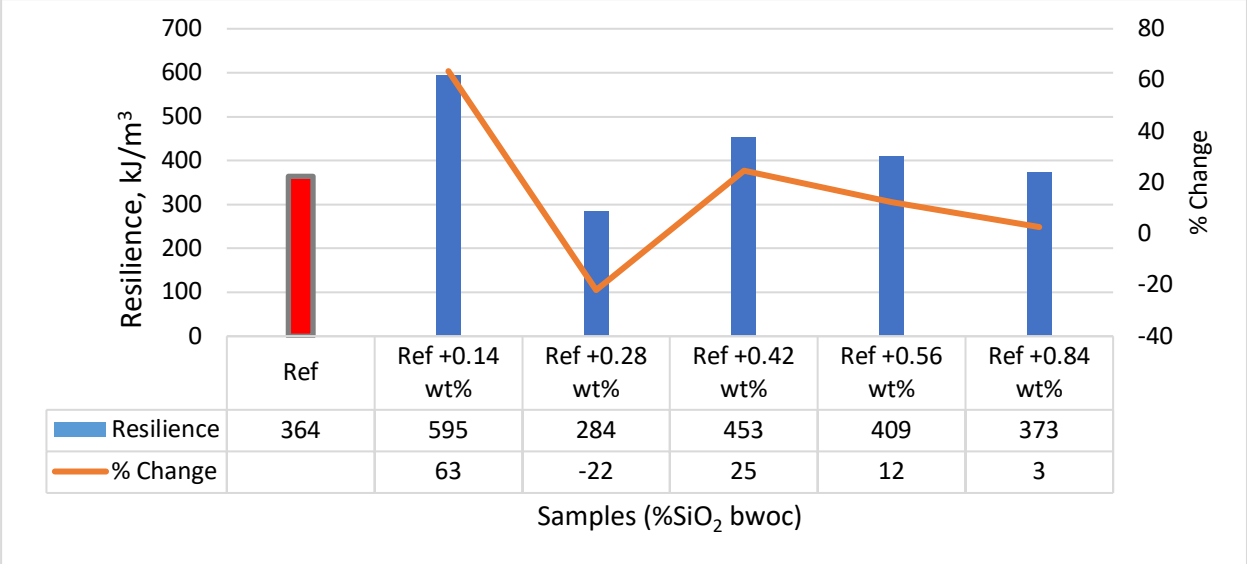


Figure 4.6 Effect of $SiO_2$ on Resilience of C-class cement

## 4.2 Effect of $SiO_2$ on Environmental Cement

Portland G-class cement is the commonly used oil well cement for well construction and plug and abandonment. C-class cement is used on the top section of the wellbore with the objective of providing strong structural integrity.

In this thesis the effect of $SiO_2$ on environmental cement was tested with the objective of evaluating the cement to be used as a candidate in the industry. The experimental design is provided in section §3.1.4.3.

### 4.2.1 Effect of $SiO_2$ on Fluid Absorption of Environmental Cement

Figure 4.7 shows the average water absorption of the plugs after 3 days of immersion in water. Results show that the addition of $SiO_2$ increased by 0-0.5wt% as compared with the neat cement. However, the increment is insignificant.

Comparing with the C-class cement (Figure 4.1), the percentile water absorption of the environmental cement is higher. It is also interesting to observe that the addition of $SiO_2$ reduced the water absorption of the C-class cement and increased in the environmental cement.

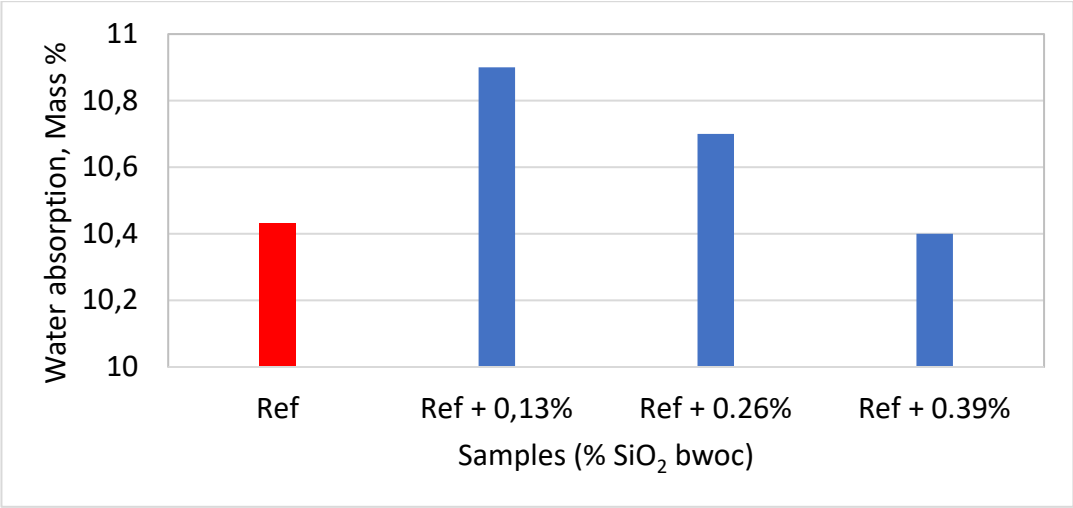


Figure 4.7 Effect of $SiO_2$ on water absorption of environmental cement

### 4.2.2 Effect of $SiO_2$ on the Modulus of Elasticity of Environmental Cement

Figure 4.8 displays the Modulus of elasticity (M) behavior of the plugs where we can observe that M increases with the addition of $SiO_2$ concentrations, and with the highest change by 10%.

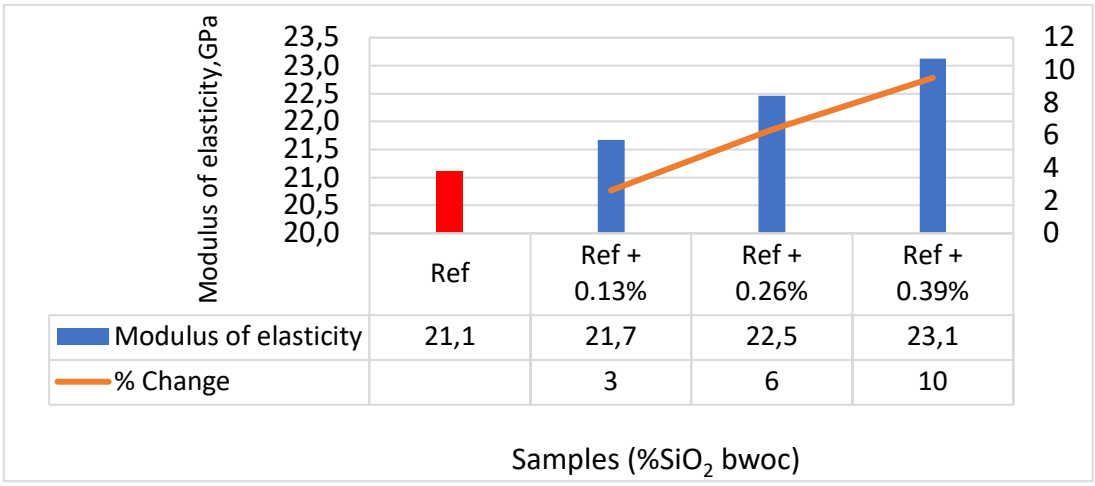


Figure 4.8 Effect of $SiO_2$ on the modulus of elasticity of environmental cement

### 4.2.3 Effect of $SiO_2$ on Uniaxial Compressive Strength of Environmental Cement

Figure 4.9 shows the effect of $SiO_2$ on the UCS of the environmental neat cement. Results show that as nanoparticle concentration increase the UCS strength increases. As the nanoparticle increases from 0.13wt%, 0.26wt%, and 0.39wt% $SiO_2$ bwoc, the UCS increase by 50%, 47%, and 27% respectively. Comparing with the C-class cement, the environmental cement exhibited a higher UCS. It can also be observed that the 0.56wt% $SiO_2$ increased the UCS of C-class cement by 17% and the 0.13wt% $SiO_2$ increased the UCS of the environmental cement by 50%. Moreover, the neat C-class UCS is 28 MPa and the neat environmental cement UCS is 27 MPa, which have nearly comparable strength for the considered WCR. However, the impact of $SiO_2$ is higher in the environmental cement than in the C-class cement. The different effects are due to the chemical interaction between the ingredients of the C-class and environmental cement with the $SiO_2$ nanoparticle. The analysis for the different performances was not conducted due to scan electron microscope (SEM) failure.

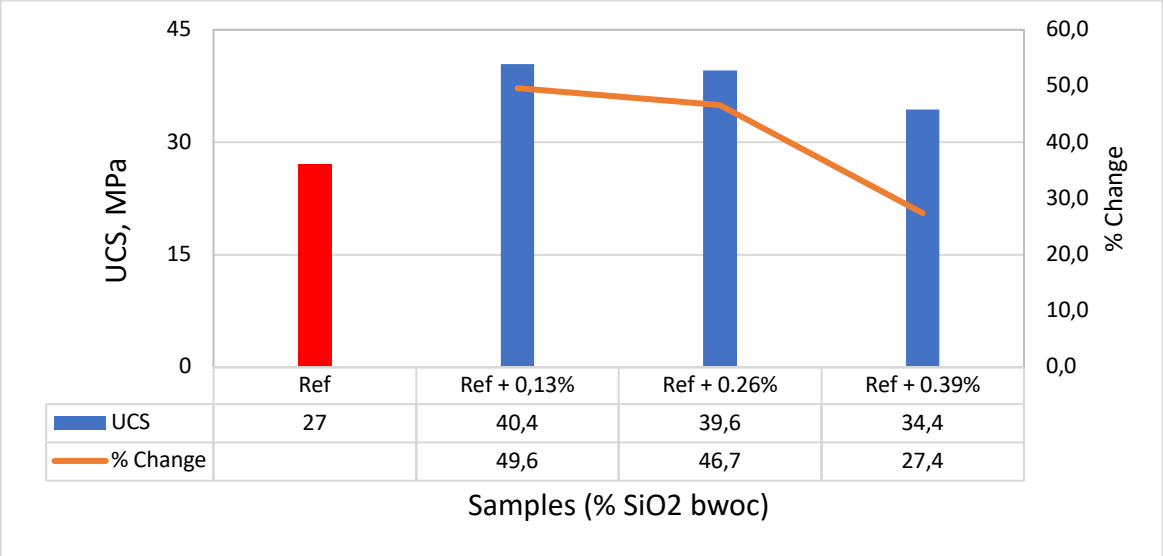


Figure 4.9 Effect of $SiO_2$ on the Uniaxial compressive strength of environmental cement

### 4.2.4 Effect of $SiO_2$ on Young´s Modulus of Environmental Cement

Figure 4.10 presents the calculated average values of the Young´s modulus of the plugs. The effect of $SiO_2$ concentration increasing showed a similar trend like the UCS of the plugs. Results showed that as the nanoparticle increases from 0.13wt%, 0.26wt%, and 0.39wt% $SiO_2$ bwoc, the Young´s modulus increase by 15%, 19%, and 5% respectively.

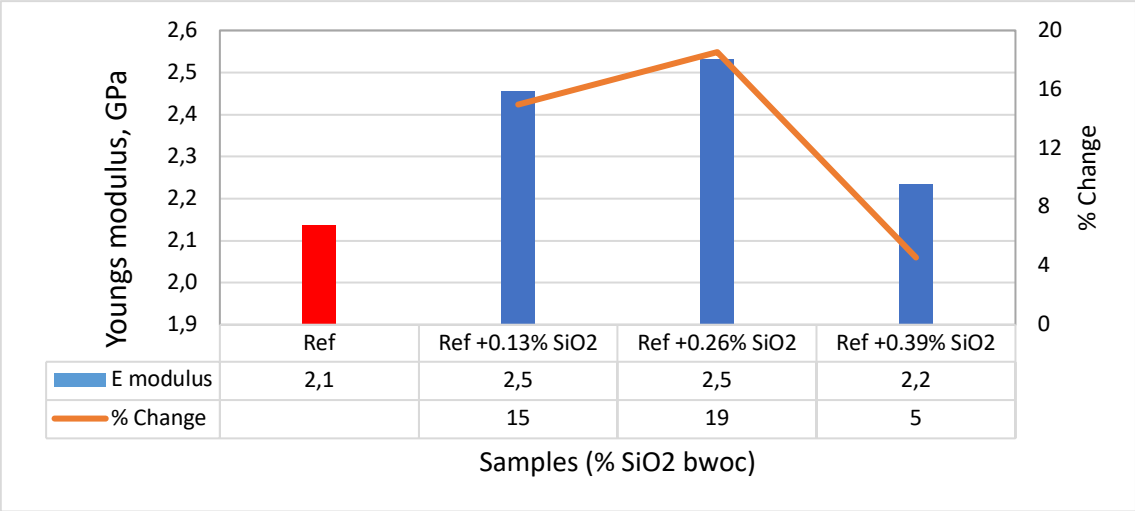


Figure 4.10 Effect of $SiO_2$ on the Youngs modulus of environmental cement

## 4.2.5 Effect of $SiO_2$ on Resilience of Environmental Cement

Figure 4.11 shows the amount of energy absorbed by the neat and the nanoparticle blended environmental cements until reaching the maximum load carry capacity. Here again, all the nanoparticle concentrations exhibited a higher resilience as compared with neat cement plug. As the nanoparticle increases from 0.13wt%, 0.26wt%, and 0.39wt% $SiO_2$ bwoc, the resilience of the neat cement increased by 62%, 46%, and 43% respectively.

The lowest concentration of $SiO_2$ has shown a significant impact on the resilience of the C-class and the environmental cements. The 0.14wt% $SiO_2$ increased the resilience of the neat C-class cement by 63% and the 0.13wt% $SiO_2$ increased the resilience of the neat environmental cement by 62%.

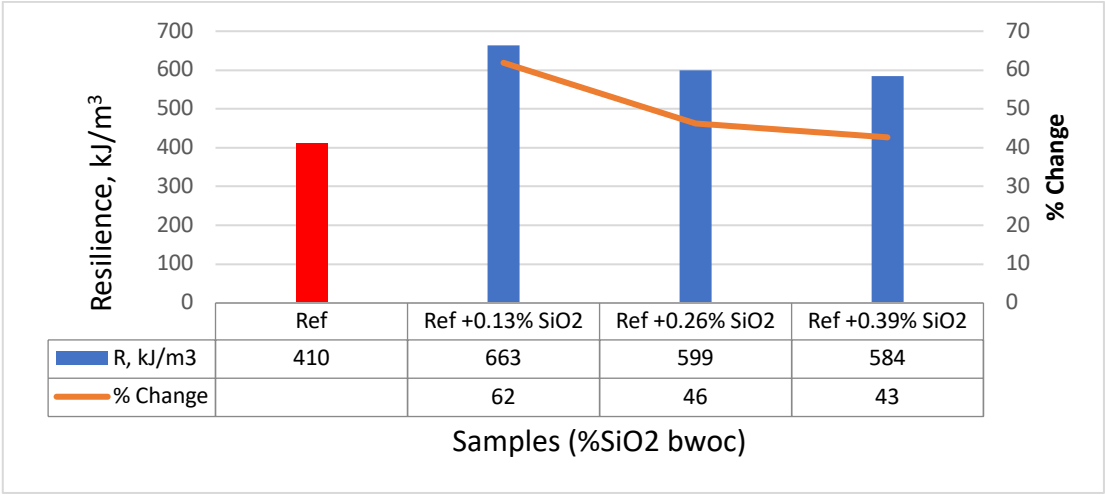


Figure 4.11 Effect of $SiO_2$ on the Resilience of environmental cement

## 4.3 Effect of $SiO_2$ - $TiO_2$ on Portland Cement - G-class cement

Portland G-class cement is the most common used oil well cement in the industry. As reviewed in Table 2.3, several investigators have experimentally investigated the single effect of $SiO_2$ and $TiO_2$ nanoparticles on G-class cement. However, up to the knowledge of this thesis author, the hybrid $SiO_2$/$TiO_2$ effect on G-class is not found. Therefore, unlike the previous experiments (Test matrix 1 and 2), this section evaluates the combined effect of $SiO_2$ and $TiO_2$ on the mechanical and elastic properties of Portland G-class cement. The test design is provided as Test Matrix 3, in Table 3.7. The nano blending was formulated by fixing 0.264% $SiO_2$ bwoc concentration and varying the concentration of $TiO_2$ as 0.044%, 0.088, and 0.132% bwoc.

### 4.3.1 Effect of $SiO_2$ - $TiO_2$ on Fluid Absorption of Portland Cement

Figure 4.12 shows the water absorption of the plugs after being immersed in water for 3 days. Comparing with the nano-free neat cement plug, all the nanoparticle blended slurries absorb more water by 0-0.3wt%, which is insignificant.

On the other hand, comparing with C-class cement (Figure 4.1) and environmental cement (Figure 4.7), the lowest water absorption is observed in G-class cement.

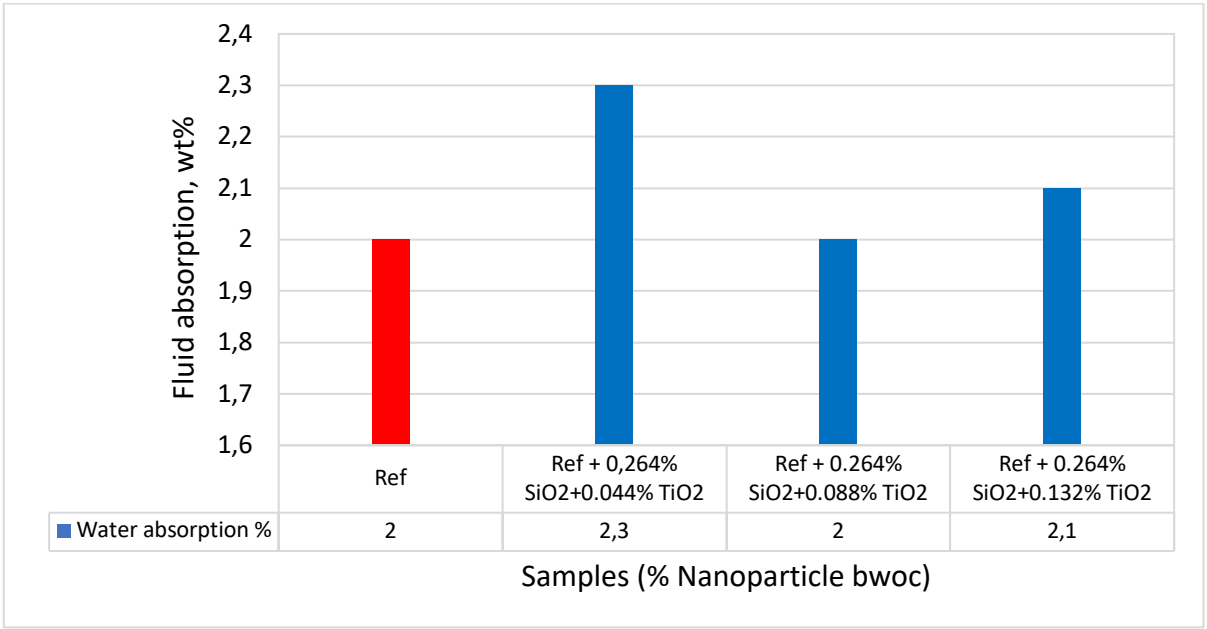


Figure 4.12 Effect of SiO2 - TiO2 hybrid on water absorption of G-class cement

### 4.3.2 Effect of $SiO_2$ - $TiO_2$ on Uniaxial Compressive Strength of Portland Cement

Figure 4.13 displays the effect of $SiO_2$ - $TiO_2$ hybrid on the UCS of the G-class Portland cement. Results show that all the nano-based plugs have a higher UCS strength compared to the neat cement. As the titanium oxide increases from 0.044wt%, 0.088wt%, and 0.132wt% $TiO_2$ bwoc, the UCS increase by 9%, 8%, and 1% respectively.

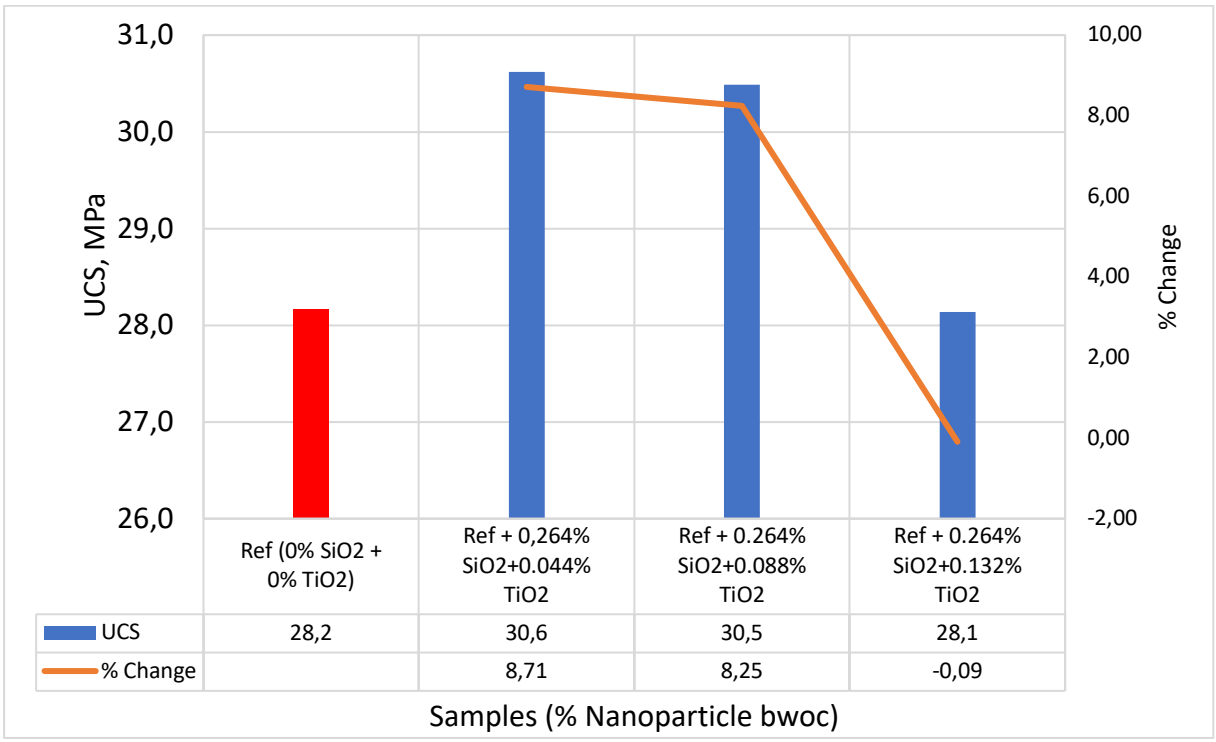


Figure 4.13 Effect of $SiO_2$ - $TiO_2$ hybrid on the Uniaxial compressive strength of G-class cement

### 4.3.3 Effect of $SiO_2$ - $TiO_2$ on Young´s Modulus of Portland Cement

The calculated average values of the Young´s modulus of the plugs are presented in Figure 4.14. It is shown that all the nano-based plugs have a higher Young´s modulus compared to the neat cement plugs. As the nanoparticle increases from 0.044wt%, 0.088wt%, and 0.132wt% $TiO_2$ bwoc, the Young´s modulus increases by 5.4%, 1.68%, and 1.95% respectively.

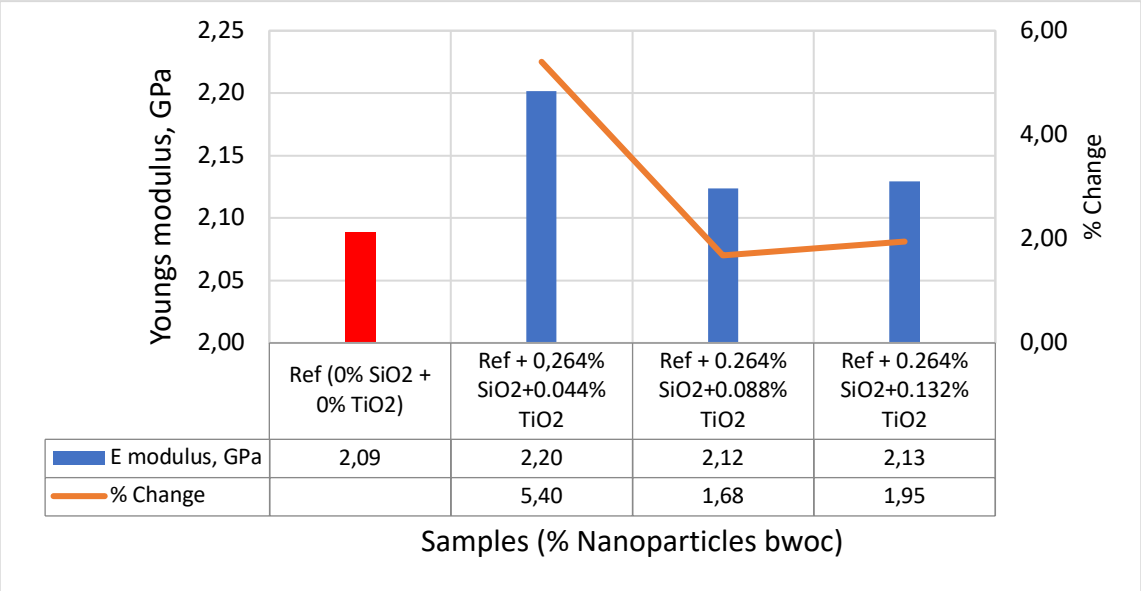


Figure 4.14 Effect of $SiO_2$ - $TiO_2$ on the Youngs modulus of G-class cement

### 4.3.4 Effect of $SiO_2$ - $TiO_2$ on Resilience of Portland Cement

Figure 4.15 shows that the 0.264wt% $SiO_2$ + 0.088wt% $TiO_2$ increases the resilience by 15.63%. On the other hand, the other nanoparticle concentrations exhibited a lower resilience compared to the neat cement plugs by 19.5% and 10.48%.

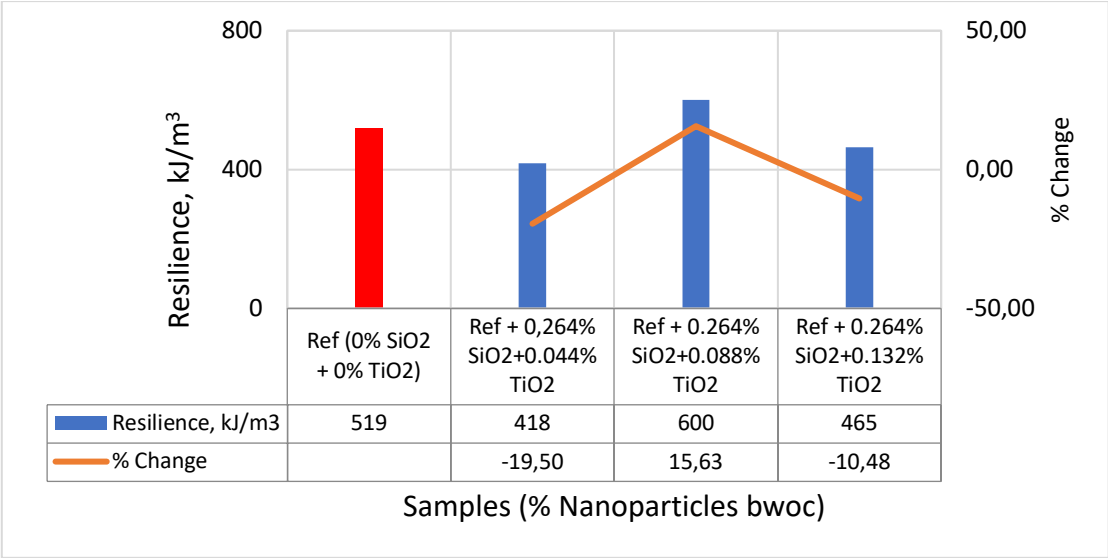


Figure 4.15 Effect of $SiO_2$ - $TiO_2$ on the Resilience of G-class cement

## 4.4 Effect of Nanoparticles on Rheology of Cement Slurries

The pumpability of cement slurries is one of the parameters to be in consideration for the cement placement in an oil well. The flow of cement in the well is controlled by the viscosities of the cement slurry. The effect of nanoparticles on the rheological properties of three cement types are compared with the nanoparticle untreated neat cement slurries. The nano particle concentrations in the three cement slurries were selected based on the highest uniaxial compressive strength.

Figures 4.16, 4.17, and 4.18 show the measured viscometer responses of the industry cement (C-class), environmental cement, and G-class cements respectively. As shown the addition of nanoparticles reduces the viscometer responses.

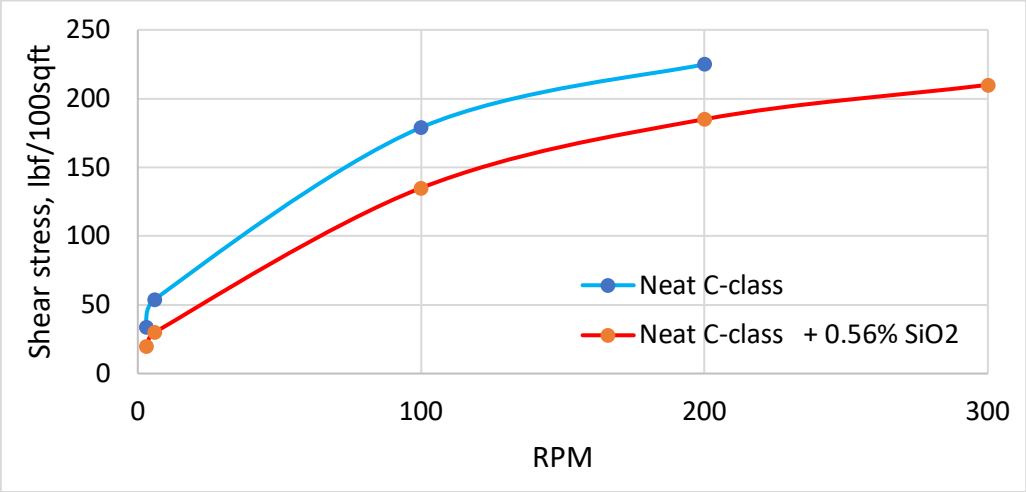


Figure 4.16 Viscometer responses of the neat and 0.56% $SiO_2$ treated C-class cement

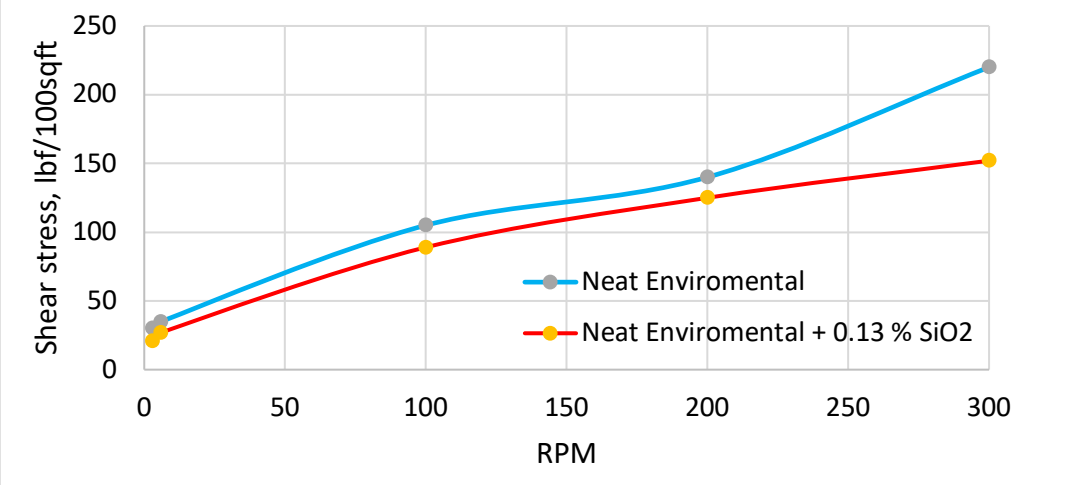


Figure 4.17 Viscometer responses of the neat and 0.13% $SiO_2$ treated Environmental cement

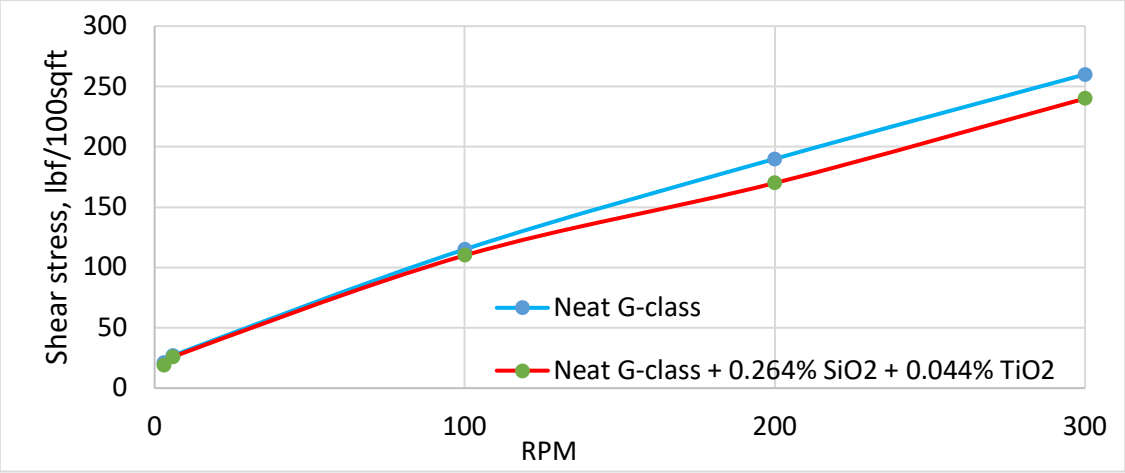


Figure 4.18 Viscometer responses of the neat and 0.264% $SiO_2$ + 0.044% $TiO_2$ blended G-class cement

Table 4.1 provides the calculated yield stress and plastic viscosity for the neat and nano treated cements. For all the cement types, nanoparticles reduced the viscosities and reduced the flow resistances for the cement placement job.

Table 4.1 Casson Yield stresses and Casson plastic viscosities

| **Temperature ($^0$C)** | **Neat C-class** | **Neat C-class+ 0.14% SiO2** | **Neat Environmental** | **Neat Environmental +0.13% SiO2** | **Neat G-class** | **Neat G-class + 26% SiO2 + 0.044% TiO2** |
|---|---|---|---|---|---|---|
| **Yield stress (Pa)** | 4,0 | 7,7 | 10,1 | 8,0 | 5,7 | 5,5 |
| **Plastic viscosity (cP)** | 138,2 | 131,6 | 97,7 | 75,8 | 163,4 | 148,1 |

## 4.5 Effect of Nanoparticles on the Heat Development of Cement Slurries

As mentioned in section §2.2, heat is liberated (i.e., exothermic reaction) when cement mixed with water. In this thesis, the heat development phenomenon is indirectly evaluated by measuring the temperature development of the neat and nanoparticle blended C-class, environmental, and G-class cements. Based on the highest uniaxial compressive strength results obtained from the three cements, the nanoparticle concentrations were selected and its effect on the temperature development was measured.

The cement slurries were mixed and poured into a plastic bag, and it was then placed in insulated polystyrene boxes to isolate cement temperature from the laboratory temperature. The temperature sensors were installed in the cement slurries before closing the boxes and storing them in a dry closet. During the hydration process, the sensors were measuring the temperature of the cements every 5 minutes for three days. From figures 4.19 and 4.20, temperature development shows a similar trend except a minor deviation until 20hr testing. It can be observed that the peak temperature for the neat industry cement is measured to be 70.5ºC and the nano treated cement recorded 65 ºC.

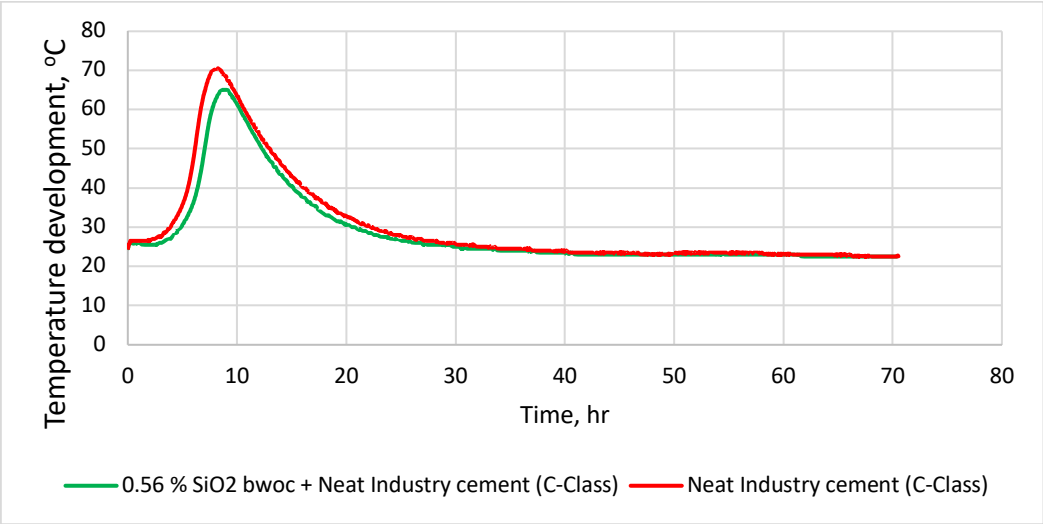


Figure 4.19 Temperature development in the neat-and 0.56% $SiO_2$ treated C-class cement

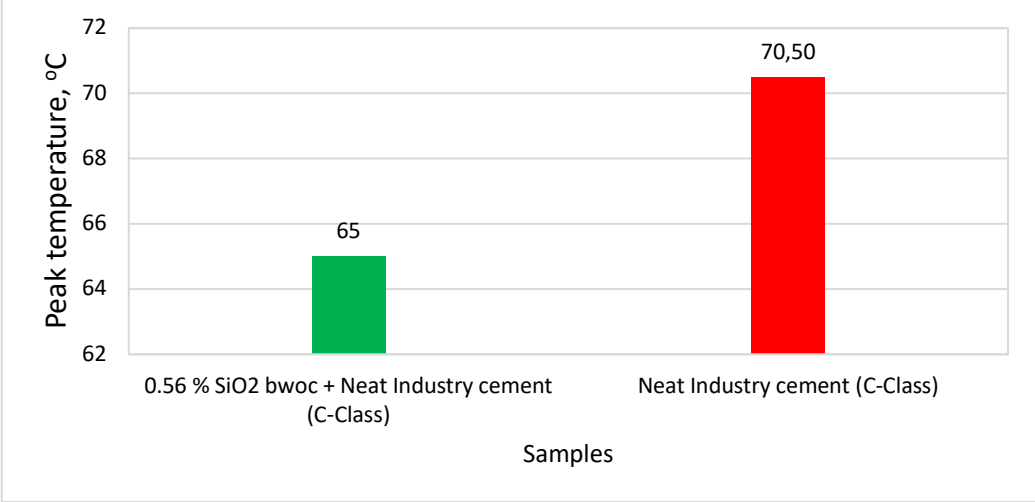


Figure 4.20 Peak temperatures of the neat and 0.56% $SiO_2$ treated C-class cement

Figures 4.21 and 4.22 display the temperature development and the peak temperature values for neat environmental cement and nano-treated environmental cements, respectively. As shown, the nanoparticles increase the peak temperature of the neat cement by 4°C.

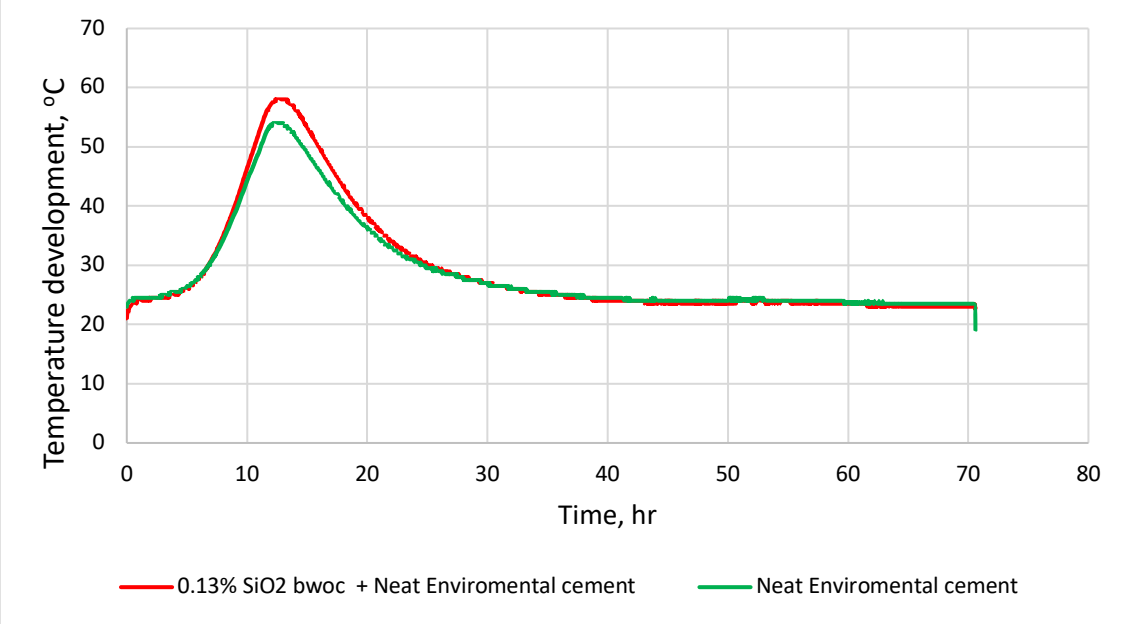


Figure 4.21 Temperature development in the neat and 0.13% $SiO_2$ treated Environmental cement

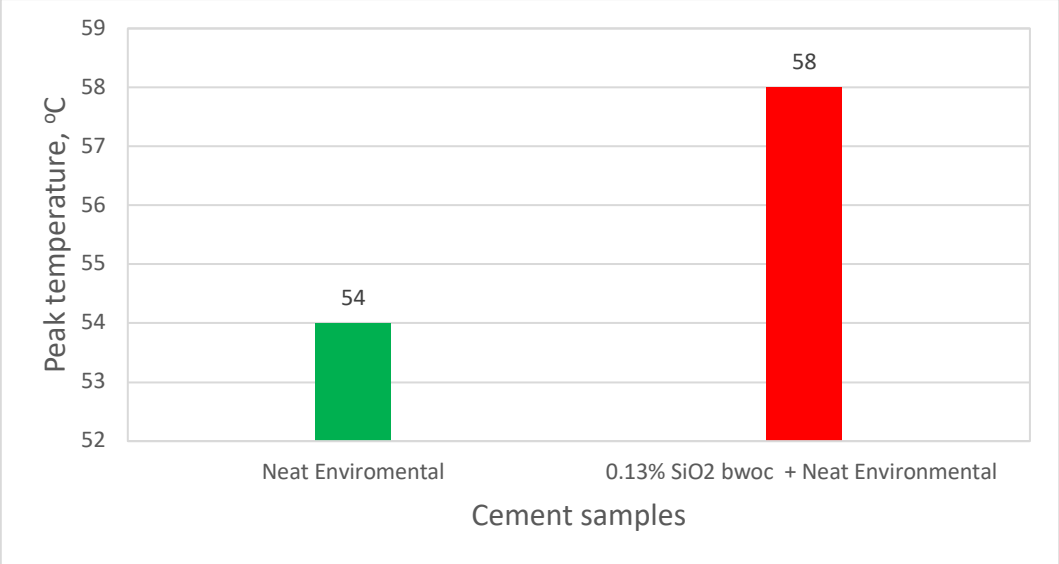


Figure 4.22 Peak temperatures of the neat and 0.13% $SiO_2$ treated Environmental cement

Figures 4.23 and 4.24 show the temperature development and the peak temperature values for the neat G-class cement and blended with hybrid nanoparticles, respectively. It is also observed that amongst the three cements, the lowest peak temperature values are obtained

for G-class cement. Another observation is that the speed of temperature development of the neat cement is higher than the nano-treated cement until reaching the peak temperatures. However, both cement systems recorded the same peak temperature.

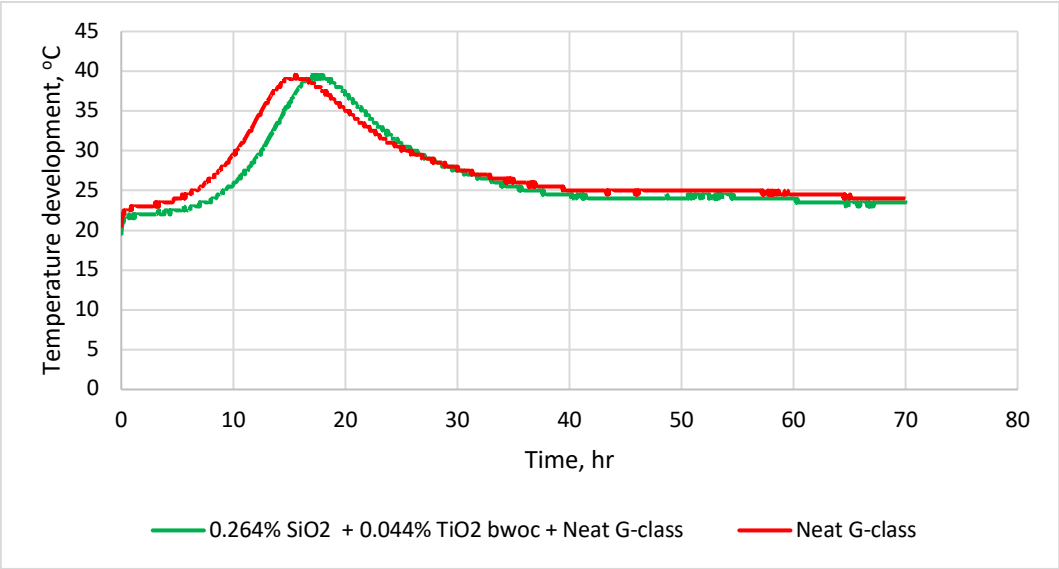


Figure 4.23 Temperature development in the neat and 0.264% $SiO_2$ + 0.044% $TiO_2$ blended G-class cement

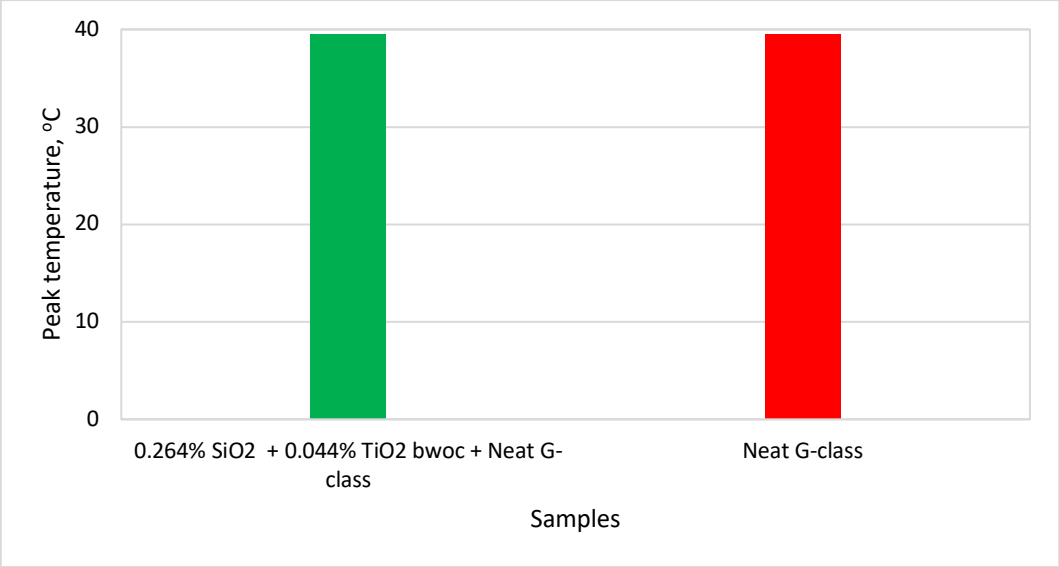


Figure 4.24 Peak temperature in the neat and 0.264% $SiO_2$ + 0.044% $TiO_2$ blended G-class cement

# 5 MODELLING AND TESTING

An empirical model was derived by coupling the destructive (UCS) with the non-destructive (compressional wave velocity). Similar UCS vs Vp models are available in literature, that have been developed based on cementitious and rock-based dataset. The following presents new model development and testing of the model with data measured by other investigators.

## 5.1 Modelling

During the process of empirical model development, the average values of the UCS and the compressional velocities of the plugs are used. The velocity data was measured the day when the cement plugs were tested with mechanical destructive test. The data used are from the C-class and environmental cement-based plugs that have been measure at 7 days and 28 days. Due to defects and poor measurement, outlier datasets are removed since it is not representative. Figure 5.1 shows the scattered datasets and the power law model that fits the measurements with $R^2$ =0.8334. The model reads:

$$UCS = 0{,}1255Vp^{4{,}4748} \quad 5.1$$

Where, UCS is in MPa and Vp in km/s

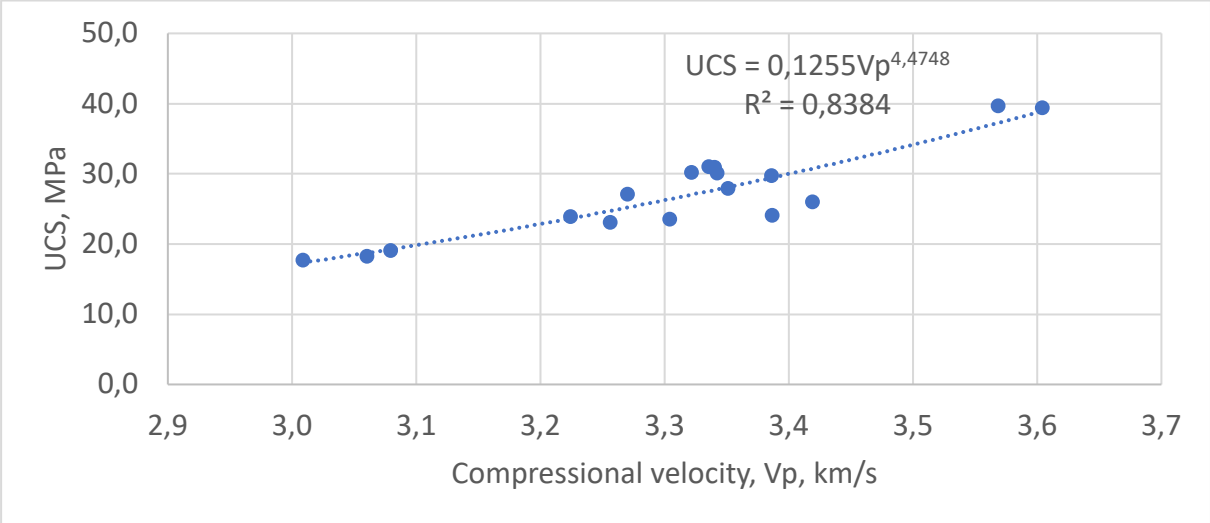


Figure 5.1 UCS vs Compressional wave velocity modelling

The model prediction of the newly developed model is compared with Horsrud's (2001) [44] empirical model, which was derived from several shale data from the North Sea. The Horsrud´s UCS – compressional velocity (Vp) model reads:

$$UCS\ (MPa) = 0.77Vp^{2.92} \qquad 5.2$$

Where, UCS is in MPa and Vp in km/s

## 5.2 Testing

This thesis work model (Eq 5.1) and the Horsrud's model (Eq. 5.2) predictions are tested against the dataset measured by Henrik Nerhus (2020) [45]. The datasets are based on cement plugs treaded with different types of nanoparticles.

Figure 5.2 displays the comparisons of the model prediction of Henrik's data set. Results show that this thesis model records a deviation from the measurement in range of 0.3-9.2% and the Horsrud´s model deviation is in the range of 0.3-13.9%.

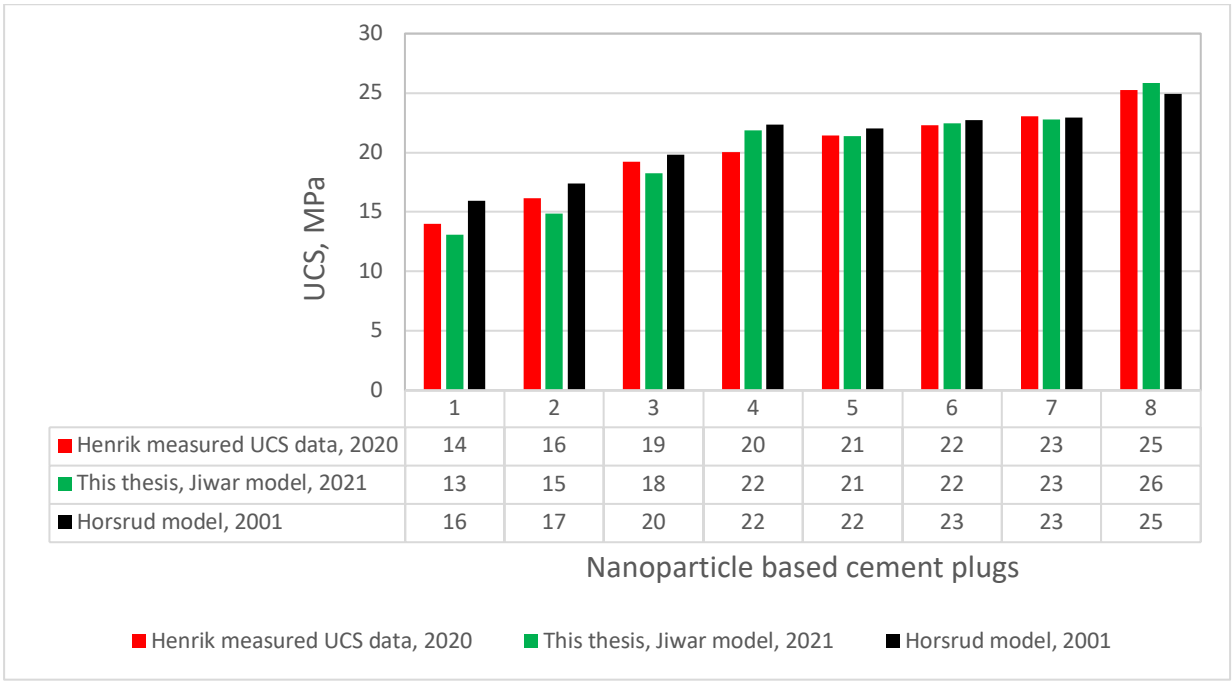


Figure 5.2 This thesis work and Horsrud's models prediction of Henrik´s dataset

# 6 SUMMARY AND CONCLUSION

Cement is a crucial barrier element used for well construction having several purposes such as to provide good structural integrity as well as to prevent undesired leakage from formation laterally or from reservoir axially. Moreover, when the well cease to produce an economical hydrocarbon, or uncontrollable leakages/flows to the surface, the fate of the well is to be plugged and abandoned. For this, again, the quality of cement and cement job during placements are the key that determine successful performances.

The desire of the NORSOK D-010 for the cement is to have a long term well barrier performance. However, well integrity survey results indicated that the conventional cement has shown integrity issue.

With the objective of improving the properties of C-class, environmental, and G-class cement, this thesis experimentally investigated the impact of $SiO_2$ and $TiO_2$ nanoparticles on the neat cements.

Results from the study are summarized as:

- The impact of Nanoparticles on the neat cements (C-class, environmental, and G-class) is not a linear function of the concentration.
- As the concentration nanoparticles reaches to the optimum value, a desired cement property can be obtained. A single concentration will not provide all the mechanical and elastic properties.
- It was found that amongst C-class with 0.56 WCR and environmental cement with 0.52 WCR, the optimal $SiO_2$ concentration showed greater impact on the mechanical and elastic properties of the environmental cement.
- Among the three test designs, it is observed that $SiO_2$ nanoparticle has shown a significant impact on the UCS of the environmental cement.
- Comparing the three cements, the neat G-class cement and $SiO_2$ nanoparticle has shown the lowest water absorption and the lowest resilience.
- The optimum $SiO_2$ concentration selected based on UCS showed that nanoparticle reduced the peak temperature developments of the neat C-class and the environmental cement. The hybrid $SiO_2/TiO_2$ did not show any impact on the neat G-class cement.

- The optimum $SiO_2$ concentration selected based on UCS showed that nanoparticle reduced the viscosity of the C-class and the environmental cement. Similarly, the optimum hybrid $SiO_2/TiO_2$ reduced the viscosity of the G-class neat cement.

**Results summary from TM#1 - Effect of $SiO_2$ on Industry C-class cement**

Table 6.1 An optimal 0.56%bwoc effect on the UCS of the neat Industry cement

| TM | Nanoparticle | Concentration (%bwoc) | WCR | Curing (days) | UCS (MPa) | UCS increase (%) |
|---|---|---|---|---|---|---|
| TM#1 | None | - | ≈0.56 | 28 | 28 | - |
| TM#1 | $SiO_2$ | 0.56 | ≈0.56 | 28 | 33 | 16.7 |

Table 6.2 An optimal 0.84%bwoc effect on the Modulus of elasticity of the neat Industry cement

| TM | Nanoparticle | Concentration (%bwoc) | WCR | Curing (days) | M (GPa) | M increase (%) |
|---|---|---|---|---|---|---|
| TM#1 | None | - | ≈0.56 | 7 | 20.7 | - |
| TM#1 | $SiO_2$ | 0.84 | ≈0.56 | 28 | 19.7 | 8.2 |

Table 6.3 An optimal 0.14%bwoc effect on the Resilience of the neat Industry cement

| TM | Nanoparticle | Concentration (%bwoc) | WCR | Curing (days) | R ($kJ/m^3$) | R increase (%) |
|---|---|---|---|---|---|---|
| TM#1 | None | - | ≈0.56 | 28 | 364 | - |
| TM#1 | $SiO_2$ | 0.14 | ≈0.56 | 28 | 595 | 63 |

Table 6.4 An optimal 0.42%bwoc effect on the Youngs modulus of the neat Industry cement

| TM | Nanoparticle | Concentration (%bwoc) | WCR | Curing (days) | E (GPa) | E increase (%) |
|---|---|---|---|---|---|---|
| TM#1 | None | - | ≈0.56 | 28 | 1.30 | - |
| TM#1 | $SiO_2$ | 0.42 | ≈0.56 | 28 | 1.63 | 26 |

## Results summary from TM#2 - Effect of $SiO_2$ on Environmental cement

Table 6.5 An optimal 0.13%bwoc effect on the UCS of the neat Environmental cement

| TM | Nanoparticle | Concentration (%bwoc) | WCR | Curing (days) | UCS (MPa) | UCS increase (%) |
|---|---|---|---|---|---|---|
| TM#2 | None | - | ≈0.52 | 28 | 27 | - |
| TM#2 | $SiO_2$ | 0.13 | ≈0.52 | 28 | 40.4 | 49.6 |

Table 6.6 An optimal 0.39%bwoc effect on the Modulus elasticity of the neat Environmental cement

| TM | Nanoparticle | Concentration (%bwoc) | WCR | Curing (days) | M (GPa) | M increase (%) |
|---|---|---|---|---|---|---|
| TM#2 | None | - | ≈0.52 | 28 | 21.1 | - |
| TM#2 | $SiO_2$ | 0.39 | ≈0.52 | 28 | 23.1 | 10 |

Table 6.7 An optimal 0.13%bwoc effect on the Resilience of the neat Environmental cement

| TM | Nanoparticle | Concentration (%bwoc) | WCR | Curing (days) | R ($kJ/m^3$) | R increase (%) |
|---|---|---|---|---|---|---|
| TM#2 | None | - | ≈0.52 | 28 | 410 | - |
| TM#2 | $SiO_2$ | 0.13 | ≈0.52 | 28 | 663 | 62 |

Table 6.8 An optimal 0.26%bwoc effect on the Youngs modulus of the neat Environmental cement

| TM | Nanoparticle | Concentration (%bwoc) | WCR | Curing (days) | E (GPa) | E increase (%) |
|---|---|---|---|---|---|---|
| TM#2 | None | - | ≈0.52 | 28 | 2.1 | - |
| TM#2 | $SiO_2$ | 0.26 | ≈0.52 | 28 | 2.5 | 19 |

## Results summary from TM#3 - Effect of $SiO_2$-$TiO_2$ on G-class cement

Table 6.9 An optimal 0.264%$SiO_2$-0.044%$TiO_2$ bwoc effect on the UCS of the neat G-class cement

| TM | Nanoparticle | Concentration (%bwoc) | WCR | Curing (days) | UCS (MPa) | UCS increase (%) |
|---|---|---|---|---|---|---|
| TM#3 | None | - | ≈0.44 | 28 | 28 | - |
| TM#3 | $SiO_2$/$TiO_2$ | 0.264/0.044 | ≈0.44 | 28 | 31 | 8.5 |

Table 6.10 An optimal 0.264%$SiO_2$-0.044%$TiO_2$ bwoc effect on the Youngs modulus of the neat G-class cement

| TM | Nanoparticle | Concentration (%bwoc) | WCR | Curing (days) | E (GPa) | E increase (%) |
|---|---|---|---|---|---|---|
| TM#3 | None | - | ≈0.44 | 28 | 2.09 | - |
| TM#3 | $SiO_2$/$TiO_2$ | 0.264/0.044 | ≈0.44 | 28 | 2.20 | 5.40 |

Table 6.11 An optimal 0.264%$SiO_2$-0.088%$TiO_2$ bwoc effect on the Resilience of the neat G-class cement

| TM | Nanoparticle | Concentration (%bwoc) | WCR | Curing (days) | R ($kJ/m^3$) | R increase (%) |
|---|---|---|---|---|---|---|
| TM#3 | None | - | ≈0.44 | 28 | 519 | - |
| TM#3 | $SiO_2$/$TiO_2$ | 0.264/0.088 | ≈0.44 | 28 | 600 | 15.63 |

# REFERENCES

[1] PetroWiki. ***Cementing operations***. https://petrowiki.spe.org/index.php?title=Cementing_operations&oldid=53699 (accessed 11 January 2021)

[2] Salami, O.T. ***Synthesis and Working Mechanism of Humic Acid Graft Copolymer Fluid Loss Additives Suitable for Cementing High Pressure/High Temperature oil and Gas Wells***. München: TECHNISCHE UNIVERSITÄT MÜNCHEN; 2014.

[3] T. Vrålstad, A. Saasen, E. Fjær, T. Øia, J. D. Ytrehus, and M. Khalifeh, *"**Plug & abandonment of offshore wells: Ensuring long-term well integrity and cost-efficiency,**"* J. Pet. Sci. Eng., vol. 173, pp. 478–491, Feb. 2019, doi: 10.1016/j.petrol.2018.10.049

[4] Erik B. Nelson and Dominique Guillot// ***Well Cementing*, Second Edition** ISBN-13: 978-097885300-6, ISBN-10: 0-9788530-0-8

[5] Bennett T. ***Well Cement Integrity and Cementing Practices***. Australia: The university of Adelaide; 2016.

[6] NORSOK Standard. D-010 Rev. 5. ***Well integrity in drilling and well drilling operations***. Norway: Standards Norway; 2021.

[7] B. Vignes and B. S. Aadnoy, "***Well-Integrity Issues Offshore Norway***," presented at the IADC/SPE Drilling Conference, Jan. 2008, doi: 10.2118/112535-MS.

[8] Theresa L. Watson, and Stefan Bachu, //***Evaluation of the Potential for Gas and CO2 Leakage Along Wellbores***// March 2009 SPE Drilling & Completion *l* 24 (01): 115–126. Paper Number: SPE-106817-PA

[9] SCENIHR/002/05 // ***The appropriateness of existing methodologies to assess the potential risks associated with engineered and adventitious products of nanotechnologies*** (2006)

[10] "Nanoparticles - ***what they are, how they are made***," Nanowerk. https://www.nanowerk.com/how_nanoparticles_are_made.php (accessed May. 07, 2021)

[11] Salih, A. H., & Bilgesu, H. (2017, April). ***Investigation of rheological and filtration properties of water-based drilling fluids using various anionic nanoparticles***. In SPE Western regional meeting. Society of Petroleum Engineers.

[12] Zhang, Jie, et al. "***Novel micro and nano particle-based drilling fluids: Pioneering approach to overcome the borehole instability problem in shale formations***." SPE Asia Pacific Unconventional Resources Conference and Exhibition. Society of Petroleum Engineers, 2015.

[13] Vryzas, Z., Nalbandian, L., Zaspalis, V. T., & Kelessidis, V. C. (2019). ***How different nanoparticles affect the rheological properties of aqueous Wyoming sodium bentonite suspensions*.** Journal of Petroleum Science and Engineering, 173, 941-954.

[14] Ismail, A. R., Aftab, A., Ibupoto, Z. H., & Zolkifile, N. (2016). ***The novel approach for the enhancement of rheological properties of water-based drilling fluids by using multi-walled carbon nanotube, nanosilica and glass beads***. Journal of Petroleum Science and Engineering,
139, 264-275.

[15] N. M. Taha, S. Lee, et al. //***Nano graphene application improving drilling fluids performance***// In International Petroleum Technology Conference. International Petroleum Technology Conference, 2015.

[16] William, J.K.M.; Ponmani, S.; Samuel, R.; Nagarajan, R.; Sangwai, J.S**.** ***Effect of CuO and ZnO nanofluids in xanthan gum on thermal, electrical and high-pressure rheology of water-based drilling fluids***. J. Pet. Sci. Eng. 2014, 117, 15–27

[17] Charles O. Nwaoji, Geir Hareland, Maen Husein, Runar Nygaard, and Mohammad Ferdous Zakaria, 2013//***Wellbore Strengthening-Nano-Particle Drilling Fluid Experimental Design Using Hydraulic Fracture Apparatus***// **SPE** 163434 SPE / IADC Drilling Conference and Exhibition, Mar 05 -07, 2013 2013, Amsterdam, The Netherlands

[18] H. A. Son, K. Y. Yoon, G. J. Lee, J. W. Cho, S.K. Choi, J. W. Kim, K. C. Im, H.T. Kim, K. S. Lee, W. M Sung. 2014. ***The potential application in oil recovery with silica nanoparticle and polyvinyl alcohol stabilized emulsion***.//Journal of Petroleum Science and Engineering Volume 126, February 2015, Pages 152-161

[19] M. Mohajeri, M. Hemmati and A.S. Shekarabi. 2014. ***An experimental study on using a nanosurfactant in an EOR process of heavy oil in a fractured micromodel***. Journal of Petroleum Science and Engineering Volume 126, February 2015, Pages 162-173

[20] M. O. Onyekonwu, N. A. Ogolo. 2010. ***Investigating the use of Nanoparticles in Enhancing Oil Recovery.*** //Paper presented at the Nigeria Annual International Conference and Exhibition, Tinapa - Calabar, Nigeria, July 31 2010. SPE-140744-MS

[21] B. Moradi, P. Pourafshary, F. J. Farahani, M. Mohammadi, and M. A. Emadi, "***Application of SiO2 Nano Particles to Improve the Performance of Water Alternating Gas EOR Process*****,"** presented at the SPE Oil & Gas India Conference and Exhibition, Nov. 2015, doi: 10.2118/178040-MS.

[22]: M. Khalil, B. M. Jan, C. W. Tong, and M. A. Berawi, "***Advanced nanomaterials in oil and gas industry: Design, application and challenges***," Appl. Energy, vol. 191, pp. 287–310, Apr. 2017, doi: 10.1016/j.apenergy.2017.01.074.

[23] Li, H., Xiao, H., Yuan, J. and Ou, J. (2004) ***Microstructure of Cement Mortar with Nano-Particles***. Composites Part B: Engineering, 35, 185-189.

[24] V. Ershadi, T. Ebadi, A. R Rabani, L. Ershadi, H. Soltanian (2011) ***The Effect of Nano silica on Cement Matrix Permeability in Oil Well to Decrease the Pollution of Receptive Environment***. International Journal of Environmental Science and Development, Vol. 2, No. 2, 128-132 January 2011.

[25] Mohammad Rahimirad, Javad Dehghani Baghbadorani 2012// ***Properties of Oil Well Cement Reinforced by Carbon Nanotubes*** **//** Paper presented at the SPE International Oilfield Nanotechnology Conference and Exhibition, June 12–14, 2012 Paper Number: SPE-156985-MS

[26] R. Roji, C. Egyed, J.P. Lips. 2012. ***Nano-engineered oil well cement improves flexibility and increases compressive strength: a laboratory study.*** //Paper presented at the SPE International Oilfield Nanotechnology Conference and Exhibition, Noordwijk, The Netherlands, June 2012. SPE-156501-MS

[27] Patil, R. C., & Deshpande, A. (2012, January). ***Use of nanomaterials in cementing applications****. In SPE International Oilfield Nanotechnology Conference and Exhibition*. Society of Petroleum Engineers.

[28] Pang, X., Boul, P. J., & Cuello Jimenez, W. (2014). ***Nanosilicas as accelerators in oilwell cementing at low temperatures***. SPE Drilling & Completion, 29(01), 98-105.

[29] Moradi, S. S. T., & Nikolaev, N. I. (2015, October*).* ***Developing High Resistant Cement Systems for High-Pressure, High-Temperature Applications*** (Russian). In SPE Russian Petroleum Technology Conference. Society of Petroleum Engineers.

[30] Murtaza, M., Rahman, M. K., & Al-Majed, A. A. (2016, November). ***Mechanical and Microstructural Studies of Nanoclay Based Oil Well Cement Mix under High Pressure and Temperature Application.*** In International Petroleum Technology Conference. International Petroleum Technology Conference.

Rehman et al. (2016)
[31] Rahman, M. K., Khan, W. A., Mahmoud, M. A., & Sarmah, P. (2016, March**).** ***MWCNT for Enhancing Mechanical and Thixotropic Properties of Cement for HPHT Applications***. In Offshore Technology Conference Asia. Offshore Technology Conference.

[32] Jafariesfad, N., Gong, Y., Geiker, M. R., & Skalle, P. (2016, April). ***Nano-Sized MgO with Engineered Expansive Property for Oil Well Cement Systems***. In SPE Bergen One Day Seminar. Society of Petroleum Engineers.

[33] Heathman, J., Fuller, G., Taylor, R., Arumugam, G., Sullivan, P., Thapa, S., & Veedu, V. (2017, May). ***Development of Nanotechnology Pipe Treatment to Improve Acoustic Cement Evaluation***. In Offshore Technology Conference. Offshore Technology Conference.

[34] Peyvandi, A., Taleghani, A. D., Soroushian, P., & Cammarata, R. (2017, October). ***The Use of Low-Cost Graphite Nanomaterials to Enhance Zonal Isolation in Oil and Gas Wells.*** In SPE Annual Technical Conference and Exhibition. Society of Petroleum Engineers.

[35] Baig, M. T., Rahman, M. K., & Al-Majed, A. (2017, October). ***Application of Nanotechnology in Oil Well Cementing***. In SPE Kuwait Oil & Gas Show and Conference. Society of Petroleum Engineers.

[36] Nazari, A., Riahi, S., Shamekhi, S. F., & Khademno, A. (2010, January). ***Assessment of the effects of the cement paste composite in presence $TiO_2$ nanoparticles.*** Journal of American Science.

[37] Sorathiya, J., Shah, S., & Kacha, S. (2017, February). ***Effect on Addition of Nano "Titanium Dioxide" (TiO2) on Compressive Strength of Cementitious Concrete***. In International Conference on Research and Innovations in Science, Engineering & Technology. Kalpa Publications.

[38] NORCEM AS. Available from: https://www.norcem.no/no

[39] CEMEX Norway. Available from: https://www.epd-norge.no

[40] LUDOX® TM-50 colloidal silica 420778," Silica preparation.

[41], "Titanium Oxide (TiO2) Nanopowder / ***Nanoparticles Dispersion (TiO2 Nanoparticles Aqueous Dispersion, Anatase, 15 wt%, 5-15 nm***)." https://www.us-nano.com/inc/sdetail/630 (accessed Mar. 17, 2020).

[42] Fjær, E., R. M. Holt, P. Horsrud, A. M. Raaen and R. Risnes (2008). ***Petroleum related rock mechanics, Elsevier Science*** // Volume 53 2nd Edition ISBN: 9780444502605

[43] Arthur P. Boresi, Richard J Schmidt // ***Advanced Mechanics of Materials.*** sixth edition ISBN0-471-43881-2

[44] P. Horsrud, "***Estimating Mechanical Properties of Shale From Empirical Correlations***,"

SPE Drill. Complet., vol. 16, no. 02, pp. 68–73, Jun. 2001, doi: 10.2118/56017-PA

[45] Henrik Nerhus 2020 //***Effect of nanoparticles and elastomers on the mechanical and elastic properties of G-class Portland cement***: Experimental and Modelling studies. MSc Thesis University of Stavanger

# APPENDIX A: FORCE VS DEFORMATION TEST

**Test batch for compressive strength of C-class 3 days:**

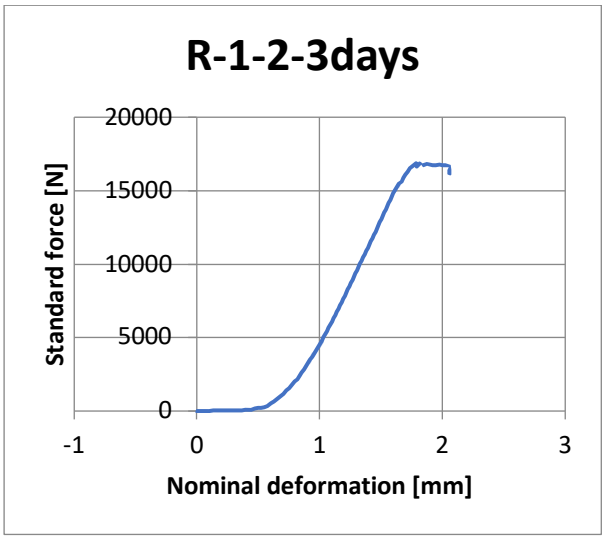


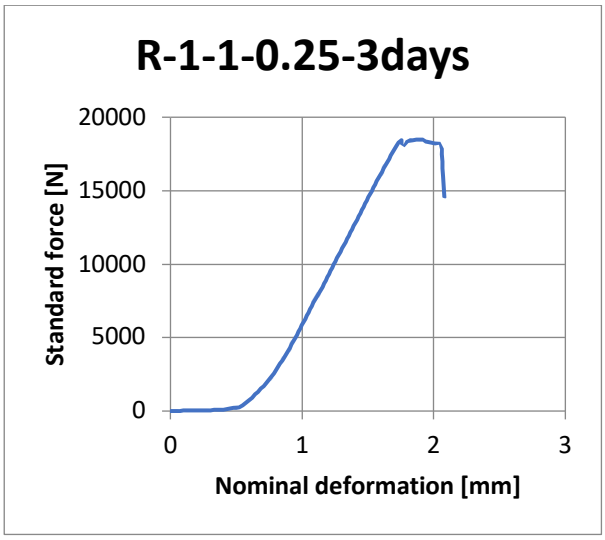


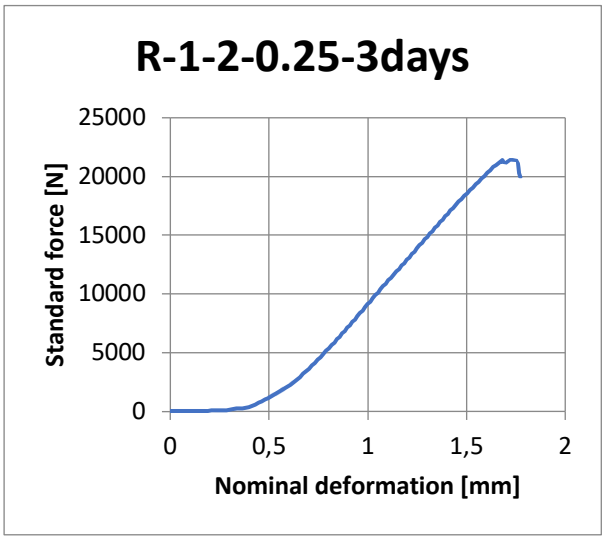


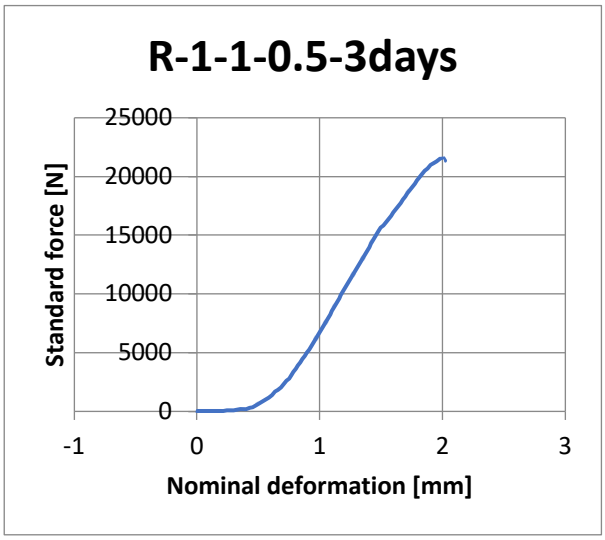

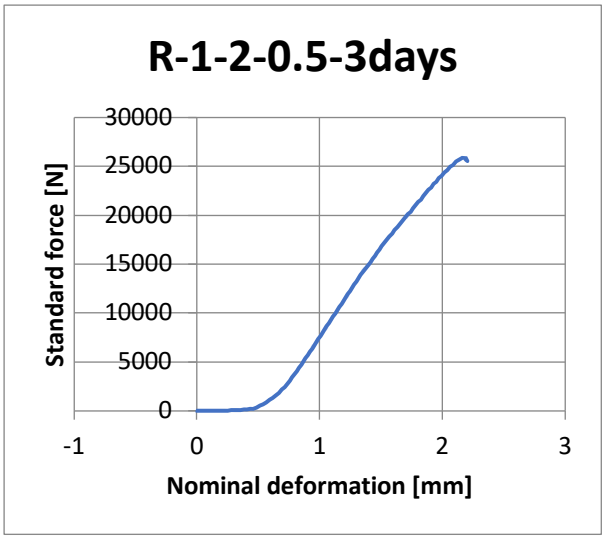
R-1-2-0.5-3days
Standard force [N]
30000
25000
20000
15000
10000
5000
0
-1
0
1
2
3
Nominal deformation [mm]

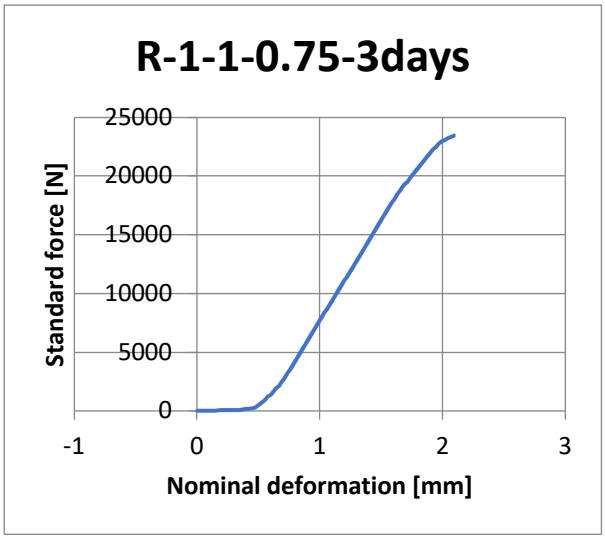
R-1-1-0.75-3days
Standard force [N]
25000
20000
15000
10000
5000
0
-1
0
1
2
3
Nominal deformation [mm]

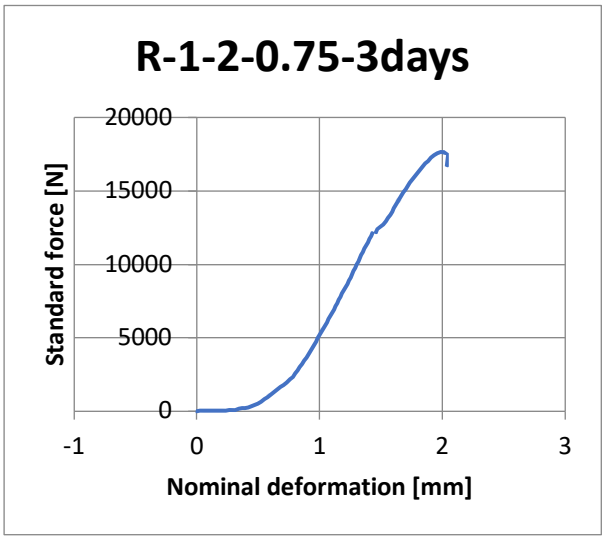
R-1-2-0.75-3days
Standard force [N]
20000
15000
10000
5000
0
-1
0
1
2
3
Nominal deformation [mm]

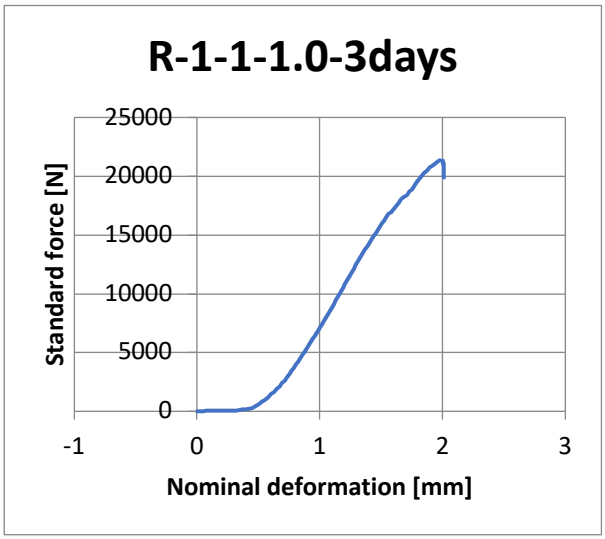
R-1-1-1.0-3days
Standard force [N]
25000
20000
15000
10000
5000
0
-1
0
1
2
3
Nominal deformation [mm]

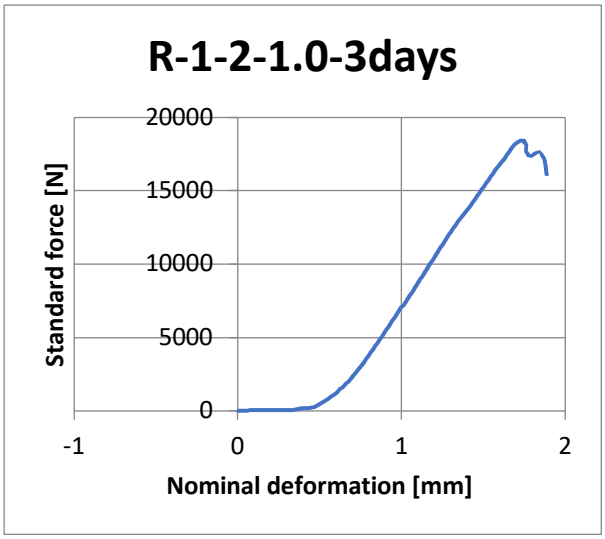
R-1-2-1.0-3days
Standard force [N]
20000
15000
10000
5000
0
-1
0
1
2
Nominal deformation [mm]

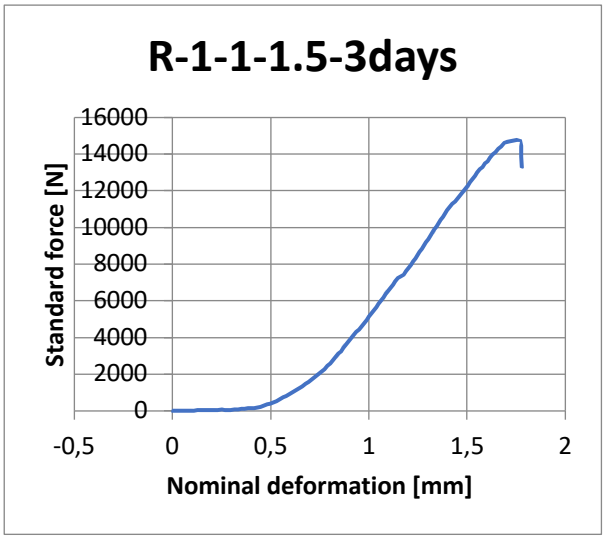
R-1-1-1.5-3days
Standard force [N]
16000
14000
12000
10000
8000
6000
4000
2000
0
-0,5
0
0,5
1
1,5
2
Nominal deformation [mm]

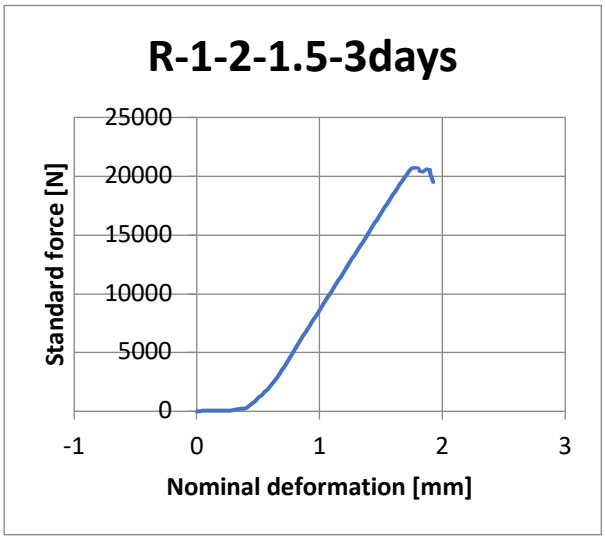
R-1-2-1.5-3days
Standard force [N]
25000
20000
15000
10000
5000
0
-1
0
1
2
3
Nominal deformation [mm]

**Test batch for compressive strength of C-class 7 days:**

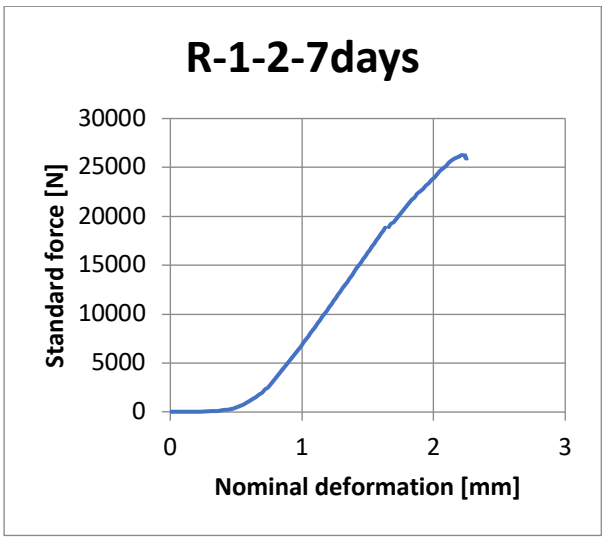


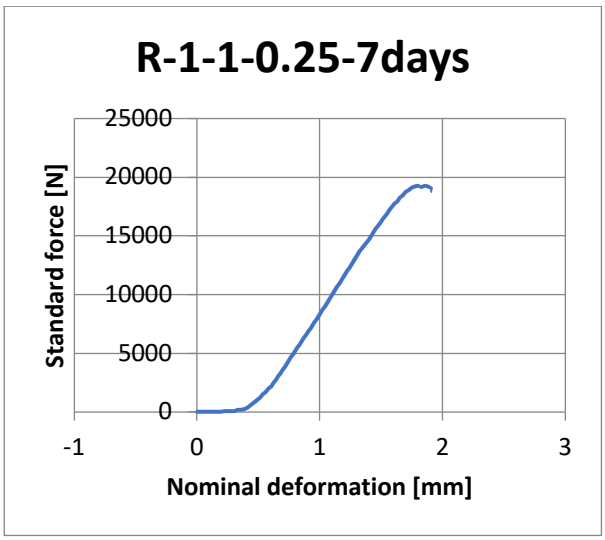


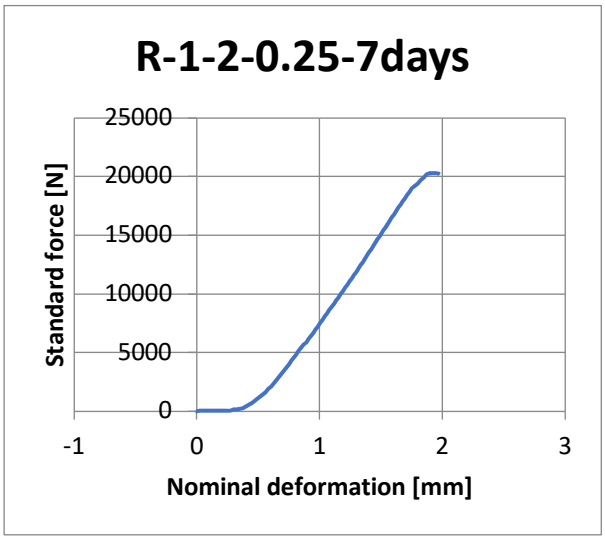


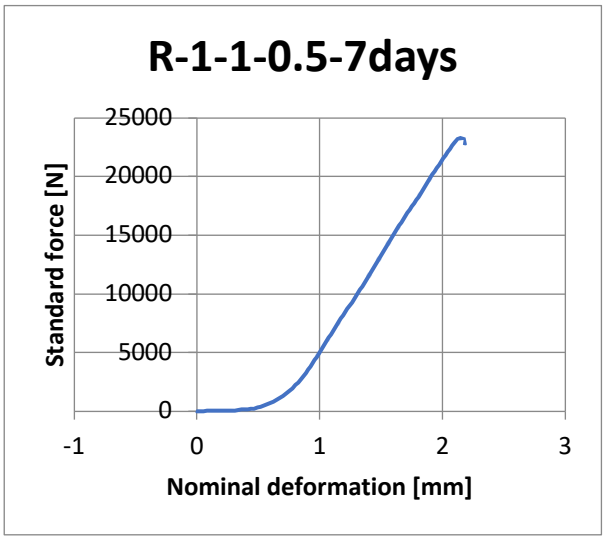


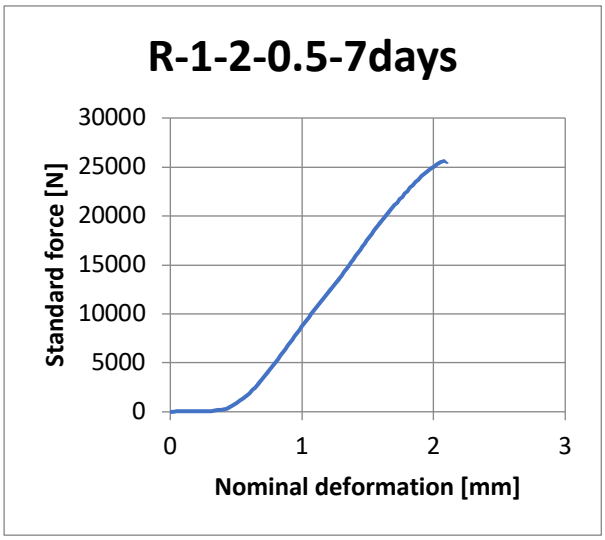


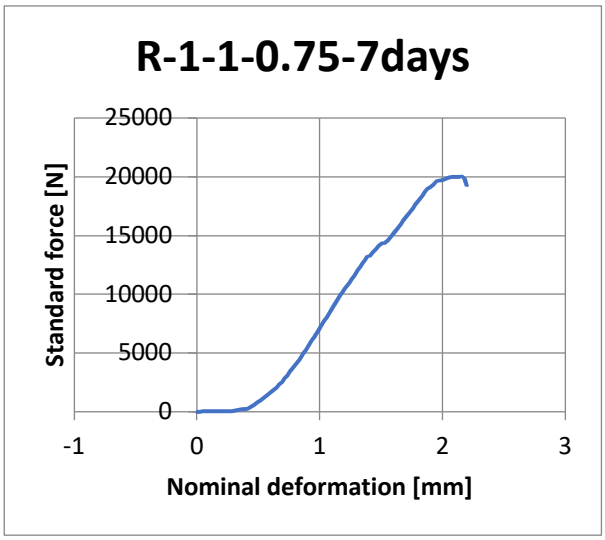

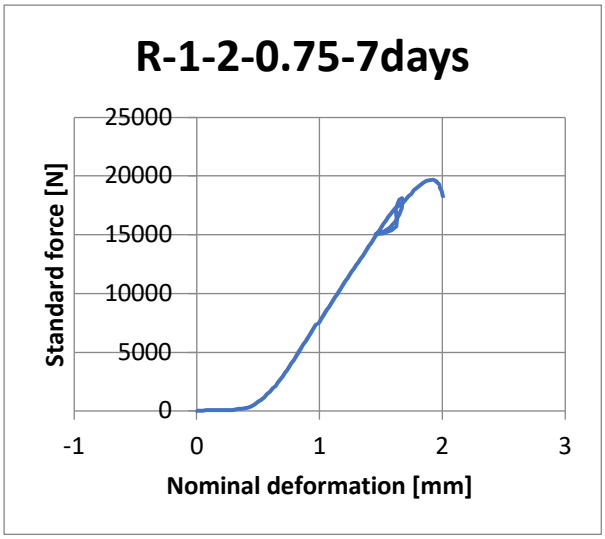
R-1-2-0.75-7days
Standard force [N]
25000
20000
15000
10000
5000
0
-1
0
1
2
3
Nominal deformation [mm]

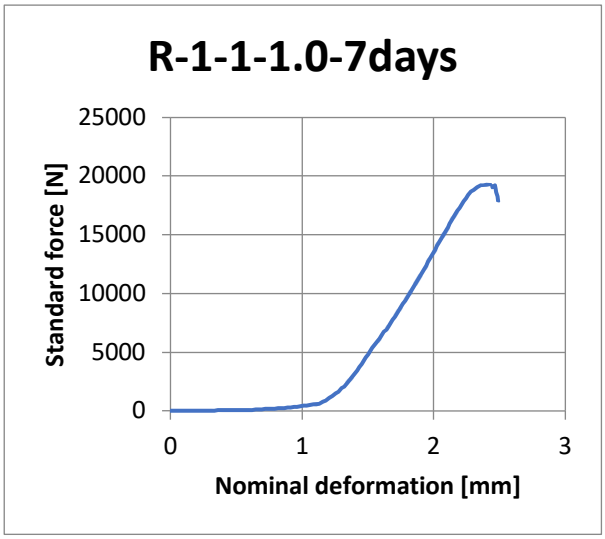
R-1-1-1.0-7days
Standard force [N]
25000
20000
15000
10000
5000
0
0
1
2
3
Nominal deformation [mm]

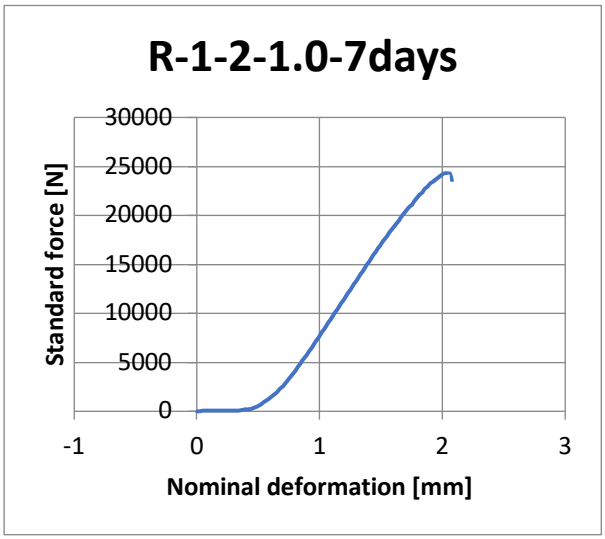
R-1-2-1.0-7days
Standard force [N]
30000
25000
20000
15000
10000
5000
0
-1
0
1
2
3
Nominal deformation [mm]

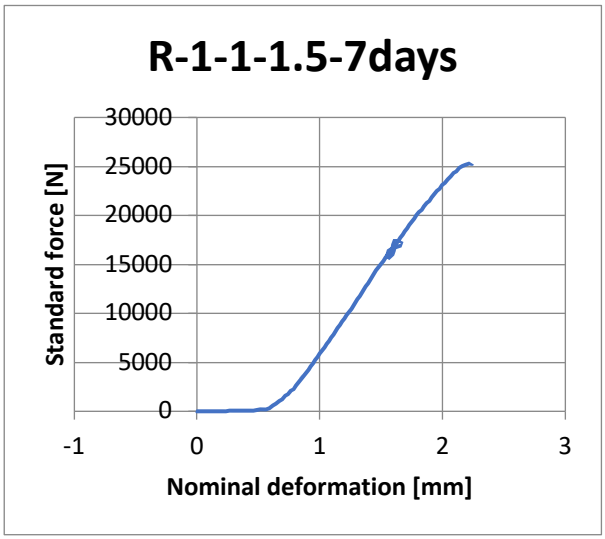
R-1-1-1.5-7days
Standard force [N]
30000
25000
20000
15000
10000
5000
0
-1
0
1
2
3
Nominal deformation [mm]

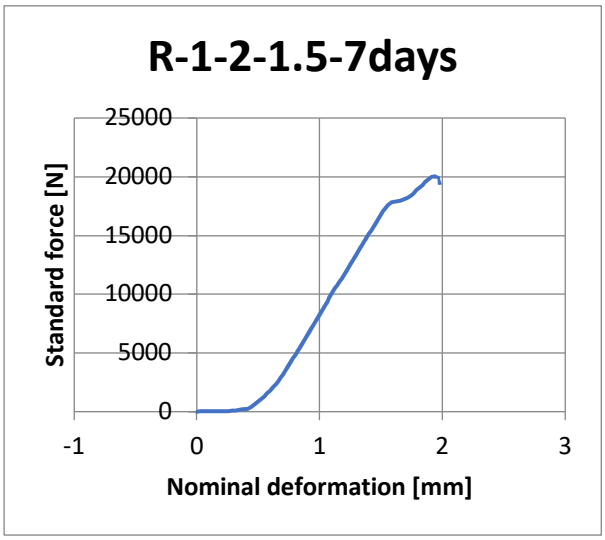
R-1-2-1.5-7days
Standard force [N]
25000
20000
15000
10000
5000
0
-1
0
1
2
3
Nominal deformation [mm]

**Test batch for compressive strength of C-class 28 days:**

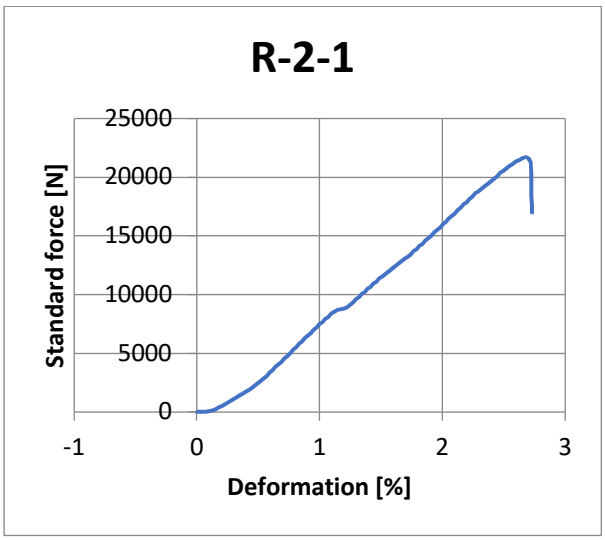


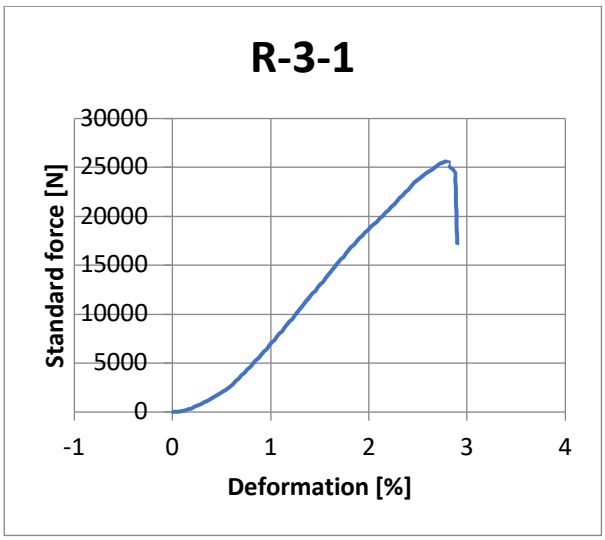


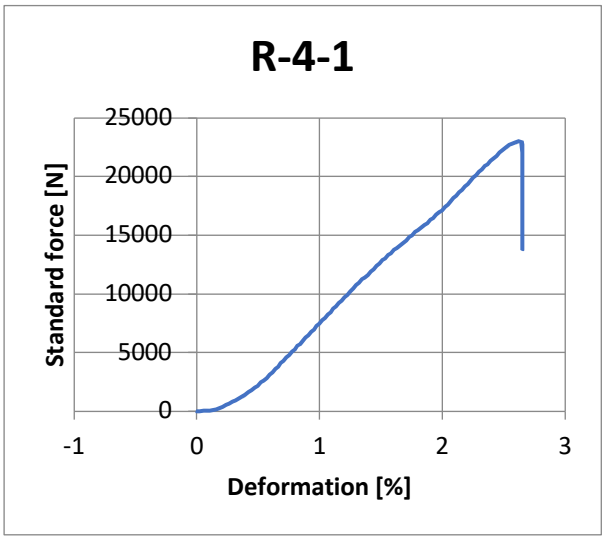


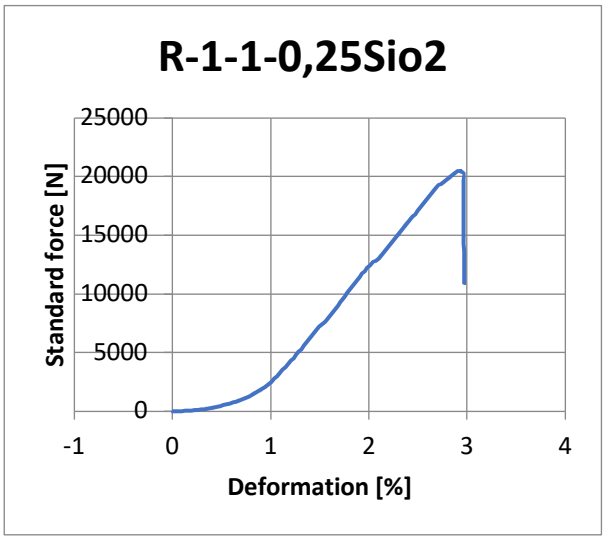


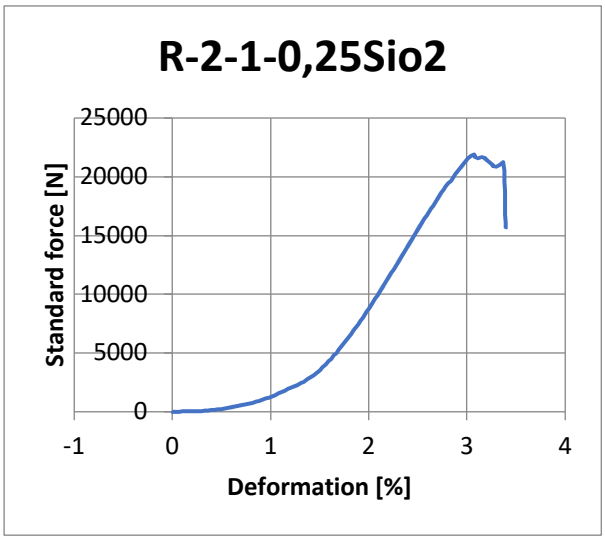


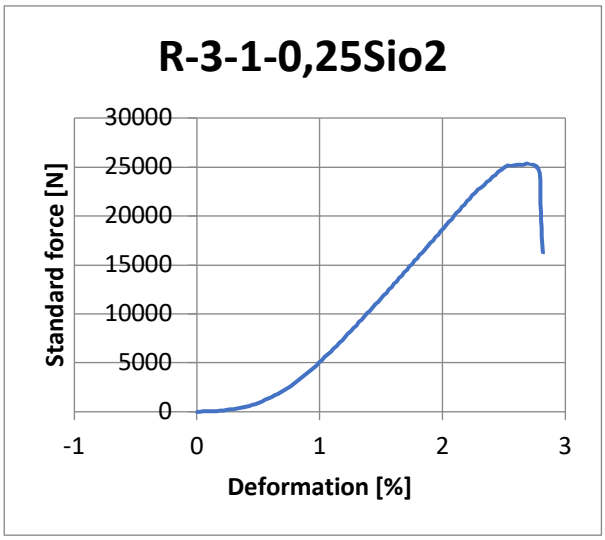

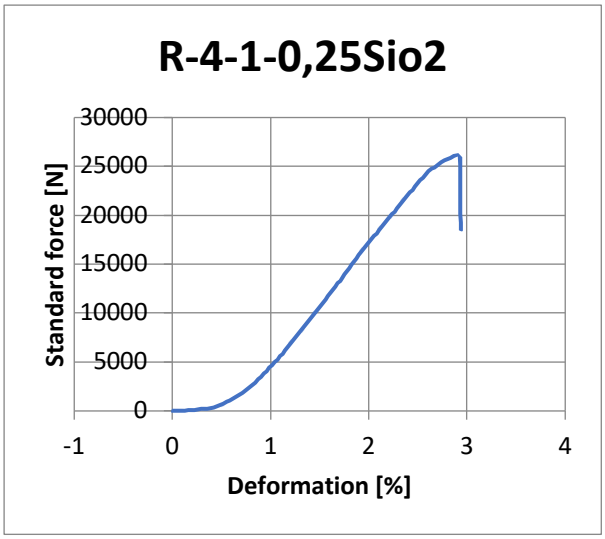
R-4-1-0,25Sio2
Standard force [N]
30000
25000
20000
15000
10000
5000
0
-1
0
1
2
3
4
Deformation [%]

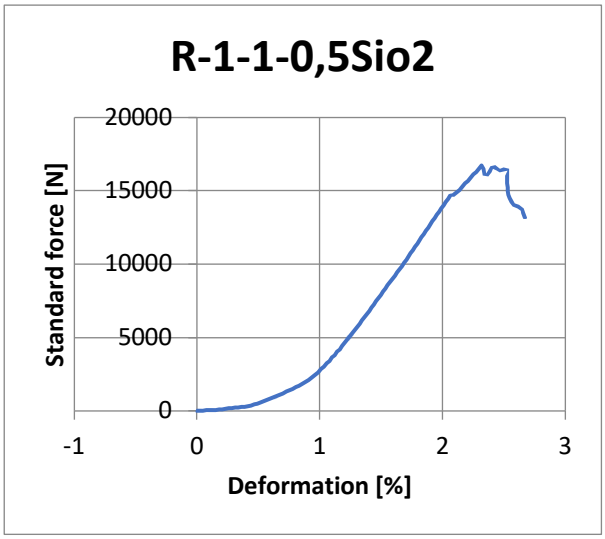
R-1-1-0,5Sio2
Standard force [N]
20000
15000
10000
5000
0
-1
0
1
2
3
Deformation [%]

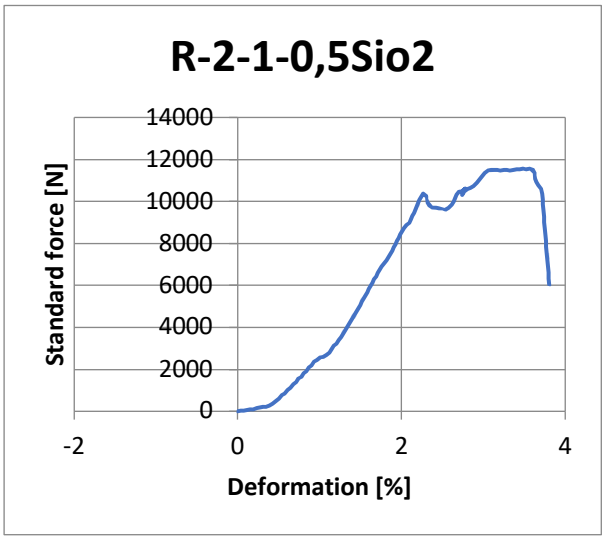
R-2-1-0,5Sio2
Standard force [N]
14000
12000
10000
8000
6000
4000
2000
0
-2
0
2
4
Deformation [%]

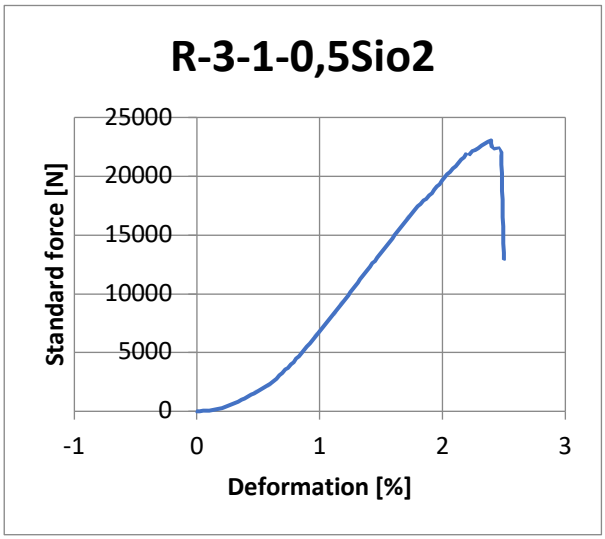
R-3-1-0,5Sio2
Standard force [N]
25000
20000
15000
10000
5000
0
-1
0
1
2
3
Deformation [%]

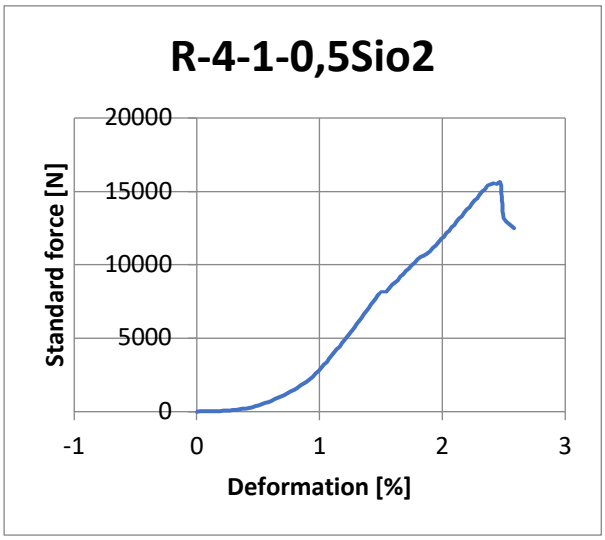
R-4-1-0,5Sio2
Standard force [N]
20000
15000
10000
5000
0
-1
0
1
2
3
Deformation [%]

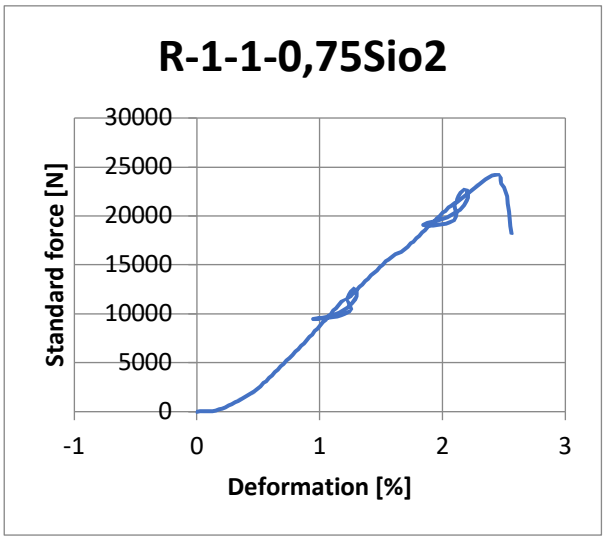
R-1-1-0,75Sio2
Standard force [N]
30000
25000
20000
15000
10000
5000
0
-1
0
1
2
3
Deformation [%]

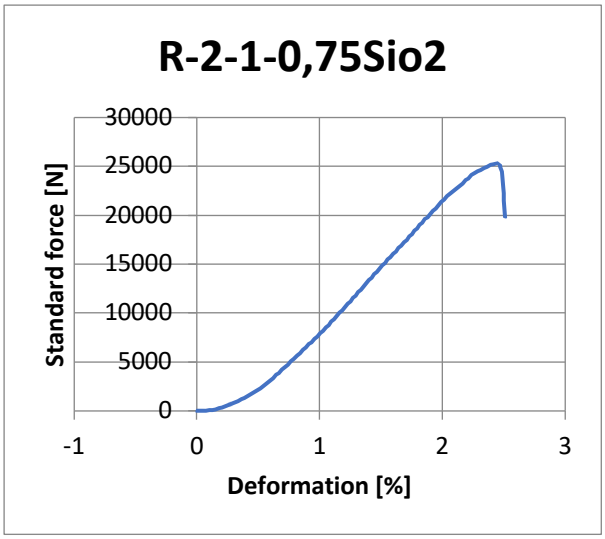
R-2-1-0,75Sio2
Standard force [N]
30000
25000
20000
15000
10000
5000
0
-1
0
1
2
3
Deformation [%]

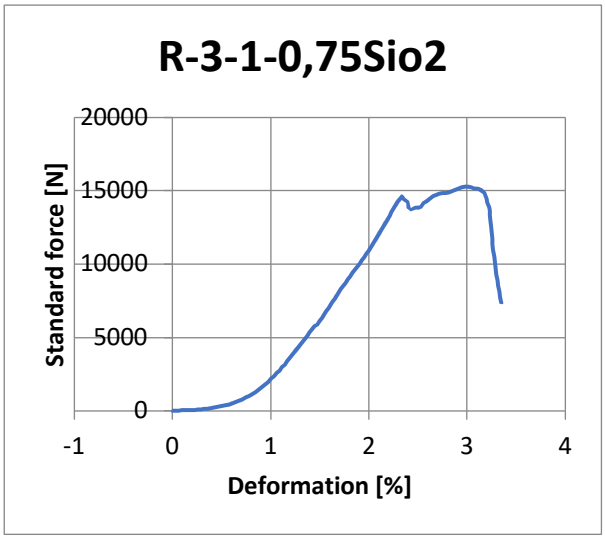
R-3-1-0,75Sio2
Standard force [N]
20000
15000
10000
5000
0
-1
0
1
2
3
4
Deformation [%]

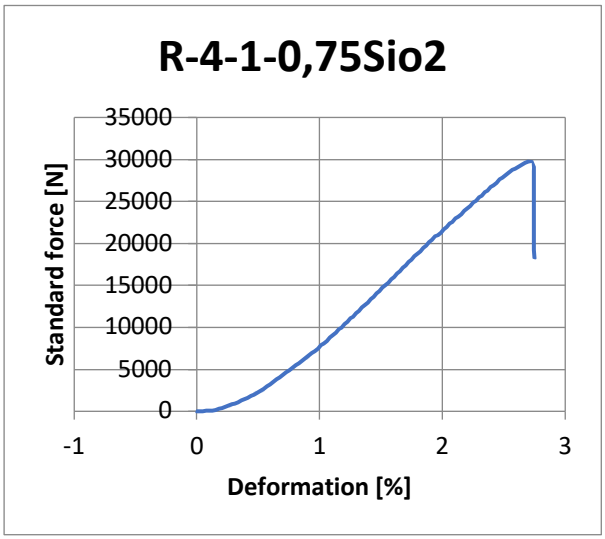
R-4-1-0,75Sio2
Standard force [N]
35000
30000
25000
20000
15000
10000
5000
0
-1
0
1
2
3
Deformation [%]

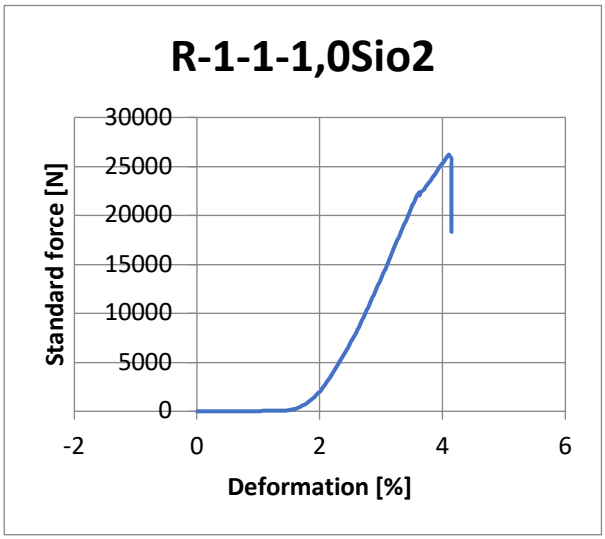
R-1-1-1,0Sio2
Standard force [N]
30000
25000
20000
15000
10000
5000
0
-2
0
2
4
6
Deformation [%]

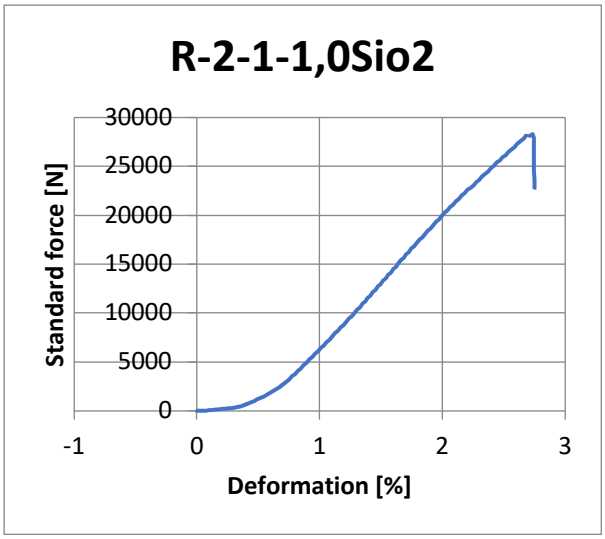
R-2-1-1,0Sio2
Standard force [N]
30000
25000
20000
15000
10000
5000
0
-1
0
1
2
3
Deformation [%]

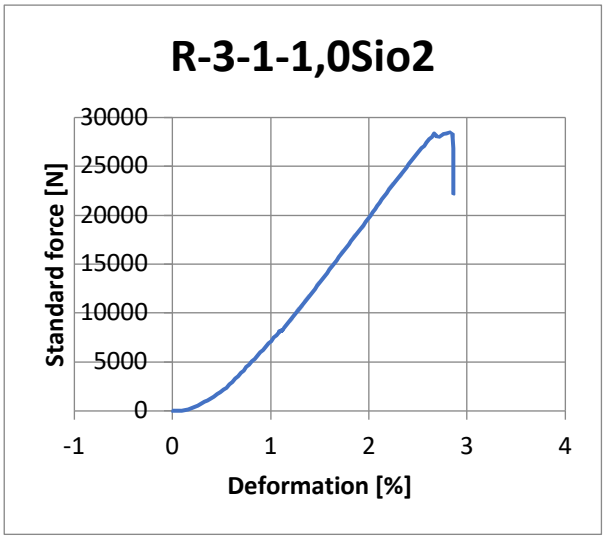
R-3-1-1,0Sio2
Standard force [N]
30000
25000
20000
15000
10000
5000
0
-1
0
1
2
3
4
Deformation [%]

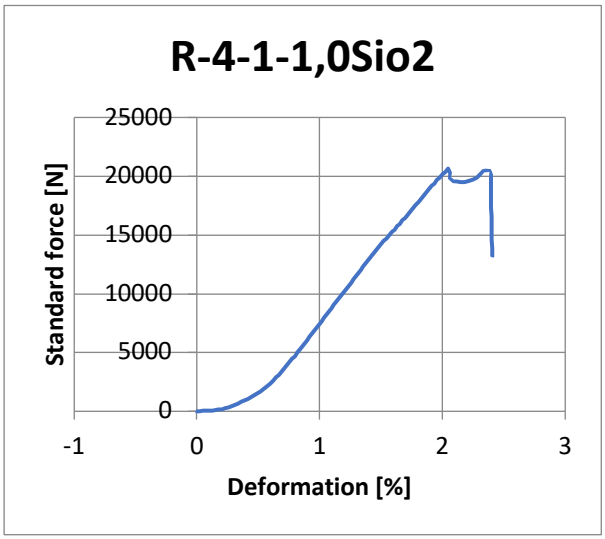
R-4-1-1,0Sio2
Standard force [N]
25000
20000
15000
10000
5000
0
-1
0
1
2
3
Deformation [%]

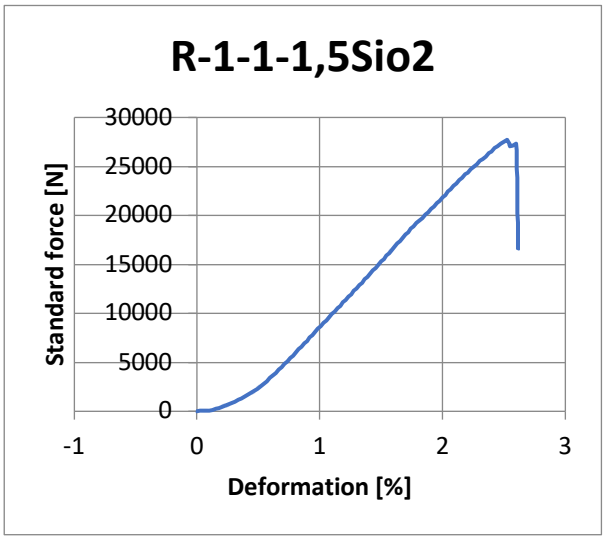
R-1-1-1,5Sio2
Standard force [N]
30000
25000
20000
15000
10000
5000
0
-1
0
1
2
3
Deformation [%]

**Test batch for tensile strength of C-class 28 days:**

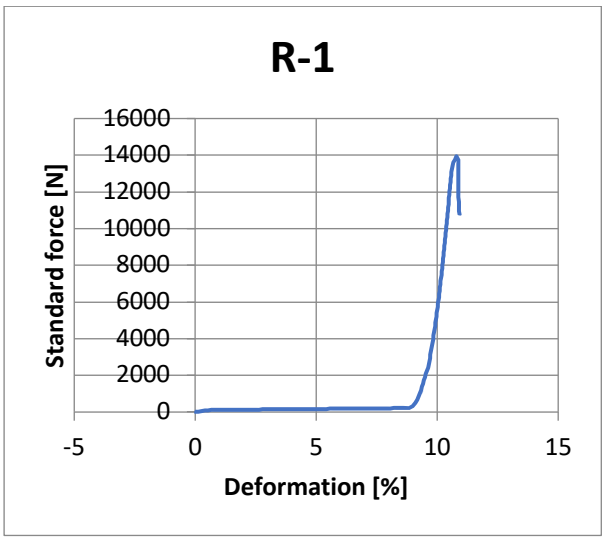


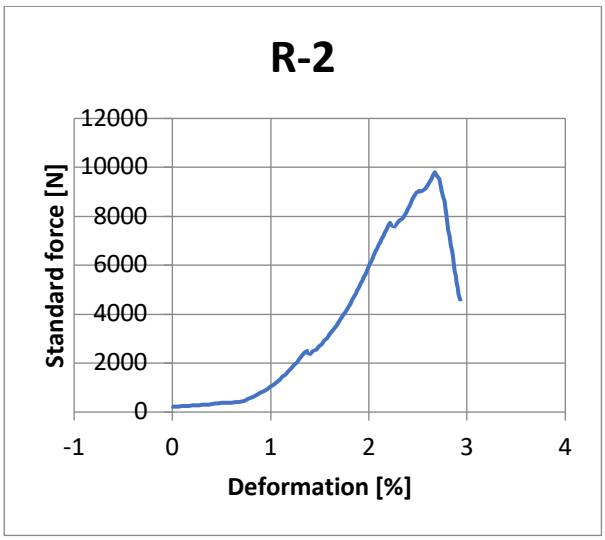


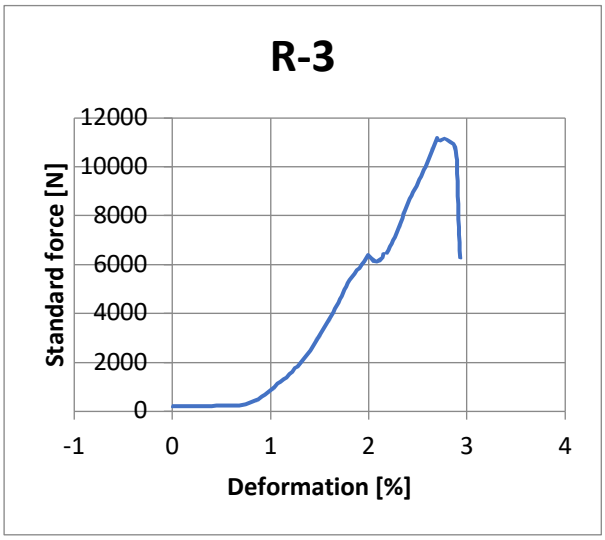


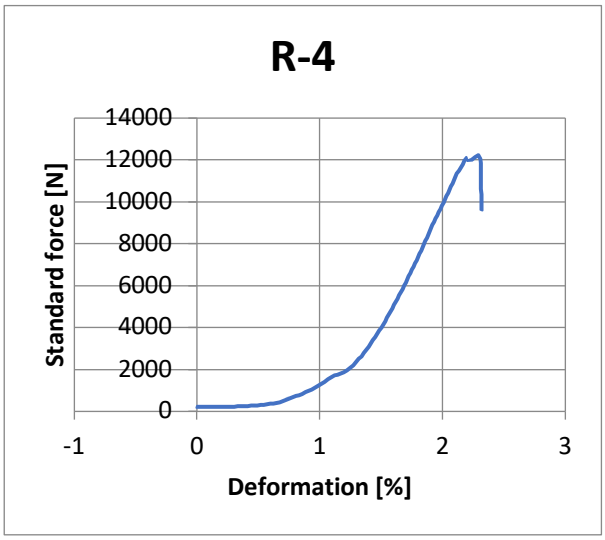


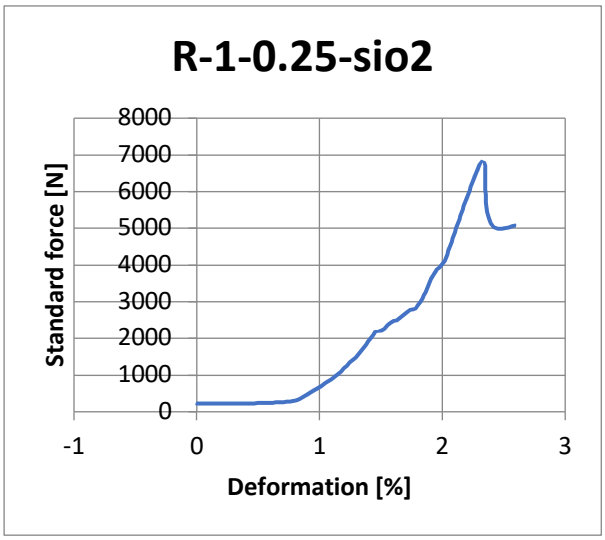


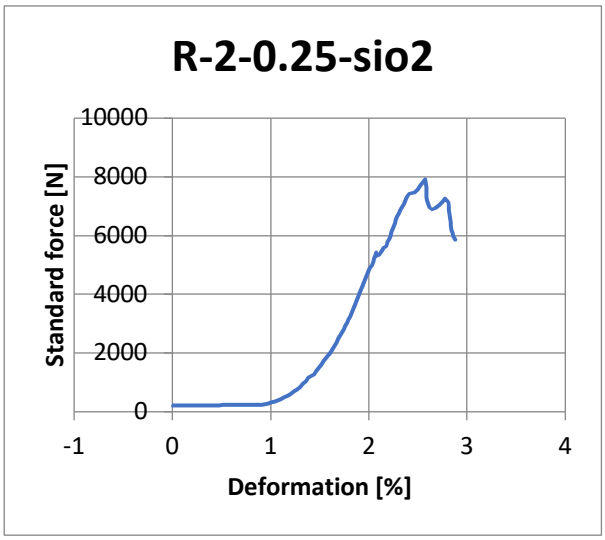

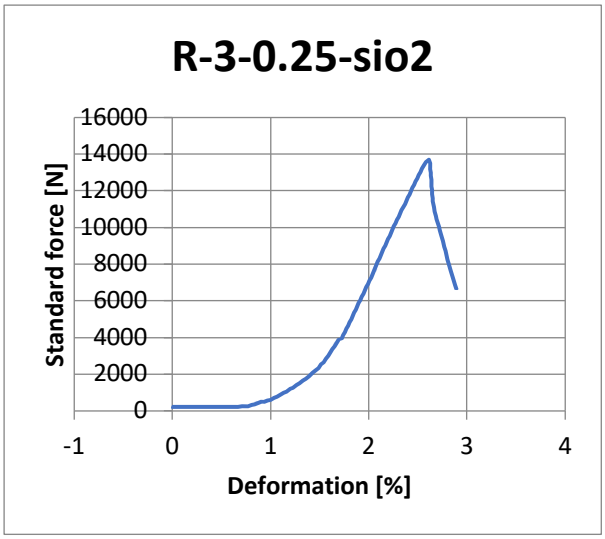
R-3-0.25-sio2
Standard force [N]
16000
14000
12000
10000
8000
6000
4000
2000
0
-1
0
1
2
3
4
Deformation [%]

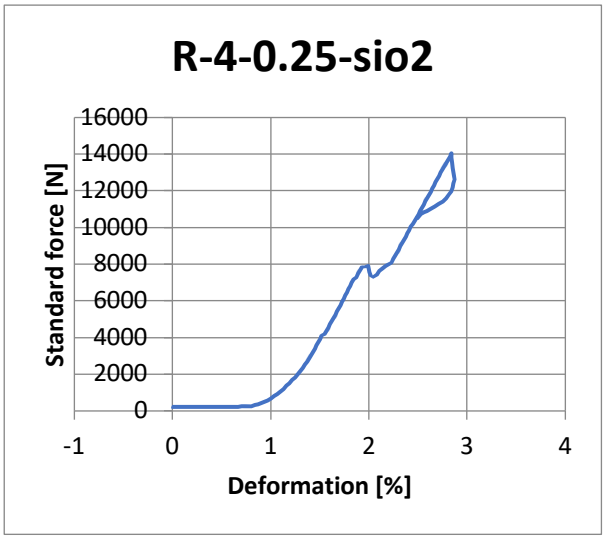
R-4-0.25-sio2
Standard force [N]
16000
14000
12000
10000
8000
6000
4000
2000
0
-1
0
1
2
3
4
Deformation [%]

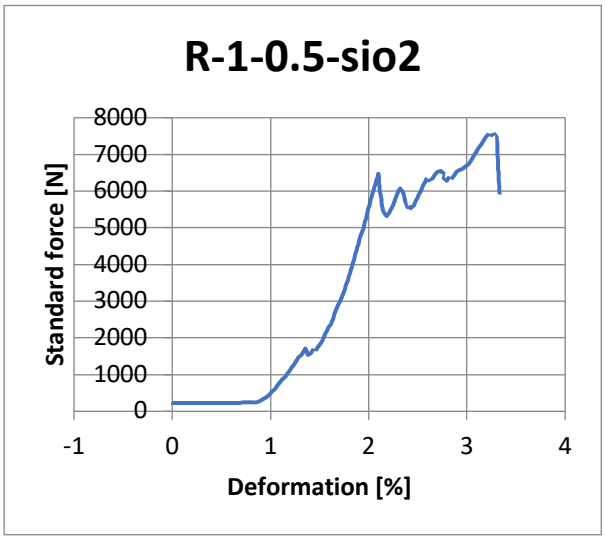
R-1-0.5-sio2
Standard force [N]
8000
7000
6000
5000
4000
3000
2000
1000
0
-1
0
1
2
3
4
Deformation [%]

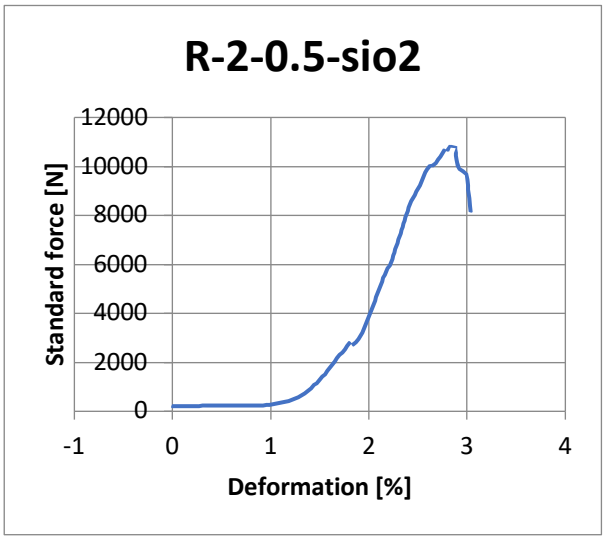
R-2-0.5-sio2
Standard force [N]
12000
10000
8000
6000
4000
2000
0
-1
0
1
2
3
4
Deformation [%]

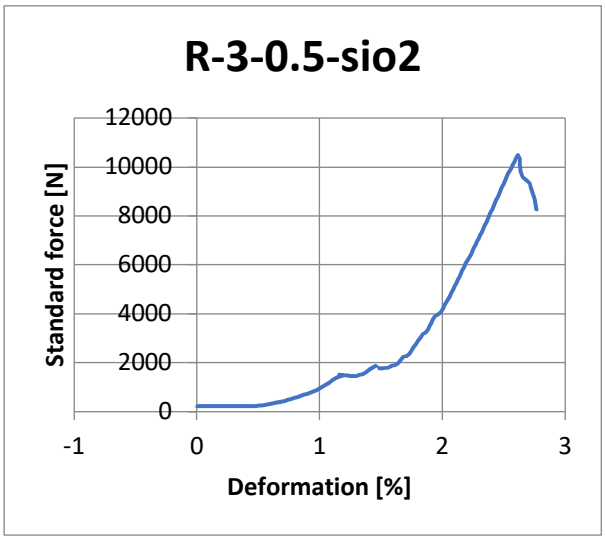
R-3-0.5-sio2
Standard force [N]
12000
10000
8000
6000
4000
2000
0
-1
0
1
2
3
Deformation [%]

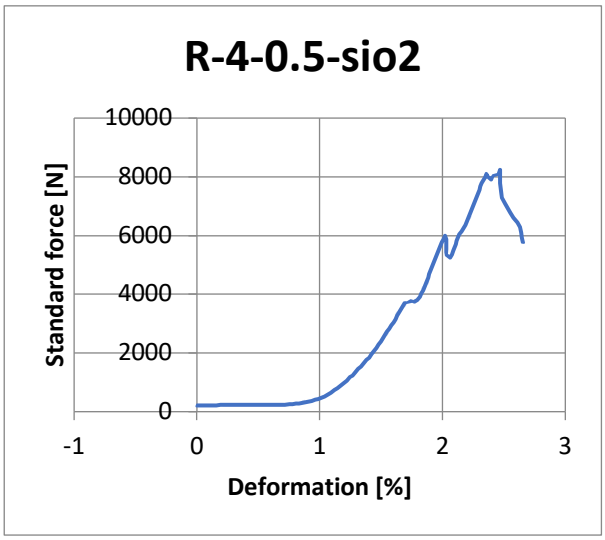
R-4-0.5-sio2
Standard force [N]
10000
8000
6000
4000
2000
0
-1
0
1
2
3
Deformation [%]

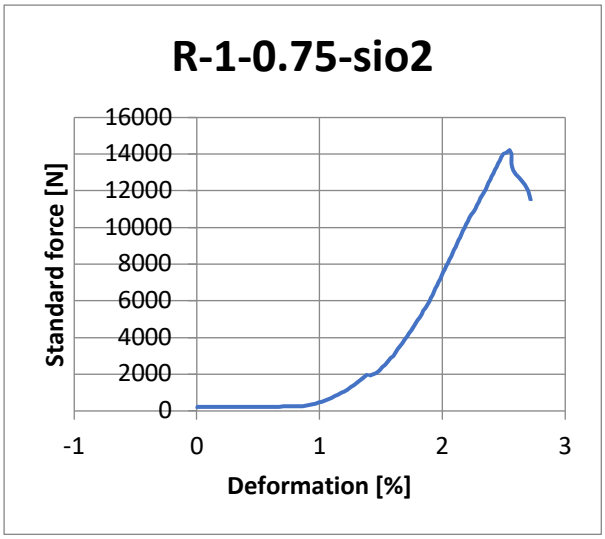
R-1-0.75-sio2
Standard force [N]
16000
14000
12000
10000
8000
6000
4000
2000
0
-1
0
1
2
3
Deformation [%]

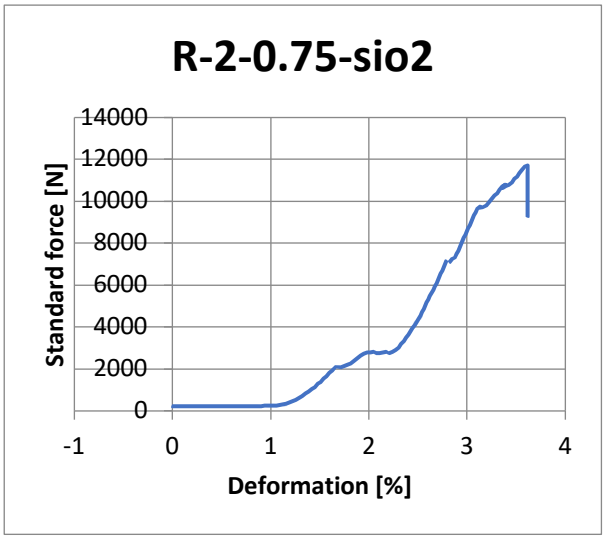
R-2-0.75-sio2
Standard force [N]
14000
12000
10000
8000
6000
4000
2000
0
-1
0
1
2
3
4
Deformation [%]

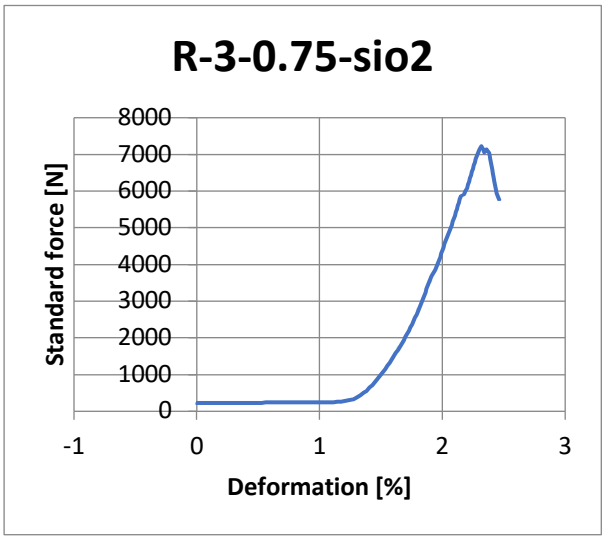
R-3-0.75-sio2
Standard force [N]
8000
7000
6000
5000
4000
3000
2000
1000
0
-1
0
1
2
3
Deformation [%]

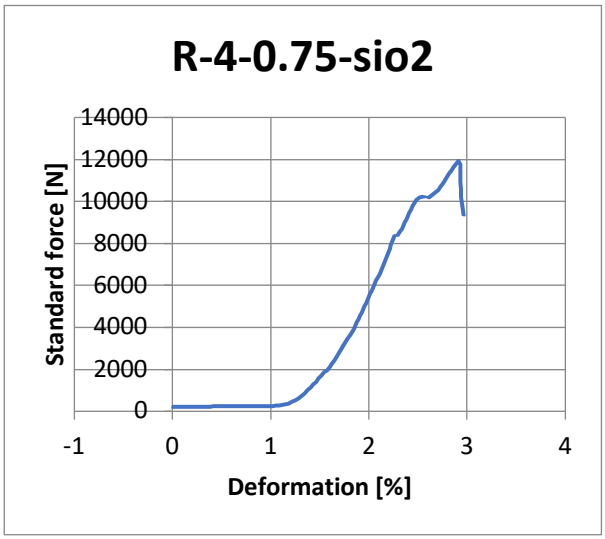
R-4-0.75-sio2
Standard force [N]
14000
12000
10000
8000
6000
4000
2000
0
-1
0
1
2
3
4
Deformation [%]

**Test batch for compressive strength of Environmental cement 28 days:**

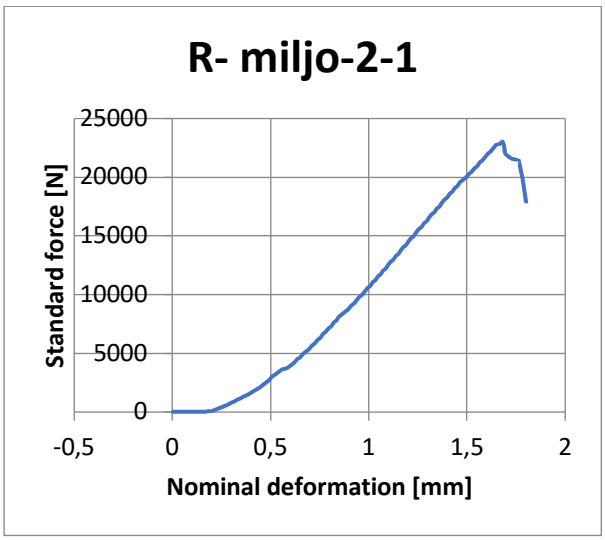


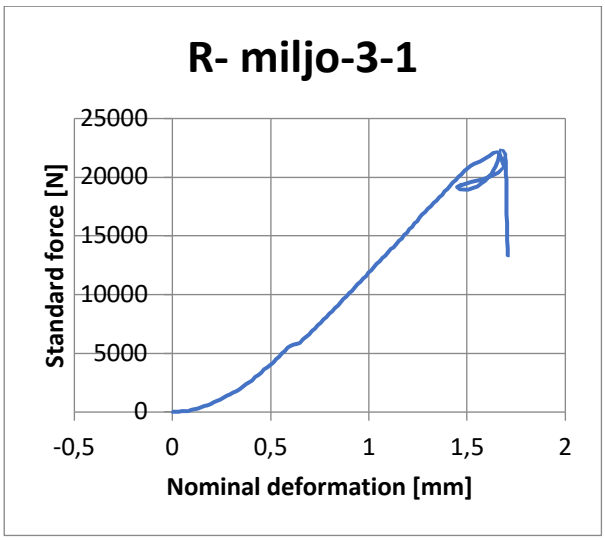


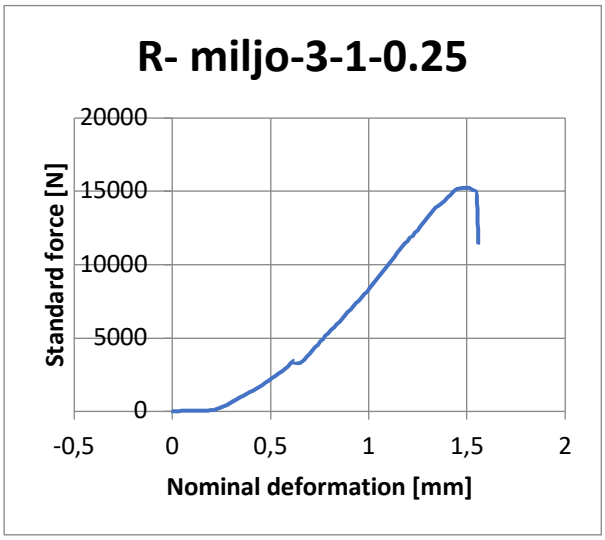


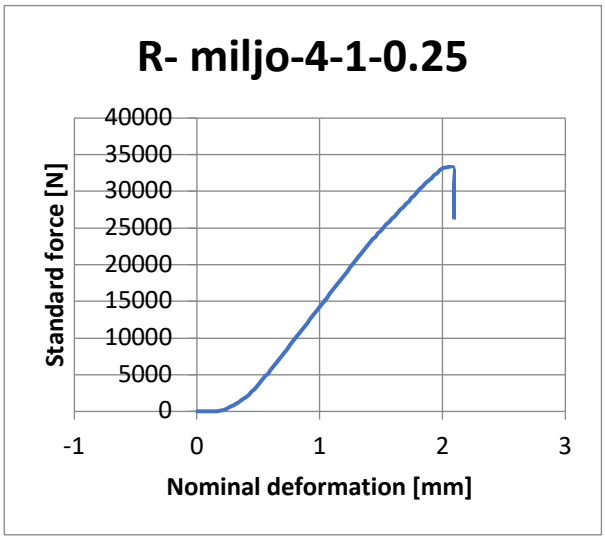


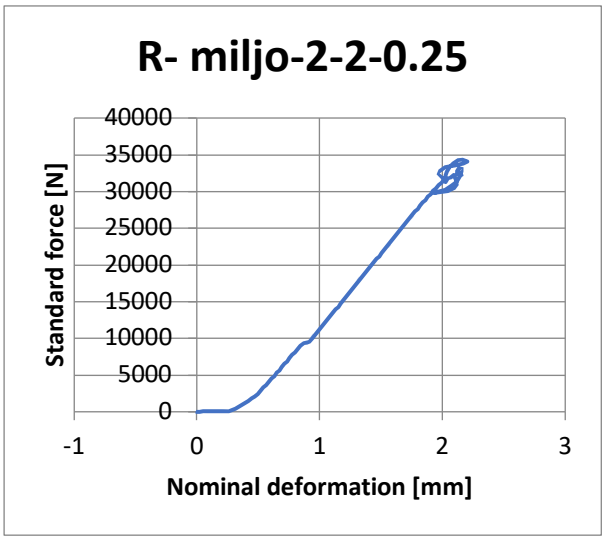


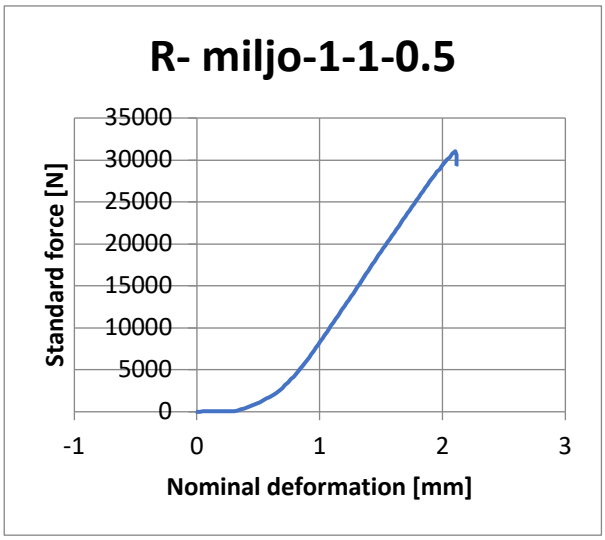

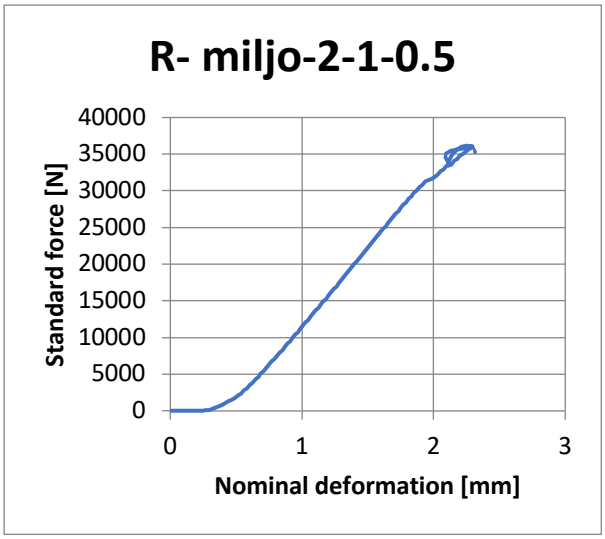
R- miljo-2-1-0.5
Standard force [N]
40000
35000
30000
25000
20000
15000
10000
5000
0
0
1
2
3
Nominal deformation [mm]

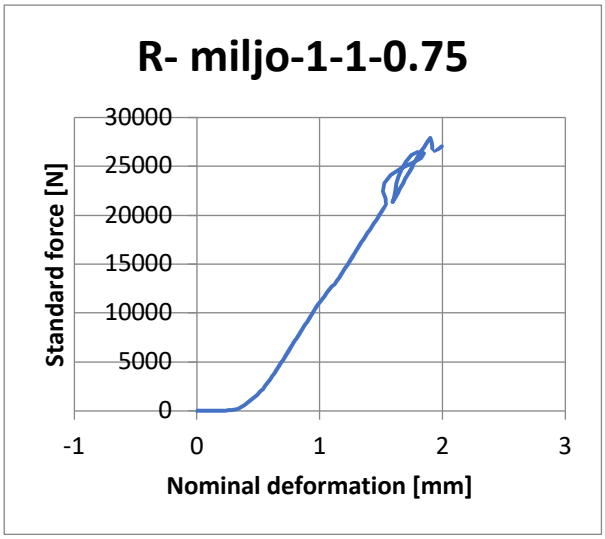
R- miljo-1-1-0.75
Standard force [N]
30000
25000
20000
15000
10000
5000
0
-1
0
1
2
3
Nominal deformation [mm]

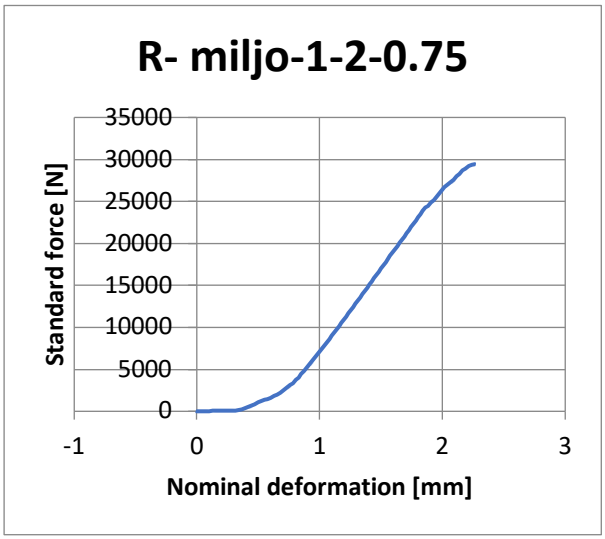
R- miljo-1-2-0.75
Standard force [N]
35000
30000
25000
20000
15000
10000
5000
0
-1
0
1
2
3
Nominal deformation [mm]

**Test batch for tensile strength of Environmental cement 28 days:**

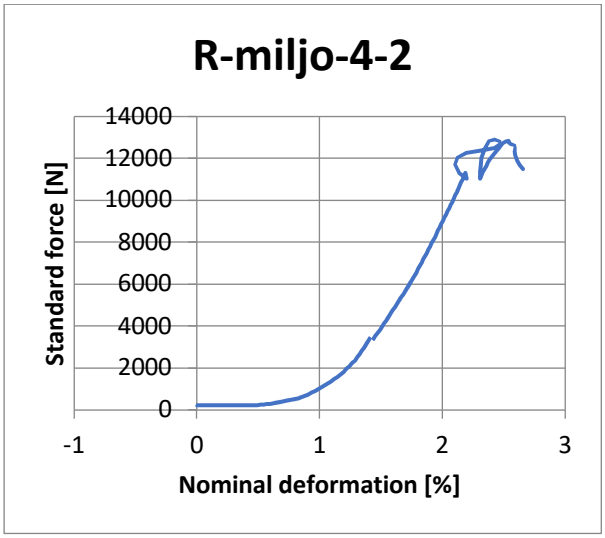


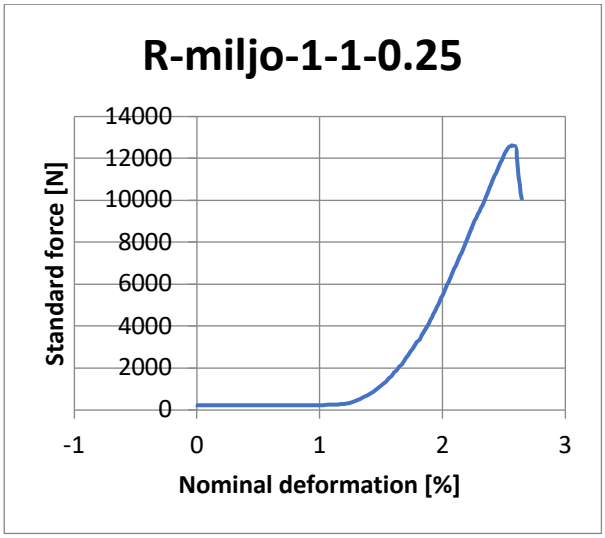


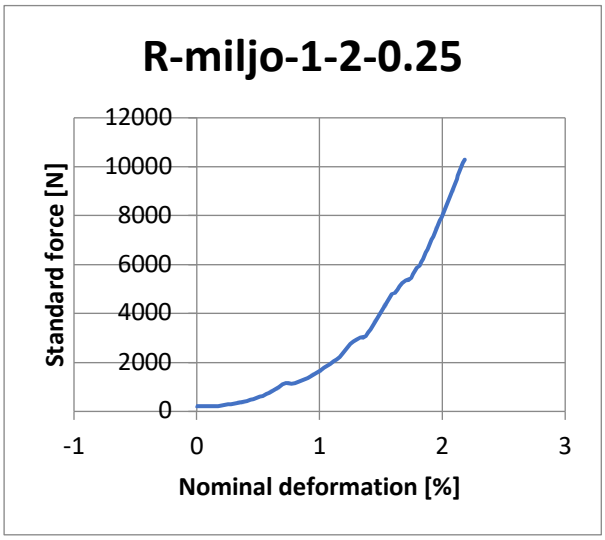


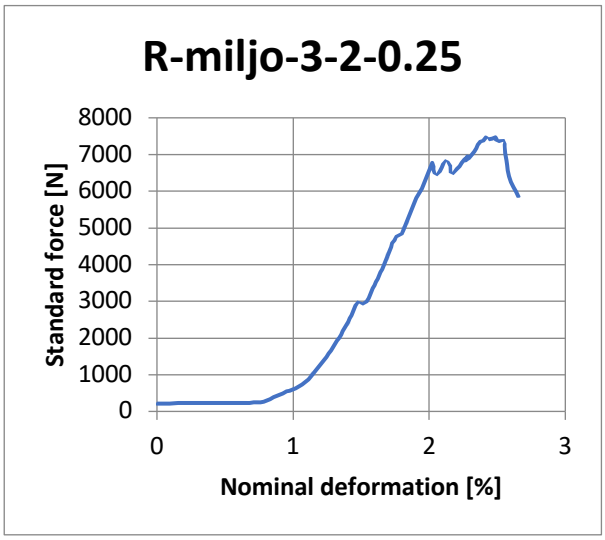


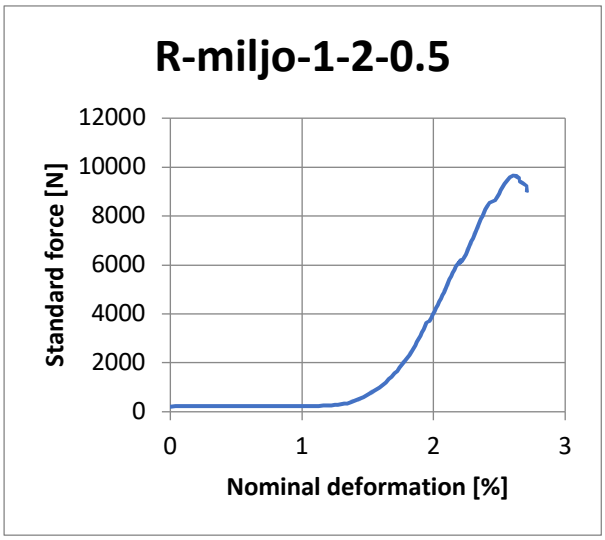


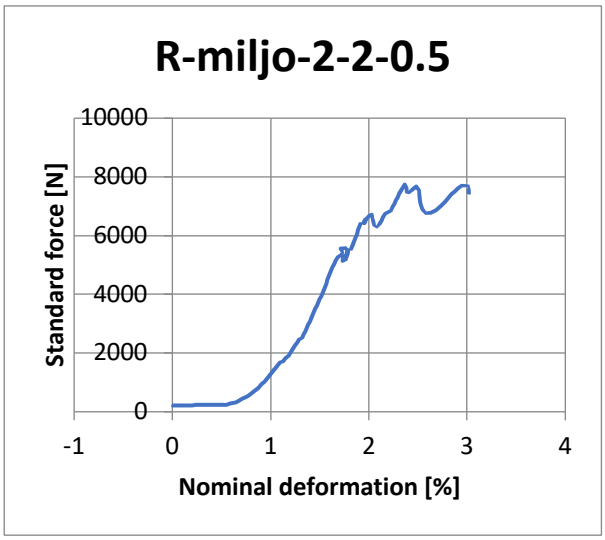

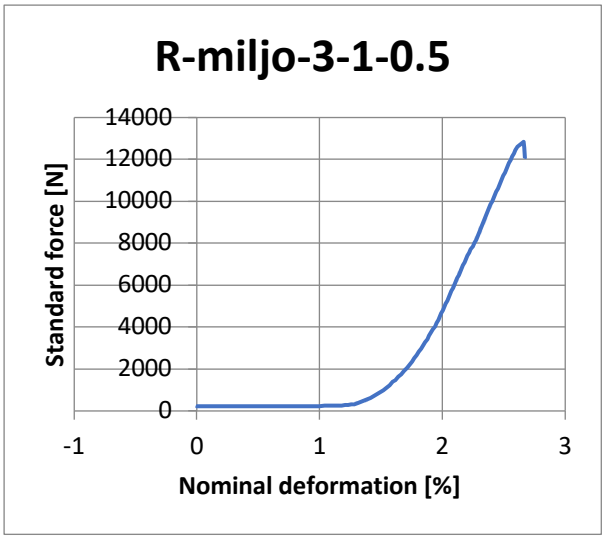
R-miljo-3-1-0.5
Standard force [N]
14000
12000
10000
8000
6000
4000
2000
0
-1
0
1
2
3
Nominal deformation [%]

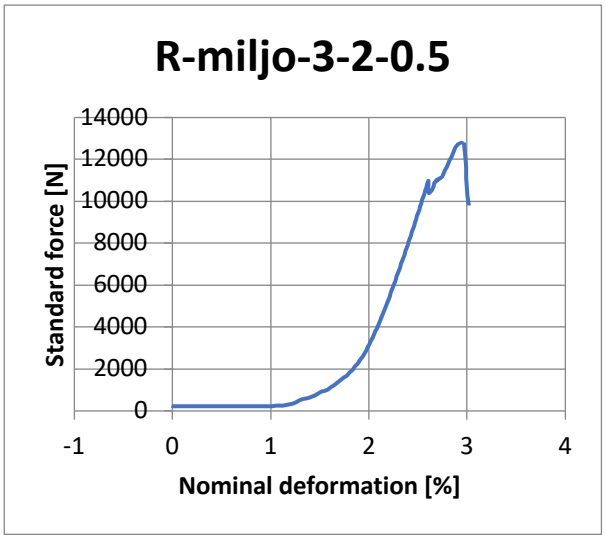
R-miljo-3-2-0.5
Standard force [N]
14000
12000
10000
8000
6000
4000
2000
0
-1
0
1
2
3
4
Nominal deformation [%]

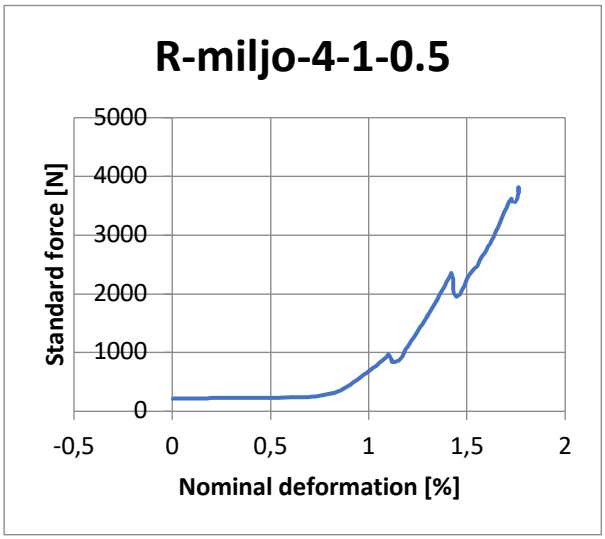
R-miljo-4-1-0.5
Standard force [N]
5000
4000
3000
2000
1000
0
-0,5
0
0,5
1
1,5
2
Nominal deformation [%]

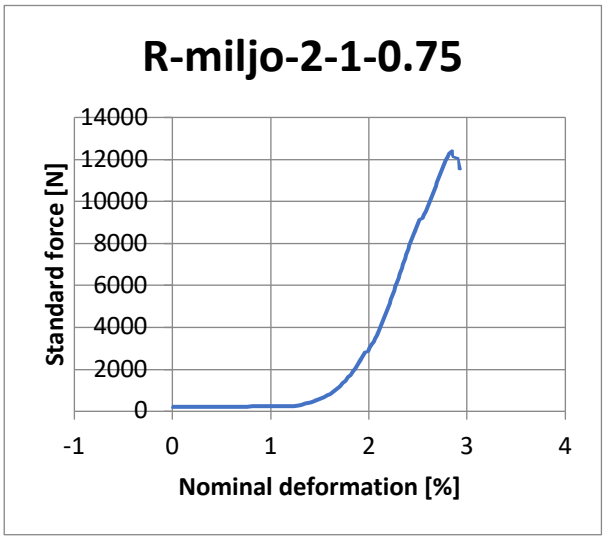
R-miljo-2-1-0.75
Standard force [N]
14000
12000
10000
8000
6000
4000
2000
0
-1
0
1
2
3
4
Nominal deformation [%]

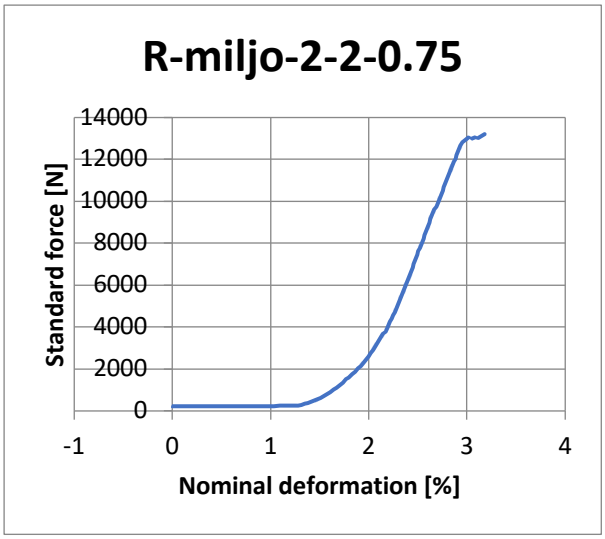
R-miljo-2-2-0.75
Standard force [N]
14000
12000
10000
8000
6000
4000
2000
0
-1
0
1
2
3
4
Nominal deformation [%]

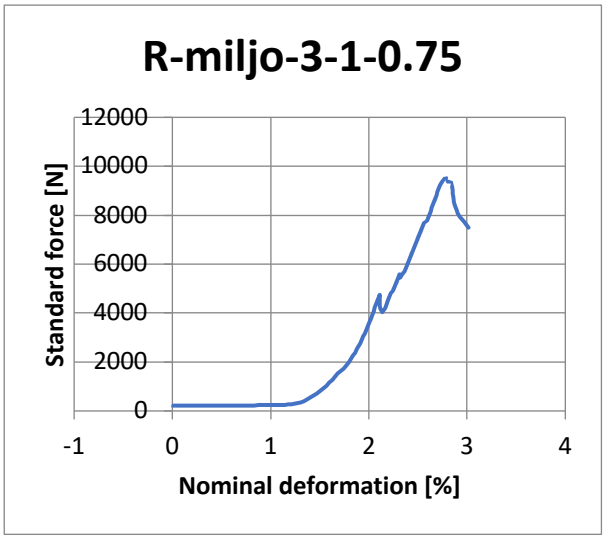
R-miljo-3-1-0.75
Standard force [N]
12000
10000
8000
6000
4000
2000
0
-1
0
1
2
3
4
Nominal deformation [%]

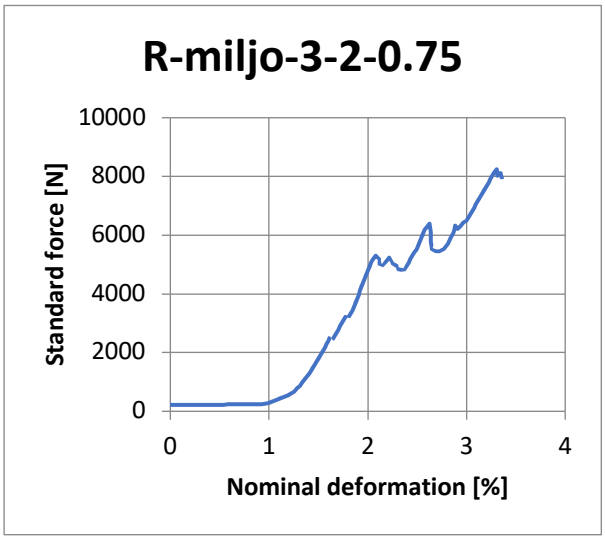
R-miljo-3-2-0.75
Standard force [N]
10000
8000
6000
4000
2000
0
0
1
2
3
4
Nominal deformation [%]

**Test batch for compressive strength of G-class 28 days:**

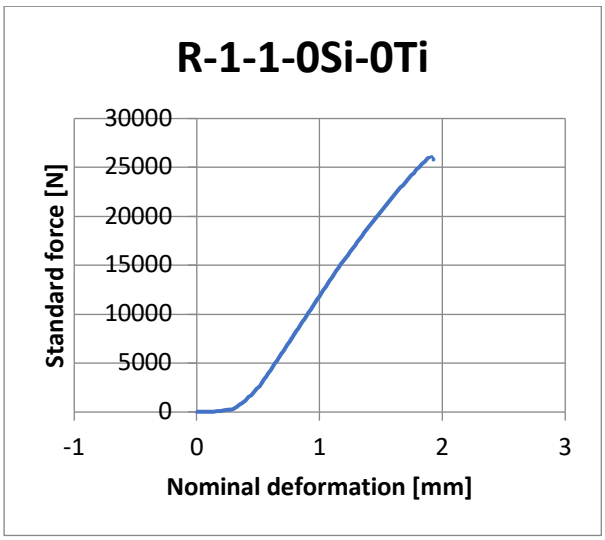


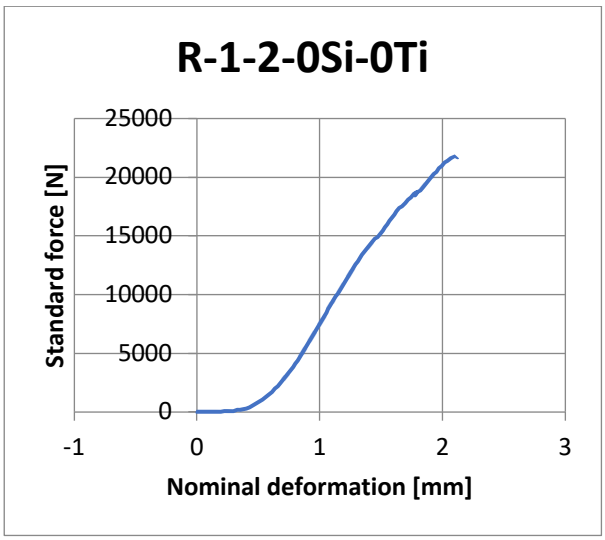


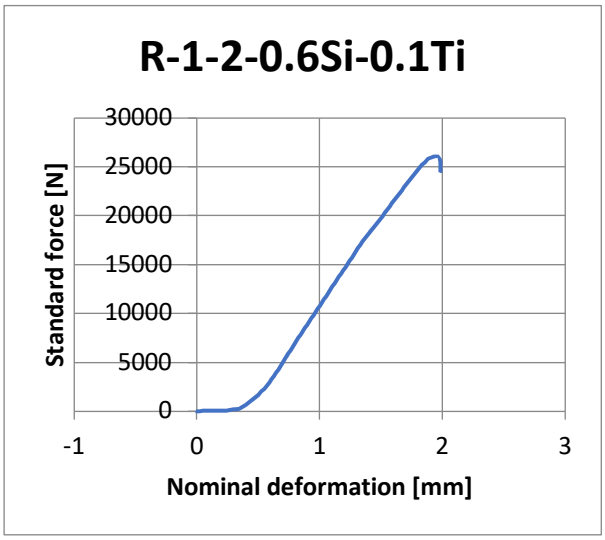


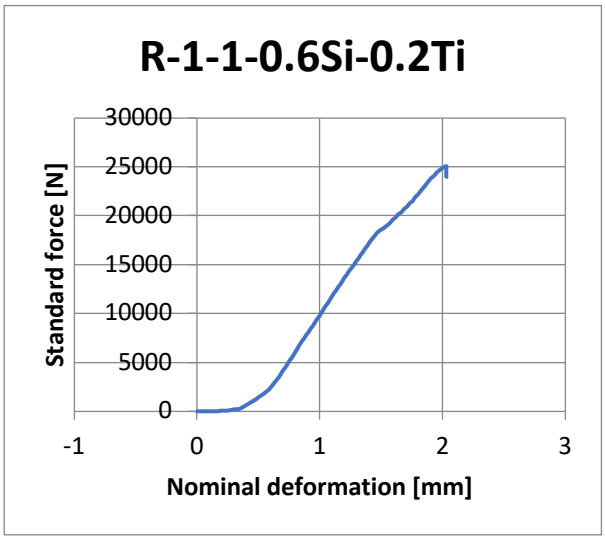

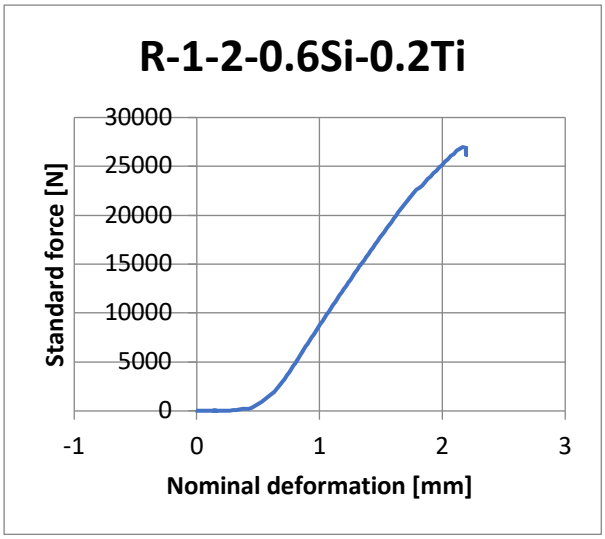
R-1-2-0.6Si-0.2Ti
Standard force [N]
30000
25000
20000
15000
10000
5000
0
-1
0
1
2
3
Nominal deformation [mm]

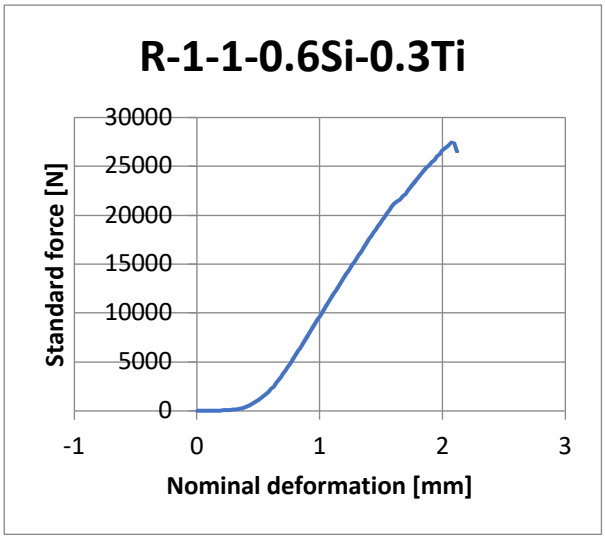
R-1-1-0.6Si-0.3Ti
Standard force [N]
30000
25000
20000
15000
10000
5000
0
-1
0
1
2
3
Nominal deformation [mm]

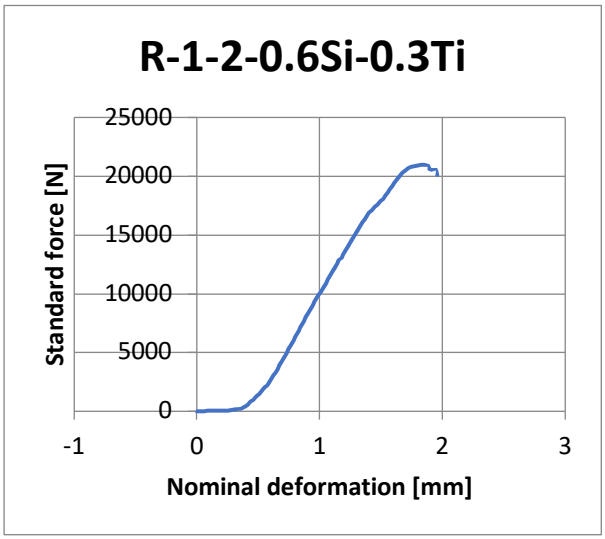
R-1-2-0.6Si-0.3Ti
Standard force [N]
25000
20000
15000
10000
5000
0
-1
0
1
2
3
Nominal deformation [mm]

# APPENDIX B: NON-DESTRUCTIVE MEASUREMENTS

**Test batch for non-destructive of C-class 3 days samples:**

| Plug # | OD, mm | Length, mm | Mass | Volume, m3 | Sonic, µs | Density, kg/m3 | Velocity, m/s | (M), Gpa |
|---|---|---|---|---|---|---|---|---|
| R-1-1 | 33,01 | 67,77 | 103,26 | 5,79987E-05 | 20,9 | 1780 | 3243 | 18,7 |
| R-1-2 | 33,01 | 68,89 | 100,43 | 5,89572E-05 | 19,3 | 1703 | 3569 | 21,7 |
| R-1-1-0,25Sio2 | 33,01 | 68,5 | 105,3 | 5,86235E-05 | 20,5 | 1796 | 3341 | 20,1 |
| R-1-2-0,25Sio2 | 33,01 | 67,75 | 104,64 | 5,79816E-05 | 19,8 | 1805 | 3422 | 21,1 |
| R-1-1-0,5Sio2 | 33,01 | 67,47 | 102,5 | 5,7742E-05 | 20,6 | 1775 | 3275 | 19,0 |
| R-1-2-0,5Sio2 | 33,01 | 67,86 | 103,06 | 5,80757E-05 | 19,8 | 1775 | 3427 | 20,8 |
| R-1-1-0,75Sio2 | 33,01 | 67,62 | 103,54 | 5,78703E-05 | 19,6 | 1789 | 3450 | 21,3 |
| R-1-2-0,75Sio2 | 33,01 | 66,12 | 100,67 | 5,65866E-05 | 19,9 | 1779 | 3323 | 19,6 |
| R-1-1-1,0Sio2 | 33,01 | 67,74 | 102,85 | 5,7973E-05 | 20 | 1774 | 3387 | 20,4 |
| R-1-2-1,0Sio2 | 33,01 | 67,85 | 102,94 | 5,80672E-05 | 19,9 | 1773 | 3410 | 20,6 |
| R-1-1-1,5Sio2 | 33,01 | 67,23 | 97,75 | 5,75366E-05 | 19,2 | 1699 | 3502 | 20,8 |
| R-1-2-1,5Sio2 | 33,01 | 68,33 | 102,75 | 5,8478E-05 | 21,2 | 1757 | 3223 | 18,3 |

**Test batch for non-destructive of C-class 7 days samples:**

| Plug # | OD, mm | Length, mm | Mass | Volume, m3 | Sonic, µs | Density, kg/m3 | Velocity, m/s | (M), Gpa |
|---|---|---|---|---|---|---|---|---|
| R-1-1 | 33,01 | 67,7 | 104,84 | 5,79388E-05 | 19,8 | 1809 | 3419 | 21,2 |
| R-1-2 | 33,01 | 67,46 | 104,47 | 5,77334E-05 | 20,2 | 1810 | 3340 | 20,2 |
| R-1-1-0,25Sio2 | 33,01 | 67,55 | 102,13 | 5,78104E-05 | 20,2 | 1767 | 3344 | 19,8 |
| R-1-2-0,25Sio2 | 33,01 | 68,03 | 103,06 | 5,82212E-05 | 21,1 | 1770 | 3224 | 18,4 |
| R-1-1-0,5Sio2 | 33,01 | 67,54 | 103,15 | 5,78019E-05 | 21 | 1785 | 3216 | 18,5 |
| R-1-2-0,5Sio2 | 33,01 | 68,18 | 103,89 | 5,83496E-05 | 20,4 | 1780 | 3342 | 19,9 |
| R-1-1-0,75Sio2 | 33,01 | 68,39 | 104,03 | 5,85293E-05 | 20,7 | 1777 | 3304 | 19,4 |
| R-1-2-0,75Sio2 | 33,01 | 68,37 | 104,5 | 5,85122E-05 | 21 | 1786 | 3256 | 18,9 |
| R-1-1-1,0Sio2 | 33,01 | 67,3 | 102,85 | 5,75965E-05 | 20,2 | 1786 | 3332 | 19,8 |
| R-1-2-1,0Sio2 | 33,01 | 68,45 | 104,28 | 5,85807E-05 | 20,7 | 1780 | 3307 | 19,5 |
| R-1-1-1,5Sio2 | 33,01 | 68,4 | 104,24 | 5,85379E-05 | 20,2 | 1781 | 3386 | 20,4 |
| R-1-2-1,5Sio2 | 33,01 | 67,78 | 103,58 | 5,80073E-05 | 20,4 | 1786 | 3323 | 19,7 |

**Test batch for non-destructive of C-class 28 days samples:**

| Plug # | OD, mm | Length, mm | Mass | Volume, m3 | Sonic, µs | Density, kg/m3 | Velocity, m/s | (M), Gpa |
|---|---|---|---|---|---|---|---|---|
| R-2-1 | 33,01 | 67,28 | 99,14 | 5,75794E-05 | 20,8 | 1722 | 3235 | 18,0 |
| R-3-1 | 33,01 | 67,96 | 100,1 | 5,81613E-05 | 20,9 | 1721 | 3252 | 18,2 |
| R-4-1 | 33,01 | 67,35 | 99,46 | 5,76393E-05 | 20,7 | 1726 | 3254 | 18,3 |
| R-1-1-0,25Sio2 | 33,01 | 68,03 | 99,39 | 5,82212E-05 | 22 | 1707 | 3092 | 16,3 |
| R-2-1-0,25Sio2 | 33,01 | 67,85 | 99,3 | 5,80672E-05 | 20,8 | 1710 | 3262 | 18,2 |
| R-3-1-0,25Sio2 | 33,01 | 67,36 | 99,47 | 5,76478E-05 | 20,3 | 1725 | 3318 | 19,0 |
| R-4-1-0,25Sio2 | 33,01 | 67,49 | 99,46 | 5,77591E-05 | 20,3 | 1722 | 3325 | 19,0 |
| R-1-1-0,5Sio2 | 33,01 | 67,18 | 99,7 | 5,74938E-05 | 20,4 | 1734 | 3293 | 18,8 |
| R-2-1-0,5Sio2 | 33,01 | 67,14 | 100 | 5,74596E-05 | 20,5 | 1740 | 3275 | 18,7 |
| R-3-1-0,5Sio2 | 33,01 | 67,69 | 99,36 | 5,79303E-05 | 20,7 | 1715 | 3270 | 18,3 |
| R-4-1-0,5Sio2 | 33,01 | 67,67 | 99,48 | 5,79131E-05 | 21 | 1718 | 3222 | 17,8 |
| R-1-1-0,75Sio2 | 33,01 | 67,64 | 102,19 | 5,78875E-05 | 19,5 | 1765 | 3469 | 21,2 |
| R-2-1-0,75Sio2 | 33,01 | 67,67 | 102,14 | 5,79131E-05 | 20,3 | 1764 | 3333 | 19,6 |
| R-3-1-0,75Sio2 | 33,01 | 67,92 | 99,62 | 5,81271E-05 | 20,3 | 1714 | 3346 | 19,2 |
| R-4-1-0,75Sio2 | 33,01 | 67,93 | 99,68 | 5,81357E-05 | 21,2 | 1715 | 3204 | 17,6 |
| R-1-1-1,0Sio2 | 33,01 | 67,17 | 101,29 | 5,74852E-05 | 20,4 | 1762 | 3293 | 19,1 |
| R-2-1-1,0Sio2 | 33,01 | 67,49 | 100,21 | 5,77591E-05 | 21,4 | 1735 | 3154 | 17,3 |
| R-3-1-1,0Sio2 | 33,01 | 67,57 | 99,73 | 5,78276E-05 | 20,8 | 1725 | 3249 | 18,2 |
| R-4-1-1,0Sio2 | 33,01 | 67,93 | 101,42 | 5,81357E-05 | 20,2 | 1745 | 3363 | 19,7 |
| R-1-1-1,5Sio2 | 33,01 | 67,32 | 101,38 | 5,76136E-05 | 20,5 | 1760 | 3284 | 19 |

**Test batch for non-destructive of C-class 28 days Brazilian samples:**

| Plug # | OD, mm | Length, mm | Mass | Volume, m3 | Sonic, µs | Density, kg/m3 | Velocity, m/s | (M), Gpa |
|---|---|---|---|---|---|---|---|---|
| R-1-1 | 33,01 | 66,57 | 97,89 | 5,69717E-05 | 18,5 | 1718 | 3598 | 22,2 |
| R-1-2 | 33,01 | 67 | 95,67 | 5,73397E-05 | 19,3 | 1668 | 3472 | 20,1 |
| R-1-3 | 33,01 | 67,11 | 97,47 | 5,74339E-05 | 19,7 | 1697 | 3407 | 19,7 |
| R-1-4 | 33,01 | 66,87 | 94,79 | 5,72285E-05 | 19,1 | 1656 | 3501 | 20,3 |
| R-1-1-0,25Sio2 | 33,01 | 66,95 | 97,69 | 5,7297E-05 | 19,1 | 1705 | 3505 | 20,9 |
| R-2-1-0,25Sio2 | 33,01 | 66,88 | 98,07 | 5,7237E-05 | 19,6 | 1713 | 3412 | 19,9 |
| R-3-1-0,25Sio2 | 33,01 | 66,85 | 97,59 | 5,72114E-05 | 19,5 | 1706 | 3428 | 20,0 |
| R-4-1-0,25Sio2 | 33,01 | 67,03 | 98,22 | 5,73654E-05 | 19,5 | 1712 | 3437 | 20,2 |
| R-1-1-0,5Sio2 | 33,01 | 67,13 | 98,17 | 5,7451E-05 | 18,7 | 1709 | 3590 | 22,0 |
| R-2-1-0,5Sio2 | 33,01 | 66,62 | 96,66 | 5,70145E-05 | 19,2 | 1695 | 3470 | 20,4 |
| R-3-1-0,5Sio2 | 33,01 | 66,77 | 97,63 | 5,71429E-05 | 19 | 1709 | 3514 | 21,1 |
| R-4-1-0,5Sio2 | 33,01 | 66,81 | 97,03 | 5,71771E-05 | 18,8 | 1697 | 3554 | 21,4 |
| R-1-1-0,75Sio2 | 33,01 | 66,71 | 95,94 | 5,70916E-05 | 18,7 | 1680 | 3567 | 21,4 |
| R-2-1-0,75Sio2 | 33,01 | 66,6 | 96,88 | 5,69974E-05 | 18,5 | 1700 | 3600 | 22,0 |
| R-3-1-0,75Sio2 | 33,01 | 67,23 | 97,21 | 5,75366E-05 | 18,2 | 1690 | 3694 | 23,1 |
| R-4-1-0,75Sio2 | 33,01 | 66,04 | 96,15 | 5,65182E-05 | 18,9 | 1701 | 3494 | 20,8 |

**Test batch for non-destructive of environmental cement 28 days samples:**

| Plug # | OD, mm | Length, mm | Mass | Volume, m3 | Sonic, µs | Density, kg/m3 | Velocity, m/s | (M), Gpa |
|---|---|---|---|---|---|---|---|---|
| R-1-2 | 33,01 | 67,77 | 99,39 | 5,79987E-05 | 19,1 | 1714 | 3548 | 21,6 |
| R-2-1 | 33,01 | 67,51 | 100,32 | 5,77762E-05 | 19,3 | 1736 | 3498 | 21,2 |
| R-3-1 | 33,01 | 67,92 | 100,56 | 5,81271E-05 | 19,5 | 1730 | 3483 | 21,0 |
| R-2-2-0,25Sio2 | 33,01 | 67,33 | 99,68 | 5,76222E-05 | 18,5 | 1730 | 3639 | 22,9 |
| R-3-1-0,25Sio2 | 33,01 | 67,77 | 99,87 | 5,79987E-05 | 19,4 | 1722 | 3493 | 21,0 |
| R-4-1-0,25Sio2 | 33,01 | 67,17 | 99,05 | 5,74852E-05 | 19,2 | 1723 | 3498 | 21,1 |
| R-1-1-0,5Sio2 | 33,01 | 67,57 | 99,82 | 5,78276E-05 | 19,1 | 1726 | 3538 | 21,6 |
| R-2-1-0,5Sio2 | 33,01 | 67,9 | 100,59 | 5,811E-05 | 18,5 | 1731 | 3670 | 23,3 |
| R-1-1-0,75Sio2 | 33,01 | 68,07 | 100,32 | 5,82555E-05 | 18,5 | 1722 | 3679 | 23,3 |
| R-1-2-0,75Sio2 | 33,01 | 67,31 | 99,86 | 5,7605E-05 | 18,5 | 1734 | 3638 | 22,9 |

**Test batch for non-destructive of environmental cement 28 days Brazilian samples:**

| Plug # | OD, mm | Length, mm | Mass | Volume, m3 | Sonic, µs | Density, kg/m3 | Velocity, m/s | (M), Gpa |
|---|---|---|---|---|---|---|---|---|
| R-1-1 | 33,01 | 67,41 | 96,23 | 5,76906E-05 | 20,7 | 1668 | 3257 | 17,7 |
| R-2-2 | 33,01 | 68,33 | 98,67 | 5,8478E-05 | 20,8 | 1687 | 3285 | 18,2 |
| R-3-2 | 33,01 | 67,56 | 98,98 | 5,7819E-05 | 19,6 | 1712 | 3447 | 20,3 |
| R-4-1 | 33,01 | 67,83 | 97,18 | 5,80501E-05 | 19,8 | 1674 | 3426 | 19,6 |
| R-4-2 | 33,01 | 67,34 | 97,36 | 5,76307E-05 | 19,7 | 1689 | 3418 | 19,7 |
| R-1-1-0,25Sio2 | 33,01 | 67,7 | 98,65 | 5,79388E-05 | 21,9 | 1703 | 3091 | 16,3 |
| R-1-2-0,25Sio2 | 33,01 | 67,74 | 98,2 | 5,7973E-05 | 20,7 | 1694 | 3272 | 18,1 |
| R-2-1-0,25Sio2 | 33,01 | 67,67 | 97,97 | 5,79131E-05 | 19,6 | 1692 | 3453 | 20,2 |
| R-3-2-0,25Sio2 | 33,01 | 67,88 | 98,45 | 5,80929E-05 | 21,4 | 1695 | 3172 | 17,1 |
| R-4-2-0,25Sio2 | 33,01 | 67,62 | 97,52 | 5,78703E-05 | 19,7 | 1685 | 3432 | 19,9 |
| R-1-2-0,5Sio2 | 33,01 | 67,58 | 98,36 | 5,78361E-05 | 19,9 | 1701 | 3396 | 19,6 |
| R-2-2-0,5Sio2 | 33,01 | 67,86 | 98,71 | 5,80757E-05 | 20,3 | 1700 | 3343 | 19,0 |
| R-3-1-0,5Sio2 | 33,01 | 67,47 | 97,59 | 5,7742E-05 | 20,6 | 1690 | 3275 | 18,1 |
| R-3-2-0,5Sio2 | 33,01 | 67,87 | 98,17 | 5,80843E-05 | 19,7 | 1690 | 3445 | 20,1 |
| R-4-1-0,5Sio2 | 33,01 | 67,95 | 98,69 | 5,81528E-05 | 19,9 | 1697 | 3415 | 19,8 |
| R-4-2-0,5Sio2 | 33,01 | 68,45 | 98,06 | 5,85807E-05 | 20,3 | 1674 | 3372 | 19,0 |
| R-2-1-0,75Sio2 | 33,01 | 67,67 | 98,38 | 5,79131E-05 | 20,2 | 1699 | 3350 | 19,1 |
| R-2-2-0,75Sio2 | 33,01 | 67,57 | 97,31 | 5,78276E-05 | 21,1 | 1683 | 3202 | 17,3 |
| R-3-1-0,75Sio2 | 33,01 | 68,13 | 96,85 | 5,83068E-05 | 21,9 | 1661 | 3111 | 16,1 |
| R-3-2-0,75Sio2 | 33,01 | 68,04 | 97,32 | 5,82298E-05 | 19,7 | 1671 | 3454 | 19,9 |
| R-4-1-0,75Sio2 | 33,01 | 67,56 | 97,59 | 5,7819E-05 | 20 | 1688 | 3378 | 19,3 |
| R-4-2-0,75Sio2 | 33,01 | 67,31 | 97,21 | 5,7605E-05 | 19,8 | 1688 | 3399 | 19,5 |

**Test batch for non-destructive of G-class 7 days samples:**

| Plug # | OD, mm | Length, mm | Volume, m3 | Sonic, µs | Velocity, m/s |
|---|---|---|---|---|---|
| G-0/0-1-1 | 33,01 | 67,27 | 5,75708E-05 | 22 | 3058 |
| G-0/0-1-2 | 33,01 | 67,27 | 5,75708E-05 | 21,7 | 3100 |
| G-0.6/0.1-1-1 | 33,01 | 67,24 | 5,75451E-05 | 22,3 | 3015 |
| G-0.6/0.1-1-2 | 33,01 | 67,24 | 5,75451E-05 | 22,4 | 3002 |
| G-0.6/0.2-1-1 | 33,01 | 67,21 | 5,75195E-05 | 22 | 3055 |
| G-0.6/0.2-1-2 | 33,01 | 67,2 | 5,75109E-05 | 21,4 | 3140 |
| G-0.6/0.3-1-1 | 33,01 | 66,97 | 5,73141E-05 | 21,8 | 3072 |
| G-0.6/0.3-1-2 | 33,01 | 67,05 | 5,73825E-05 | 22 | 3048 |

**Test batch for non-destructive of G-class 28 days samples:**

| Plug # | OD, mm | Length, mm | Mass | Volume, m3 | Sonic, µs | Density, kg/m3 | Velocity, m/s | (M), Gpa |
|---|---|---|---|---|---|---|---|---|
| G-0/0-1-1 | 33,01 | 67,38 | 112,18 | 5,7665E-05 | 19,5 | 1945 | 3455,38462 | 23,2 |
| G-0/0-1-2 | 33,01 | 67,3 | 112,42 | 5,75965E-05 | 19,3 | 1952 | 3487,04663 | 23,7 |
| G-0.6/0.1-1-1 | 33,01 | 67,68 | 112,35 | 5,79217E-05 | 19,9 | 1940 | 3401,00503 | 22,4 |
| G-0.6/0.1-1-2 | 33,01 | 67,32 | 112,09 | 5,76136E-05 | 19,6 | 1946 | 3434,69388 | 23,0 |
| G-0.6/0.2-1-1 | 33,01 | 67,25 | 112,08 | 5,75537E-05 | 19,9 | 1947 | 3379,39698 | 22,2 |
| G-0.6/0.2-1-2 | 33,01 | 67,32 | 112,05 | 5,76136E-05 | 19,5 | 1945 | 3452,30769 | 23,2 |
| G-0.6/0.3-1-1 | 33,01 | 67,49 | 112,12 | 5,77591E-05 | 19,9 | 1941 | 3391,45729 | 22,3 |
| G-0.6/0.3-1-2 | 33,01 | 67,68 | 113,02 | 5,79217E-05 | 19,5 | 1951 | 3470,76923 | 23,5 |